IGF-1R EXPRESSION IN FETAL RAT HARD AND SOFT TISSUES IN RESPONSE TO CIGARETTE SMOKE EXTRACT

By

Harpradeep Ratia

A Thesis submitted to the Faculty of Graduate Studies

of

The University of Manitoba

in partial fulfilment of the requirements of the degree

of

MASTER OF SCIENCE

Department of Oral Biology

Faculty of Dentistry

University of Manitoba

2008

THE UNIVERSITY OF MANITOBA

FACULTY OF GRADUATE STUDIES

*****

COPYRIGHT PERMISSION

IGF-1R Expression in Fetal Rat Hard and Soft Tissues in Response to Cigarette Smoke Extract

BY

Harpradeep Ratia

A Thesis/Practicum submitted to the Faculty of Graduate Studies of The University of Manitoba in partial fulfillment of the requirement of the degree

Of

Master of Science

Acknowledgements

I would like to take this opportunity to Thank the almighty GOD for choosing me and bestowing me with his unconditional blessings in the form of knowledge and righteousness. I am very greatful to my parents who have encouraged me through out my life unconditionally and never discriminated against my gender for my inclination for education. My brother and sister for their immense emotional support. My school teachers, friends, university professors, clinicans, colleagues and patients (Delhi, Manipal India) who formed the building blocks of my being the person I am today.

I would like to Thank my committee members Dr. J.E. Scott (Supervisor), Dr. J Thliveris and Dr. A C. Karim (Co-Supervisors) for accepting to form the examining committee inspite of their busy schedules and gave their valuable inputs to this project. I am truly greatful to Dr. Scott for his financial support as a student research assistant and for BOB, MICH studentship, especially at the time of intense trials and tribulations and when I least expected it to come my way. Dr. Maria Vrontakis for being so empathetic and non judgemental towards my academic decisions which I personally believe till today were in the best interest of everyone. Dr. Fleming's communications course was a turning point in my life and even when it was over academically, it was not over for me at least. I made every possible attempt to keep up with his teachings and in search for more, tuesday afternoons became more fun when I knocked the 35min Health Sciences communications club run by Dr. E. Frost, which kept me going for the next challenge.

I don't think I can ever Thank Dr. Scott enough, for accepting me in this program in spite of no research background. At no point he showed his disbelief or discriminated against other Canadian students in his ways of crucial decisions and imparting knowledge. This was a very supportive behavior to help Asian international students adjust. His laboratory students are a blend of the East and West which makes student interaction and learning truly worth the educational environment. His unconditional support, non judgmental and patient attitude at all times to me and my colleagues can never be ignored. I shall truly remain greatful to him all my life.

I feel honoured to have been one of the few students to have been Co-supervised by Dr. Thliveris and Dr. Karim the soon to be Superannuated professors for this running academic year. I wish them happiness always.

Last but not the least, I can never forget the immense verbal support from the Professors , technicians and friends from the Departments of Physiology, Biology of breathing journal group, Anatomy, Pathology, Oral Pathology and Oral Biology on this project. Many unmentioned names and peronalities are too acknowledged with sincere feeling. I truly wish the sacrifice of animals in our study and the research conducted on them for a tobacco free world may prove worthwhile one day. As for me research experience and education at the Univerisity of Manitoba, Faculty of Dentistry, and Oral Biology was a life's way of teaching me some unlearnt lessons and in bonus it opened the doors to the real journey known as LIFE.

TABLE OF CONTENTS

Abbreviations

% Percentage
2RI Code for second generation of Research index cigarette
AB Acrylamide Bis
AECs Alveoloepithelial cells
ALS Acid Labile Unit
APS Ammonium per sulphate
Approx. Approximately
BAD Bcl-2/Bcl-X_L-associated death promotor
BP Binding protein
BP BladeBarp Parker
BSA Bovine serum albumin
CDC Center for disease control
Circum Circumference
CL Chemilumonescence
CRW Cigarette rod weight
CSE Cigarette Smoke Extract
DD Deionised water
DNA Deoxy ribose nucleic acid
EDTA Ethylene di amine tetra aceticacid
GC Glycine cysteine
GH Growth Hormone
Gm Gram
GRF Growth hormone releasingfactor
HBSS Hanks Balanced Salt Solution
HCl Hydro chloric acid
HRP Horse raddish peroxidase
H2O2 Hydrogen per oxide
Ig Immunoglobulin
IGF1R Insulin-like growth factor receptor Type1
IGF-2R Insulin –like growth factor 2receptor
IGFBP Insulin-like growth factor binding proteins
IHC Immunohistochemistry
IRS-1 Insulin receptor substrate-1
kDa Kilodalton
MCC Mandibular condylar cells
MEM Minimum enriched medium
MTS3-(4,5-dimethylthiazol-2-yl)- 5-(3-carboxymethonyphenol)-2-(4-sulfophenyl)-2H-tetrazolium, inner salt
Na3VO4 Sodium Orthovandate
NaCl Sodium chloride
NADH Nicotine Adenine Dinucleotide Hydrogenase
NADPH Nicotine Adenine Dinucleotide Phosphate Dehydrogenase
NBCS New Born Calf Serum

NC Nitrocellulose membrane
ng Nanogram
NIDA National Institute on Drug Abuse
NSILA Non suppressible insulin like activity
O/N Over night
OD Optical density
PAGE Poly acrylamide gel electrophoresis
PMSF Phenyl methyl sulphonyl fluoride
RIPA Radioimmunoprecipitation buffer
RNA Ribonucleic acid
Rpm Rotation per minute
RT Room Temperature
RTD Resistance to draw
SDS Sodium do decyl sulphate
SMS Somatostatin
Sp1 Promoter specific transcription factor
TBS Tris Buffer Saline
TBST Tris Buffer Saline Tween
TEMEDN,N,N',N'-tetramethyethylenediamine
TMJ Temporomandibular joint
TPM Tar per minute
Tyr Tyrosine
UTR Un translated region
WHO World Health Organization
α Alpha
β Beta
μ Micron

LIST OF TABLES AND FIGURES

ABSTRACT

IGF-1R expression in fetal rat hard and soft tissues in response to cigarette smoke extract

H. Ratia Department of Oral Biology, Faculty of Dentistry, University of Manitoba, Winnipeg, Manitoba R3E 0W2

Introduction: *In utero* development as a whole is a complex process of developing hard and soft tissues. Among the different organ systems, the respiratory system is a complex process involving 40 different cell types. The structure remains unique in its ability to grow throughout and instantly ready to function at the time of birth. The growing fetus receives dual supply of nourishment through its own circulation and amniotic fluid. Detrimental exposure of the fetus to genotoxins in cigarette smoke through the maternal route may cause sufficient damage to the growing embryo. Enough evidence indicates maternal smoking as a primary cause for fetal growth restriction and potential respiratory ailments along with involvement of hormones on negative effects on fetal development (Kapoor et al., 2005). However, among the various hormones involved there has been little speculation over the fetal IGF axis involvement during maternal smoking. Thus this project, through an *in vitro* molecular study, is the first to fill the plausible gaps in research of the fetal IGF axis involved through maternal smoking at the cellular level. In the developing embryo and fetus good evidence supports the role of the Insulin-like Growth Factor (IGF) axis in growth regulation. One component of this axis, IGF-Type 1 receptor (IGF-1R) is a tyrosine kinase receptor and beta subunit of this receptor is essential in cellular proliferation and survival. The present

study is focused on the effects of cigarette smoke extract (CSE) and exogenous IGF-1 on IGF-1R expression in developing rat cells from lungs (soft tissue) and mandibular condyles (hard tissue). **Methods:** Primary cell cultures from two organs, lungs (fibroblasts and Type II alveolar cells (AECs) and mandibular condylar cartilage (fibroblasts) cell types were isolated from Sprague Dawley fetal rats at gestational day 21. Data were derived from 15-18 pooled litters. Isolated cell types were exposed to CSE at dilutions 1-20% for 24 hours. IGF-1R expression was determined by Western blotting. Microscopic imaging was done to assess CSE induced morphological changes. Trypan blue exclusion for cell viability, Crystal violet for cell proliferation and Mitochondrial MTS metabolic studies were done concurrently. Statistical analysis through Duncans multiple range analysis was done. **Results:** IGF-1R is expressed in all cell types. IGF-1R expression profile varies with different concentrations of CSE with different cell types with p values recorded <0.05 relative to the controls. In addition CSE concentrations above 10% for 24 hours of exposure significantly reduced cellular proliferation and viability in a dose dependent manner with $p<0.05$ considered significant compared to the controls. In contrast the receptor expression in fibroblasts from mandibular condyles remained unaffected. **Conclusions:** The level of IGF-1R expression by developing rat lung cell types suggests its importance during cellular replication and differentiation. The cellular exposure to cigarette smoke extract differentially affects developing rat cell viability, proliferation and expression of a major regulator of growth, IGF-1R in different soft and hard tissues. In humans, exposure to primary or secondary smoke products *in utero* may similarly adversely alter fetal cell growth and development. (*Supported by NSERC & MICH*).

1.0 LUNG

1.0.1 Introduction

Lungs are the primary organ of gas exchange and constitute an important part of the respiratory system. Lungs possess a unique relation to connect the internal and external environments. Any injurious stimuli or exposure through the external environment can jeopardize the efficient functioning of the lungs. The effects can be more detrimental through secondary environmental tobacco exposures to the primary smoker and the secondary passive smokers, especially *in utero* developing fetuses.

1.0.2 Prenatal Lung Development

In humans, fetal lung develops in four stages, (Figure 1a) embryonic (4-6 week), pseudoglandular (17 week), canalicular (17-24 week) and terminal sac period (24 week-term) (Boyden, 1974; Hislop and Reid, 1974). During the embryonic period lung bud develops as an endodermal projection and divides to give rise to the right and left lung primordial. By the end of six weeks the bronchopulmonary segments which characterize adult lung can be identified (McClure and Dornan, 1989). During the pseudoglandular stage the proximal, intermediate and distal airways are lined by specialized lining epithelium. Pseudostratified columnar epithelium lines the proximal airways, cuboidal epithelium lines the intermediate, and the distal airways differentiate to epithelial cells (Inselman and Mellins, 1981). By the end of this stage ciliated, non ciliated (pre-clara cells), secretory and early basal types (Inselman and Mellins, 1981) are present. These represent four of the eight epithelial cell types seen in adult lung. At the end of this stage

all the branches of the conducting (non-respiratory) airways is complete (Hislop and Reid, 1974). The canalicular stage is characterized by the transition of distal non-respiratory bronchioles into primitive respiratory bronchioles through the process known as alveolarisation and by development of terminal bronchioles (Murray, 1986). These gas exchange surfaces are known as acini. They are comprised of respiratory bronchioles, alveolar ducts and alveoli. By the end of this stage epithelium differentiates to type I and type II pneumocytes (Inselman and Mellins, 1981). The final stage is the terminal sac period, during this stage there is extensive growth of the alveolar duct system and increase in surface area of the spaces by formation of primitive alveoli or saccules (Hislop and Reid, 1974). With the greater surface area and thinning of epithelium of the saccules brings the spaces in close proximity to the developing capillaries for future gas exchange (Murray, 1986). At birth the epithelial lining is thin and continuous with the two types of alveolar epithelial cells (AECs), type I and II (Inselman and Mellins, 1981). Development of the pulmonary vasculature, capillaries and veins occurs simultaneously with the developing airways. During the early fetal development vessels form by vaculogenesis around the branching airways. In later lung development capillary bed is essential for alveolar formation (Hislop A. 2002). During development fetal lungs expand by a liquid that is secreted across the pulmonary epithelium into the lung lumen (Hooper et al., 1995) and leaves the lung via the trachea (Harding et al., 1986). This process is critical for the normal lung growth.

1.0.3 Post natal lung growth

Postnatally lung grows by formation of alveoli with production and secretion of a variety of substances within the lung. The lung undergoes considerable growth after birth as it is only partly formed in utero. The acini increase in length from 1mm at birth to 1cm in the adult (Hislop an Reid, 1975). The rate of alveolar formation also increases during the first few years of life, although the greatest rate is within the first 18 months after birth (Reid, 1979). The number of respiratory branches and ducts also increase in number until eight years of age. As a result of this further development, the alveolar surface area consequently increases until the adult value is reached by the age of 25 years (Inselman and Mellins, 1981).

1.0.4 Lung Cells

Lungs are made up of 40 different types of cells. Among them mucus producing cells of the airways, alveolar macrophages, clara cells (non ciliated bronchiolar epithelial cells), ciliated epithelial cells, fibroblasts, type I and type II AECs are a few major ones. In the present context we have studied type II AECs and lung fibroblasts for our experimental project and the following section reviews their basic characteristics.

1.0.5 Fibroblasts

The fibroblasts of the lung are derived from the mesenchymal tissues and comprise of the major cell type of the interstitium (Weibel et al., 1976). The major classes of these mesenchymal cells are based on morphology and anatomical location.

These are the interstitial fibroblasts, pericytes, and contractile interstitial cells or myofibroblasts. However the exact origin of these interstitial cells is uncertain. (Franks and Cooper, 1972). It is not known if fibroblasts of mature lung interstitium are distinctly separate cell types from those described above or whether they can transform from one to the other upon appropriate stimulation. Thus, cultured lung cells with the morphological appearance of fibroblasts may actually represent mixtures of the three classes of interstitial cells. Because of the uncertainty some culturists prefer the term "fibroblast like cell" to denote cells with the morphological, cultural, and biochemical characteristics of the true fibroblast (Schaeffer, 1979). The fibroblast is a spindle shaped, elongated cell with a large oval nucleus containing one or more nucleoli (Ross, 1968; Kuhn, 1978). The cytoplasm contains abundant rough endoplasmic reticulum, a well developed golgi apparatus, and numerous mitochondria. A primary role for the interstitial fibroblast is the maintenance of the integrity of the alveolar compartment through its anatomic location and its production of collagens and other matrix components (Bradley et al., 1980; Hance and Crystal, 1975). Types I and III collagen are major secretory products of lung fibroblasts. The connective tissue matrix is composed of 60-65% collagen. The fibroblasts also play an important role during early lung development and maturation of the alveolar epithelium. The fibroblasts produce a pneumocyte factor that stimulates the synthesis of pulmonary surfactant by the alveolar type II cells. This process is regulated by glucocorticoids which induce the production of the fibroblast pneumocyte factor (Floros et al., 1985).

1.0.6 Type II Alveoloepithelial cells

Alveolar type II epithelial cells are one of the two main epithelial cells that line the wall of the alveolus. Type II cells comprise only 15% of the adult lung cells (Crapo et al., 1982). Morphologically type II cells are characterized by cuboidal shape with a diameter of approx. 10μm and a volume of approx. 450-900μm and occupy only approx. 5% of the surface area (Liu et al., 2004). The presence of lamellar bodies store intracellular pulmonary surface-active materials (Williams, 1977; 1978). The functions of type II cells include synthesis, storage, and secretion of pulmonary surface-active material. They also play a significant role in the re-epithelisation of the alveolar wall after lung injury (Liu et al., 2004). Pulmonary surfactant secretion reduces surface tension within the lungs and prevents lung collapse at maximum exhalation (Johansson et al., 1997). It is a complex mixture of phospholipids (approx. 90%) and lung specific surfactant protein (approx. 8-10%) SP-A, SP-B, SP-C and SP-D (Mason et al., 1997). The pulmonary surfactants must transit the aqueous lining layer and adsorb very rapidly into a tensoactive layer within the alveoli (Perez-Gil et al., 1998) thereby facilitating alveoli expansion and prevent collapse at maximum end expiration. The type II AECs is a considered to be the progenitor cell that gives rise to type I cells by division and differentiation (Uhal et al., 1997). Cell shape influence both morphology and phenotypic expression of alveoloepithelial cells grown in culture (Uhal et al., 1997). It is, largely determined by the exertion of intracellular tensile forces onto a substrate through focal adhesion sites regulating AEC differentiation (Sims et al., 1992).

1.1 The Mandibular Condyle

Mandibular condyle is an important constituent articulatory unit of the temporomandibular joint (TMJ) complex which brings about facial growth and movements. During fetal development Meckel's cartilage is the primary cartilage of the lower jaw. Between the 8^{th} and 12^{th} week of fetal life the cone shaped cartilaginous condyle develops at the superior-posterior surface of the bony mandible (Avery, 1992). With the establishment of the complete picture of joint by 12 weeks, subsequent changes in joint structure deal chiefly with growth and development of the joint in preparation for the functional demands placed upon it after birth, and throughout our lifespan (Burdi, 1992). The gross anatomical features of the mandible and the articulating complex are seen in figure 2a. Because of the clinical importance of the mandibular condyle and its developmental anomalies, it is necessary to understand the biological basis for its mode of growth and the regulatory factors involved.

The mandibular condyle is the most important site within the mandible. It is because of its pressure tolerant property which allows for the endochondral enlargement of the mandible in a functional site where intramembranous growth is not possible. Endochondral type of bone growth is required for the posterior-superior growth in the mandibular condyle because of the surface compression involved at the junction of the condyle and the cranial floor (Figure 2a). In other areas of the mandible intramembranous bone growth takes place because of the tensile relationships of the periosteum with the muscles of mastication. For example, the membranes covering the mandibular neck are not under direct surface pressure and bone growth proceeds by

remodeling as a result of endosteal and periosteal activity. This specific function of condylar cartilage is mainly to provide a regional growth mechanism for the localized joint region (Enlow, 1992). Bilateral growth sites of the mandibular condylar heads provide for development from pre to postnatal periods. From the second trimester *in utero* to 25 years of life the joint continues to enlarge, modify, and function as a cartilage covering the heads of the condyles which undergoes continuous remodeling and eventually forms the bone. It keeps pace with the growth of the face and functions during the entire developmental period.

Mandibular condylar cartilage has also been referred to as a *secondary cartilage*. Phylogenetically, the original articular part of the mandible derived from Meckel's cartilage was converted into auditory ossicles. Therefore a new cartilage was secondarily added to carry out this articular function. This probably occurred when the original periosteum in the altered part of the mandible, due the influence of pressure at its new articular contact with the basicranium, was transformed into a cartilage-forming membrane (Hall, 1970). Thus, the mandibular condylar cartilage has also been referred to as secondary cartilage, which developed secondarily after the original primary cartilage was modified for a different function elsewhere in the skull. The mandibular condylar growth process has been compared to the process of growth of cartilages of long bones. The head of the condyle and that of the long bones differ in that long bones form secondary ossification sites. These secondary ossification sites produce epiphyseal lines where lengthening of the long bones occurs (Figure 2c). The head of the condyles accomplish growth like that of a long bone by development of new chondroblasts, with growth of new cartilage matrix and replacement by bone. In long bones cartilage cells

appear to be arranged in long rows adjacent to the cartilage bone junctions. In the mandibular joint cartilage the cells appear scattered (Avery 1992; Bernick, 1994). The genetic capacity of the chondrocyte provides a primary determinant of mandibular growth rate and thickness. Because of the pressure adapted nature of cartilage, it was assumed that the upward and backward growth of the condyle has a resultant push effect against the basicranium, with a subsequent displacement of the entire mandible in a forward and downward direction. This was the classic *condylar-thrust* concept for mandibular condylar growth (Enlow, 1992).

1.1.1 Macroscopic and microscopic anatomy of the mandibular condyle

Condyles are ovoid in shape mediolaterally. They consist of a smooth bony surface covered with a fibrous connective tissue. The condyles grow laterally (Figure 2b) during development.

Histologically, the mandibular condylar cartilage has specialized zones of cellular activity. Superficially the mandibular condylar cartilage is covered with a fibrous zone. Beneath the fibrous layer lies rapidly proliferating prechondroblasts. Deep to the proliferative zone is a region of maturing chondroblasts, followed by calcifying zone and bone (Figure 2d). Due to surface pressure on the condyle and resultant ischaemia, the cells within the fibrous covering of the condyle undergo differentiation into chondroblasts rather than osteoblasts (Hall, 1970). The fibrous layer that covers the condyle is highly cellular early in development but become much denser with increasing age. It is sparsely vascularized. The chondrogenic zone of pre-chondroblasts lies just deep to the fibrous articular layer. This is the major site for proliferative activity within

the condyle (Duterloo, 1967; Meikle 1973). In this region repeated cell divisions result in the posterosuperior growth of the condylar cartilage. The growth occurs by appositional proliferation just deep to the capsular covering with simultaneous removal of cartilage with bone replacement which takes place on the internal side of the cartilage mass. Due to this mechanism the entire cartilage plate moves upward and backward, while allowing bone formation that lengthens the ramus behind the moving cartilage. This process is very specific to the endochondral growth process.The arrangement of cells within the proliferative zone as shown in (Figure 2d) are densely arranged with very little intercellular matrix. This is because of the rapid nature of the proliferative activity. The continued formation of daughter cells does not result in linear columns of cell groups. Thus, the mandibular condylar cartilage is not restricted in capacity for its growth direction. This unrestricted property of growth direction allows for growth changes in other parts of the craniofacial complex. Multiple growth directions in the craniofacial complex allow condyle to adapt to the growth changes occurring elsewhere in the craniofacial complex. However, this is in contrast to the isogenous lines of chondrocytes in the epiphyseal plate cartilages of long bones which follows a unidirectional course of growth. This is important to differentiate the complexity of architectural design of the craniofacial complex in comparison to the long bones. Deep to the proliferative zone of the mandibular condyle lies the region of maturing chondroblasts. There is an increase in intercellular matrix in this zone. However, the cells remain closely packed. The chondroblasts undergo progressive hypertrophy within this zone. In the deepest part, the scanty intercellular matrix undergoes calcification. Beneath the hypertrophied cells lies the erosive zone. In this region chondroclastic

resorption of the calcified matrix takes place. Appositional bone formation occurs within the resorbed areas, and the mandibular neck thereby extends into a region previously occupied by the condylar cartilage. A core of fine cancellous bone located specifically in the medullary part of the condyle and its neck forms as a result of endochondral bone growth. The membranes of the cortical bones in non articular regions of the condyle, and the mandibular neck, are not subjected to compressive forces. Therefore the cortices here are formed by intramembranous ossification (Enlow 1992).

1.1.2 Developmental abnormalities of the mandibular condyle

Congenital and developmental anomalies of the condyle may result from disordered embryonic development. Mandibular condylar anomalies may vary from complete agenesis or induced absence of the condyle, unilaterally or bilaterally to changes in size and shape seen in the growth dysplasias possibly due to hyperplasia and hypertrophy. The time sequence of morphodifferentiation bears an important relationship to the pathogenesis of malformation. The teratogen-sensitive period for most body structures begins at about day 20 of human embryonic development and concludes at about day 45. The TMJ develops late compared to the synovial joints in other parts of the body. When most human joints develop directly to adult form, the TMJ passes through stages in development that are seen in the evolutionary development of the jaw. The time sequence and the course of development of the jaw joint do not reduce the teratogen sensitivity of the developing structures. It is intriguing to understand how a long or complex sequence of developmental stages may enable a joint affected by teratogenic influences to catch up to its normal developmental stage before the full

sequence of differentiation is switched off genetically. The rarity of congenital anomalies of the TMJ in comparison with other human synovial joints suggests that the latter possibility may operate to the advantage of the TMJ, the most essential of human joints. However, there are specific stages in the morphogenesis of the TMJ when the risk of malformation may be high. The first of these coincides with the development of the cartilaginous bar of Meckel's cartilage in the mandibular arch. This condensation occurs in mesenchyme that is derived, to a large degree, from cells that have migrated to the first visceral arch from the neural crest. In the branchial arch, these cells combine with preaxial mesoderm to provide the basis for the visceral arch cartilages. The migration and mixing of the neural crest ectomesenchyme takes place at about day 20 in the human embryo. Any disturbance to the migration or mingling of the neural crest-derived cells may disturb the subsequent differentiation of the mandibular condyle. Developmental failure of tissues or failure of blood supply may result in associated malformations in neighboring parts derived from similar embryological origins. (Poswillo and Robinson, 1992)

1.2 Tobacco smoking

Tobacco smoking world wide is a major public health issue. It is a process of inhaling smoke from burned dried leaves of tobacco plant mostly in form of a cigarette. Currently there are 1.3 billion smokers world wide (Wang and Scott, 2005). Tobacco use causes more than 5 million deaths per year (WHO, 2008; Jacobs et al., 2001). It is estimated that tobacco use will cause more than 8 million deaths annually by 2030 (WHO, 2008).

1.2.1 Maternal smoking

Maternal tobacco smoking is a major concern due to the adverse fetal health outcomes. Currently, at least 10% of pregnant women in US smoke (Martin, 2006). In developed countries like US and other industrialized countries, 18% of women smoke (CDC, 2007). In comparison only 8% of the women smoke in developing nations (WHO, 2001). According to statistics in US from public health service it is predicted that if all pregnant women in the country stopped smoking, there would be an estimated 11% reduction in still births and 5% reduction in new born deaths (CDC, 2004).

1.2.2 Smoking and hormonal influence

Smoking may affect maternal and fetal hormonal balance (Kapoor et al., 2005). Smoking in general affects various hormone secreting organs such as pituitary, thyroid, adrenal, testicular and ovarian function. Calcium and insulin metabolism are also affected resulting in insulin resistance and type-2 diabetes mellitus. Smoking increases

risk and severity of Graves hyperthyroidism and ophthalmic disorders, osteoporosis and reduced fertility (Kapoor et al., 2005).

1.2.3 Maternal smoking and hormonal influence

Cigarette smoke is primarily composed of more than 4000 different carcinogenic compounds. Increased catecholamine production due to maternal smoking may result in underperfusion of the foetoplacental unit (Kapoor et al., 2005). Cigarette smoke constituents expose the developing fetus through both amniotic and blood circulation.

A study of Insulin-like growth factors profile in pregnant smokers did not find sufficient links between the maternal and infant serum levels of IGF-I and IGFBP-3. However, lack of receptor assessment and other components of the IGF axis cannot be ignored to assume the lack of negative involvement of IGF axis in fetal development exposed to second hand smoke (Ehrnis et al., 2004).

Cigarette smoke is primarily composed of gaseous (carbon monoxide) and particulate matter (tar). Among the different constituents within the tobacco smoke, tar, nicotine, cotinine-metabolite of nicotine and carbon monoxide have attracted greater attention. Carbon monoxide and nicotine from tobacco smoke may interfere with the oxygen supply to the fetus. Nicotine also crosses placenta, with concentrations in fetus reaching as much as 15% higher than maternal levels (Huizink and Mulder, 2006). Tar in cigarette varies from 15mg for a regular cigarette to 7mg in low-tar cigarette. Exposure to these constituents increased the risk of lung cancer, emphysema, and bronchial disorders (NIDA, 2006).

1.2.4 Maternal smoking and compromised fetal pulmonary function.

Exposure to maternal tobacco smoking or environmental tobacco smoke in the first few years of life persist into childhood and may affect the pulmonary function attained throughout the child's life (Cunnigham, 1994). Exposure to cigarette smoke constituents in developing fetus causes airway hyper responsiveness, decreased lung function, airway obstruction postnatally (Joad, 2004), reduced fertility in female off springs by two-thirds (Jurisicova et al., 2007) and reduced sperm count among male fetuses (Fowler et al., 2008) . Higher occurrence of respiratory illnesses in infants born to smoking mothers within the first year have been reported (Janoff et al., 1987). Upon inhalation, cigarette smoke crosses the layers of the respiratory epithelium as shown in figure 1b (Wang and Scott, 2005). This figure shows the paths via which the cigarette smoke reaches from respiratory to circulatory system. On the way to the alveoli, tar and particles precipitate changing the composition of cigarette smoke. Cigarette smoke might pass the lung-blood barrier by free diffusion (gases) or via cellular transport mechanisms for water, ion, macromolecules or other chemicals through the hydrophilic and hydrophobic cellular layers. On a cellular level cigarette smoke exposure is detrimental to the cellular cytoskeleton, proliferation, attachment and detachment of alveolar epithelial cells (Lannan et al., 1994). Alveolar cells exposed to whole cigarette smoke extracts are shown to have DNA damage, decreased surfactant secretion and collagen production (Lannan et al., 1994; Leanderson et al., 1992). Genetic predisposition to adverse fetal development to tobacco exposure is also well documented (Kabesch et al., 2004; Hong, 2003).

1.2.5 Maternal smoking and craniofacial defects.

Even though respiratory and intra-uterine growth retardation abnormalities are recognized fetal complications of maternal smoking, there is enough evidence of maternal smoking affecting negatively the cranio-facial structures of the developing fetus resulting in hydrocephaly, microcephaly, (Hassib, 2006). More specific associations with orofacial cleft lip and cleft palates (Lammer et al., 2004; Little et al., 2004; Hartsfield et al., 2001) have been reported. Craniofacial structures are a composite of bones and muscles forming a synchronized functional complex. Cigarette smoking is known to affect bone density in smokers (Godfrey et al., 2001) and probably of the fetus as well. Smoking is known to affect the developed periodontium adversely. Therefore exposure to smoke agents during intrauterine life may predispose the developing fetus to increased risk of osteoporosis (Javaid, 2003), and fractures of cranio-facial and other bony defects thereby jeopardizing functional efficiency of the developing system.

1.3 Insulin-like growth factors-IGFs a review

1.3.1 Evidence and Terminology

Extensive research conducted in the early 1900's to understand the basis of growth in living organisms led to the discovery of growth hormone (GH) in 1921 (Evan and Long). It was not until 1957, when IGFs were first proposed as "Sulphation factor" (Salmon and Daughaday, 1956) based on studies that confirmed that GH did not directly uptake sulfate into cartilage but acted indirectly through its action on a substance present in the serum (Salmon and Daughaday, 1957). Later "Somatomedins" was the proposed designation for "sulfation factor" based on the evidence that somatotrophins (GH) released substances from the pituitary (Daughaday et al., 1972). In further categorization ,Somatomedin C was the designated terminology for somatotrophins responsive to somatomedins (Daughaday et al., 1972). Researchers working on different biological systems discovered polypeptides in serum similar in action to insulin. Subsequently it was found that insulin activity in serum was not suppressible by addition of anti-insulin serum. This activity was referred to as "NSILA" (non suppressible insulin like activity) (Burgi et al.,1966; Jakob et al.,1968). Recognition of sulfation factors, somatomedins & NSILAs in different biological systems resulted in considerable debate as to weather these substances were related or were different proteins (Etherton, 2004). Finally chemical characterization (Klapper et al., 1983) of these factors revealed their close structural homology to proinsulin and hence termed them as insulin-like in the late 1980s (Daughaday et al., 1987).

1.3.2 Physiology of the IGF System

In animals normal tissue regeneration and response to injury can be attributed to growth promoting substances such as, growth hormones and associated growth factors. Insulin-like growth factors (IGFs) comprise of a family of polypeptides that mediate growth promoting effects of growth hormones (GH). The IGF axis includes two ligands (IGF-1, IGF-2), two receptors (IGF-1R, IGF-2R) and the six insulin-like growth factor binding proteins (IGFBP). IGFs are important growth promoting substances produced from the liver, which is a predominant source of IGFs (Figure 3a). During fetal and postnatal life, IGF ligands augment the effects systemically and locally through the IGF receptors and binding proteins expressed in most tissues during embryonic development.

a. Modes of Operation of IGFs

IGF-1 and 2 are single polypeptides that share a high degree of homology with proinsulin. They functions through the cell surface receptors primarily the type 1 IGF receptor. It is a tyrosine kinase cell surface receptor with signaling intracellular domains. IGF-2R is a single large transmembrane receptor. It is not a typical signaling receptor in response to ligand interaction and acts as a clearance receptor for IGF-2 ligand (Holly, 2004). The mechanism for making IGF available for action in tissues is interplay among IGF ligands, receptors and binding proteins. Upon secretion in circulation from the liver majority of the IGF is associated with IGFBP-3 and the acid labile subunit (ALS) which is a large glycoprotein. The binding affinity of IGF ligands to binding proteins is 20-50 fold greater than IGF-1R (Cleemon, 1997). IGFBP is distributed in interstitial fluids, cell surfaces, extracellular materials and cell surface receptors. The ALS binds to the C-

terminal region of IGFBP-3 and the ALS. The ALS binds to a C- terminal region of IGFBP-3 that also binds to proteoglycans present on cell surfaces and in the extracellular matrix (ECM). It is also possible that proteoglycans on the surface of the capillary endothelium compete for binding to IGFBP-3 and displace the ALS generating a binary complex from the ternary complex (Holly, 2004). Therefore the binary complex would then be able to cross the endothelium and transport the IGF into the tissue. This ternary complex slows the clearance even more such that in adults a total IGF-1 and IGF-2 concentration in circulation is around 100 nM. This concentration is 1000 times higher than insulin and most peptide hormones. In the tissues IGF concentrations are around a third of that in the circulation. It is still a large excess over that needed for cell regulation. Other mechanisms, where proteases act on binding proteins has been discussed in the literature for controlling regulated delivery of IGFs from the circulatory reservoir (Holly, 2004).

b. Similarities and Differences between IGFs and Insulin

Due to close association of IGFs to insulin we have reviewed a few distinguishing features among the two families which make them separate independent entities. IGFs are widely expressed throughout the body. IGFs are not stored within the secretory granules in the cells but are secreted as they are produced through constitutive secretory pathways. In contrast, insulin is restricted to beta cells in the pancreas. It is stored in secretory granules within the cells of pancreatic islets and secreted via the regulated mechanisms in response to stimuli. Insulin in circulation passess around the body until it encounters its cell receptor in target tissue. On the contrary, IGFs do not

circulate freely but is in a bound form with the soluble high affinity binding proteins (IGFBPs). The binding proteins bind the IGFs and therefore slow their clearance. This enables very high concentrations of IGFs to build up (Holly, 2004). Genetically genes for IGF-1 and insulin are homologous and probably arose from a common ancestor. IGF-1 gene is located on chromosome 12 and insulin on 11. Both share 45% amino acid homology. However C-peptide region of IGF-1 bears no homology with the proinsulin C-peptide and is not cleaved from the molecule as occurs in proinsulin processing (Laron, 2004). The promoter region of transcription machinery of IGF-1R lacks TATA or CAAT motifs and transcription starts from a unique site contained within the initiator motif whereas transcription of insulin receptor gene which also lacks TATA and CAAT boxes start from multiple sites (Le Roith et al., 1995). The IGF-1 receptor is closely related to the insulin receptor and binds IGF-1 with high affinity and insulin with low affinity (Laron, 2004). IGF-1R is similar to insulin receptor in its tyrosine kinase domain and share a overlap in their intracellular signaling mechanism These receptors exist as dimers within the cell surface but due to close similarity in structure there is a possibility that in cells where both IGF-1R and insulin receptor are expressed the receptor undergoes heterodimerization forming the hybrid IGF-1/Insulin receptors (Kim and Accili, 2002). Optimum regulation of IGF-1R is achieved with just 1-2nM at the cellular level indicating the vast excess in circulation (Holly, 2004).

c. Biological effects of IGFs

Based on experimental evidence it is proved that IGFs are ubiquitous. They have diverse biological effects on tissue repair, regeneration, antiapoptotic and others. IGF-1

is synthesized in multiple animal and human tissues (D'ercole et al., 1980; Han et al., 1988). IGF-1 produced in animal tissues in cultured explants of fetal mouse tissues in serum free medium raised the possibility of autocrine and paracrine actions at the site of origin (D'ercole et al., 1980). Animal studies were further confirmed in humans, where expression of IGF m -RNA was observed in multiple human fetal tissues, confirmed through Northern blot and dot blot analysis (Han et al., 1988). Further experimental evidence has confirmed retarded growth and death after birth in IGF transgenic animal models (Liu et al., 1993, Le Roith et al., 2001). On the other hand autocrine and paracrine nature of tissues was suggested and found that hepatic IGF-1 is unimportant for sustaining normal growth and this was proved within a mouse model with deleted liver IGF-1 gene, even though serum IGF-1 levels were reduced by approximately 75%. Thus, it was confirmed that liver, though a major source of IGF-1 production is not the sole site of synthesis and provided direct evidence for locally produced IGF-1 (Yakar et al., 2001).

1.3.3 Insulin-like growth factor-1 receptors (IGF-1R)

It was not until the early 1980s that IGF-1 receptors were identified. It was observed that explants from animal tissues released immunoreactive IGF-1 in cultured media and a large portion of it was recognized by cell surface receptors specific for IGF-1 (D'ercole et al., 1980). The majority of the physiological actions of IGFs occur via IGF-1 receptor activation upon dissociation of IGF from IGFBP.

a. *IGF-1R Gene Structure*

Human IGF-1R is located on the distal end of chromosome 15 (q25-26).This gene is more than 100kb in length and contains 21 exons.

b. IGF-1R Functional domains, promoter region and transcription factors

Functional domains

IGF-1R organized into functional domains, with exonic arrangement corresponding to the alpha and beta subunits respectively (Figure 3b). The exons 1-3 code for 5'UTR, signal peptide, non cysteine rich terminal and cysteine rich domain of alpha subunits, mainly involved in ligand binding at the cysteine rich domain. Exon 4-10 encodes the remaining alpha subunit. Exon 11 encodes the peptide cleavage site that generates alpha and beta subunits from a polypeptide precursor molecule. Beta subunit with tyrosine kinase domain encoded by exon 16-20 demonstrates highest amino acid identity between IGF-1 and IGF-1R (80-85%). Exon 21 contains extensive 3'UTR sequences approximately 5 kb in length (Le Roith et al., 1995). *IGF-1R m RNA* contains a vey long (approx. 1kb) 5'-UTR. Since the coding region of IGF-1 receptor m RNA spans approx. 5.1 kb, it can be concluded that this transcript contains an approx. 5kb 3'-UTR. Research on IGF-1R gene suggests that IGF-1R gene encodes one of the longest 5'-UTRs described to date in eukaryotic genes (Le Roith et al., 1995).

c. IGF-1R Promoter region and transcription factors

The IGF-1R promoter region lacks TATA/CAAT box that is generally required for the accurate positioning of transcription machinery and for efficient transcription initiation (Figure 3c). Transcription in the absence of TATA box/CAAT box is initiated from a unique site contained within an initiator motif (Smale and Baltimore, 1989). The

initiator is a discrete promoter element that can direct specific transcription initiation from an internal site in the absence of TATA element. The IGF-1R promoter is GC rich (80%) and contains several binding sites for members of the Sp1 family of zinc-finger nuclear proteins. IGF-1R promoter activity was extremely low in Sp1 null Drosophila-derived Schneider cells, while co-transfection of an Sp1 expression vector significantly enhanced promoter activity. Analysis of physical and functional interactions of Sp1 at the promoter revealed that Sp1 is a potent transactivator for IGF-1R gene (Sarfstein et al., 2006). The transcription of IGF-1R gene is negatively regulated by a number of tumor suppressors, including the breast cancer gene-1 (BRCA1), p 53, and the Wilms' tumor protein-1 (WT1). Transcriptional suppression of the IGF-1R gene may be responsible for IGF-1R levels below a certain threshold. Thus the interactions between stimulatory and inhibitory transcription factors perhaps determine the level of expression of the IGF-1R gene and, consequently proliferative status of the cell (Safstein et al., 2006).

d. IGF-1R protein structure, trafficking and signaling

Protein structure

IGF-1R is a single precursor molecule with 1367 amino acids. It contains 30-residue signal peptide followed by alpha and beta subunit sequences and a cleavage site. The cleavage site of proreceptor is the basic tetrapeptide Arg-Lys-Arg-Arg (residues 707 710). Proteolytic cleavage results in a separate alpha and beta subunits joined by disulphide bonds. The mature receptor is a heterotetrameric complex with $\alpha 2\beta 2$ configurations (Figure 3d).The alpha subunit is completely extracellularly placed and

contains a cysteine rich domain encoded by exon 3 and 11, potential linked glycosylation sites. IGF ligand binds to the cysteine rich alpha subunit. The beta subunit is a 24 residue hydrophobic transmembrane domain with short extracellular region and a cytoplasmic tyrosine kinase domain (residues 973-1229). The juxta membrane region has a low density lipoprotein receptor which is important for receptor internalization. The tyrosine kinase domain is highly conserved evolutionarily. A highly conserved motif is glycine rich segment (Gly-X-Gly-X-X-Gly) on residues 976-981 in the catalytic region assumed to anchor and orient the phosphate moiety of ATP for transfer to subcellular substrates (LeRoith et al., 1995).

e. Trafficking and Signaling Mechanism

The IGF-1R undergoes ligand-induced autophosphorylation. The major sites for phosphorylation are the clustered tyrosines 1131, 1135 and 1136. Another phosphotyrosine is located at position 950 and two distal to tyrosine kinase domains at residues 1250 and 1251 (Le Roith et al., 1995). Receptor mediated endocytosis governs the entry of receptors inside the cells. Tyrosine kinase receptors e.g. IGF-1R are initially located outside the internalization gates (the clathrin-coated pits) and concentrated on the thin digitations of the cell surface, the microvilli (Carpentier et al., 2004). Upon activation receptors are translocated from surface domains where they are present in an unoccupied state towards the surface areas where the clathrin-coated pits are present (Carpentier et al., 2004). The receptor localization on microvilli might be dependent, on their tight coupling to the cytoskeleton. However, little information is available on the cytoskeletal partner involved in IGF-1R localization on microvilli. Fission of the neck

membranes with constricted clathrin coated pits forms free cytoplasmic clathrin-coated vesicles. The coat constituents are then released to allow for heterotypic membrane fusion with endosomal compartments. The acidic pH of endosomes allows the dissociation of ligands from their receptors and sorting in different directions. Classically, dissociated ligands are targeted to lysosomes, where they are degraded, while membrane receptors are recycled back to the cell surface where they can be reused. However the dissociation of IGF-1 from its receptor is slow at low endosomal pH. Therefore, the fate of IGF-1R coupled to its ligand in endosomes is unclear (Carpentier et al., 2004). Additional mechanisms like ligand-induced ubiquitination may regulate the degradation of activated IGF-1R. The ubiquitin-proteasome system is a well recognized regulator of endocytosis for selected membrane receptors in order to degrade signaling molecules and control the magnitude of signaling events. However, it still remains to be established by how much the ubiquitin-proteasome pathway may contribute to the ligand-induced IGF-1R internalization and termination of IGF-1 induced signaling. The process of internalization rate and the rate of recycling determined are dependent on the number of receptors present on the cell surface and hence their availability for ligand binding. This is crucial for determining the cell sensitivity to circulating hormones (Carpentier et al., 2004).

The IGF-1R mediates mitogenic biological functions for growth and proliferation when ligands bind to the receptor present at the cell surface. Ligands bind to the alpha (α) subunit of the receptor and initiate a series of events that result in autophosphorylation of the receptor via its tyrosine kinase activity (Figure 4). This causes the interaction with certain major cellular substrates such as IRS-1 and Shc that

mediate the mitogenic and antiapoptotic signals to the cell nucleus controlled by the IRS-1/PI-3'-kinase/Akt/p70 pathway (Figure 4). This pathway is also essential for the regulation of cell size increase, which is required for the predisposition of cells to mitosis. The concluding step, which reduces apoptotic effect is phosphorylation of BAD is one of the members of Bcl-2 family of proteins, phosphorylated by Akt. (Guerreiro, et al., 2006). Issues on spatial and temporal activation of IGF-1R in signaling still remain a challenge to be established (Carpentier et al., 2004).

1.3.4 IGF system in embryonic lung development

IGFs are involved in both prenatal and postnatal growth. The IGF-1R mRNA is present in low abundance with highest levels of receptor IGF-1 m RNA seen at the embryonic stages and subsequently decreases to a much lower level in adult animals. In adult rats, highest levels of m RNA were observed in the CNS with intermediate levels in kidney, stomach, lungs, testes and heart (Werner et al., 1990). No expression of IGF-1R is seen in liver, tissues with highest levels of IGF-1 m RNA and peptide (LeRoith et al., 1995). With respect to lung embryonic tissues, IGF-1 is predominantly expressed during saccular and alveolar stages of lung development, with a peak in IGF-1R mRNA. Insufficiency in receptor expression leads to perinatal respiratory failure perhaps due to poorly formed alveoli (Liu et al., 1993). Studies have shown the predominant role of IGF-1R action in mouse fetuses that are homozygous for IGF-1R deficiency. They are severely growth retarded (approx. 30% of normal weight) and die at birth due to inadequate cellularization of the lung musculature (Roberts, 1996). IGF-2 is predominantly expressed in pseudoglandular and canalicular stages of lung

development. These levels decrease as the lung matures (Hooper and Wallace, 2004). The IGF-BPs 2, 3, 4 and 5 are distributed spatially and temporally during lung development suggesting cell specific regulation (Billie et al., 1995). IGFBP-2, type-2 receptor and IGF-2 ligand are associated with negative control of alveolar epithelial cell proliferation during lung development (Mouhieddine et al., 1994). On a cellular level based on *in-situ* hybridization analyses, both IGF-1 and IGF-2 m RNAs are expressed by cultured fetal lung fibroblasts, mesenchymal and pleural cells in fetal lung. IGF-1R receptor has been shown to be expressed by adult tracheal epithelial cells, type II AECs, A549 lung tumor cell line and fetal lung fibroblasts. IGF-2 receptor is also expressed in fetal lung (Moats-Staats et al., 1995). Thus lung development is a complex process with all the components of IGF axis involved to bring about remodeling and growth.

1.3.5 IGF system in mandibular condyles

In our present project we studied the effect of IGF-1 hormones in mandibular condylar cells in combination with cigarette smoke extracts in an *in-vitro* study model to bridge the gap between plausible possibilities of IGF axis in the condylar region affected by maternal smoking. Based on the literature endocrine disturbances in animals have a profound effect on condylar growth (Ware and Fujimoto, 1992).

Developmentally condylar cartilage of newborn rats is similar to that of 12-14 week old human fetus (Durkin et al., 1973). The condition in the condyles of newborn and very young rats, when compared with that in primates, represents a late fetal stage, rather than a true post-natal stage (Luder, 1993). Growth of skeleton and soft tissues is regulated by complex interplay of hormones and hormone-like substances, growth factors. The

localization of IGF-1R in the mandibular condyle is area specific in the TMJ to the superior and posterosuperior regions of the condylar cartilage in the fibrous articular surface of the condyle. Animal studies have shown that early post natal growth and development of the mandibular condylar cartilage may be IGF-1 dependent but not directly dependent on growth hormone (Visnapuu et al., 2001). Absence of growth hormone receptors in the condylar cartilage of young rats explains the independent action of IGFs (Visnapuu et al., 2001).

In the mandibular condyle of the young rat, mitotic activity occurs not only in the undifferentiated cells but also in the differentiated chondroblasts of the proliferative layer. At a later age, the chondroblasts are no longer dividing in the condylar cartilage (Visnapuu et al., 2000). Therfore it may be expected that undifferentiated cells constitute the target of Growth hormone in later ages (Isaksson et al., 1985; Lindahl et al., 1987; Barnard et al., 1988). *In vitro* examination of the mandibular condyle of neonatal mice indicates that the production of IGF-1 is parallel to the distribution of IGF-1 receptors, both being located in the chondroprogenitor and chondroblast layers (Maor et al., 1993). IGF-1 is proposed to be a potent chondrogenic agent which constitutes a fundamental factor in the tissue-separating morphogenic capacities of various cartilage containing structures including the mandibular condyle (Peltomaki et al., 1997). Experimental studies on rats on the mandibular condyle have found mandibular cartilage to be more sensitive to IGF-1 therefore stimulating condylar growth (Delatte, 2003).

1.3.6 IGF system as a therapeutic target

Strong links exist between circulating IGF-1 concentrations and risk of developing cancers. High concentrations of IGF-1 in an individual may be associated with increased risk of developing colorectal, breast or prostate cancers. On the contrary, low levels of IGF-1 concentrations may be associated with increased risk of cardiovascular disease, cognitive decline and predisposition to osteoporosis. The signal transduction from activated IGF-1R regulate cell proliferation and survival. The most common findings associated with deregulated IGF signaling are over expression of the IGF-1R and establishment of autocrine or paracrine signaling loops. The signaling pathway of the IGF-1R signaling mechanism may serve as target sites for development of new therapeutic approaches. IGF-1R fulfills several criteria for an ideal pharmaceutical target of cancer chemotherapy. It plays a crucial role in malignant transformation and tumor progression. The components of IGF system are differentially expressed in tumors compared to normal tissues (Guerreiro et al., 2006). The receptor and its ligands are easily measured in clinical samples. Various therapeutic strategies that target IGF-1R have demonstrated remarkable antitumor activity in tissue cultures and in mouse models of cancer. As more new molecular techniques will advance in the near future, more hormones, receptor and factors involved in processes will be identified. This will allow us to understand the effects of hormones on same and different tissues to the point of developing new therapeutic approaches to produce a physiologically significant outcome.

2.0 Material and Methods

2. 1 Materials

The following materials were purchased from the following companies. Gestational day 21 pregnant rats from Animal Care Facility University of Manitoba, Winnipeg Canada. Sodium pentobarbital (Euthanyl) Bimeda-MTC Animal Health Inc. Cambridge Ontario Canada, Hanks Balanced Salt Solution Self prepared, Antiobiotic-Antimycotic, Fungizone, Basal minimum enriched media, New Born Calf Serum, 0.5%Trypsin-Edta 10x Gibco (Burlington, ON, Canada), Tissue culture supplies (Corning costar, Fisher Scientific), Carbon, Crystal Violet stain (Fisher scientific Inc.), IGF-I Recombinant ligand, Collagenase (Sigma Chemical St.Louis, MO), Kentucky research centre research cigarettes 2RI (Kentucky Research Centre), Mini complete protease inhibitor table EDTA free, Roche, Bis Acrylamide 30%, Biomax KDKX-OMAT Films Kodak (Thermo Fisher Scientific). Precision stained molecular weight marker, BSA Lyophilised protein assay kit, Gel casting apparatus, Western Blot Transblot module, Gel Drying Cellophanes, Gel Drying Apparatus (Bio rad Missisauga Inc.) , APS, SDS, Glycine, 40%AB Acrylamide Bis 37.5:1, Temed, (Thermo Fisher Scientific Inc.), IGF-IR Tyr 1135/36 rabbit mono clonal phospho antibody (Cell signaling Inc.), IGF-IR beta C-20 Rabbit Polyclonal sc-713 Santa Cruz, IGF-IR alpha N-20 Rabbit polyclonal sc-712 ABC Immunohistology Kit (Santa Cruz, Bio technology Inc. California, USA), Beta Actin antibody mouse monoclonal Abcam, BSA Protein standards, Restore stripping buffer, Chemiluminescence ECL kits (Pierce, Fisher Thermoscientific), Jouan low speed centrifuge, Beckmans Ultracentrifuge C8-70M SW 28 rotor), Fisher scientific 550 sonic disemberator, MicromaxRF Thermo IEC Centrifuge, Alpha Ease Software Infotech.

2.2 Animal model and cell cultures

2.2.1 Lung Fibroblasts

To isolate fetal lung fibroblasts, we purchased gestational day 21 timed pregnant Sprague Dawley rats (Full term 22.5 days) from Central Animal Services University of Manitoba. Pregnant rats were sacrificed by intraperitoneal injection with 1ml Euthanyl (240 mg/ml sodium pentobarbital). Death was confirmed by the absence of pedal reflex. Thereafter the rat was scrubbed with 70% ethanol aseptically and using a sterile BP blade # 21 a vertical incision across the abdomen was placed to extract the fetuses intact from the uterus. Under aseptic conditions fetuses were decapitated and separated from the umbilical cord and immersed in Hanks Balanced salt solution (HBSS). Fetuses were counted. On average a gestational day 21 pregnant rat bore 15-18 rat pups. Under a tissue culture hood using sterile surgical forceps and blade a fine incision was placed on the thoracic region extending from the mid sternal region extending to the diaphragm, thereafter with a fine sharp pair of scissors, ribs were cut across exposing the upper thoracic rib cage with a pair of surgical tweezers in a locked position. The lungs were removed *en bloc* with the heart and trachea attached. Thereafter the lungs were placed in HBSS until all the lungs were dissected out. The lungs were cleaned from the trachea, bronchi, heart and any contaminating fetal tissues. The cleaned lungs were rinsed in HBSS before they were minced finely with a flat Sorval tissue blade into small chunks; this was followed by digesting with Trypsin-EDTA: HBSS in 1:9 dilution to dissociate the cells from in a self stirred glass module bottle for 45 minutes at 37 °C. The minced lung tissue was sieved through 3 nitex gauze filters of 150 μm thickness in a sterile

bottle. To stop the enzymatic action NBC serum (10%) and antimycotic-antibiotic (1%), fungizone (1%) at 250 μg/ml concentration substituted MEM with 2.2mg/ml $NaHCO_3$ was added. The suspension was aliquoted in sterile corning tubes and centrifuged at 1100 rpm (250g) for 10 minutes in a Jouan centrifuge. The pellet was resuspended in 6 mls of NBCS supplemented MEM based on the cell count. Cells were counted on a Beckmans Coulter counter, and plated at density of $3x10^6$ cells per $75cm^2$ flasks at 5% CO_2, 37°C, and 100% humidity. From 15-18 pooled litters usually a mixed population of 40 different lung cells types is averagely estimated as 3.4x 10^6cells/ml. Following two hours of initial plating, fibroblasts adhered to the plates. The supernates were collected for isolation of fetal type II AECs as described subsequently. After 24 hours, media were changed and subsequently every two days thereafter. Fetal lung fibroblasts came to confluence within two days of plating which also depends on the density of cell plating. A similar protocol was followed for culturing cells from postnatal rat lungs.

2.2.2 Type II AEC isolation

To isolate type II alveoloepithelial (AECs), following the initial two hours of fibroblast adherence, the supernate media were aspirated and based on the cell count plated in 25 cm^2 flasks at a cell density of $1.5x10^5$ per flask incubated in 5% CO_2 and 37°C. These cells were deprived of growth factors responsible for fibroblast growth therefore media supplemented with 10% carbon stripped serum. Carbon was added for stripping the growth factors at a concentration of 60 mg/ml O/N at 4°C and subjected to 3 cycles of high speed centrifugation at 25000 rpm for 1 hour and 30 minutes at 4°C in Beckmans Ultracentrifuge C8-70M SW 28 Rotor. Antibiotics and fungizone were added

to culture the type II AECs. Type II AECs grow in colonies and display a cuboidal cobble stone shaped morphology. The purity of the cultures is 95% as determined by previous studies in our laboratory. The colonies reach near confluence by 5-7 days following which they are subjected to 24 hour serum starved condition followed by specific cigarette smoke extract treatments (CSE) and harvested through appropriate experimental protocols. Type II AECs were harvested in passage zero (P0) stages and are not passaged in contrast to the lung fibroblasts.

2.2.3 Mandibular Condylar Fibroblasts isolation

Morphologically fetal rat mandible is similar to human mandible. At gestational day 21 fetal rat mandible possesses a body, and three projections representing the condyle, coronoid and angular process of the mandible. To isolate the fetal rat mandibular condylar fibroblasts we followed the protocol established in our laboratory to isolate fetal condylar fibroblasts from rabbits. However, the size for gestational day 21 fetal rat mandibular condylar projections are within 1 mm medio-lateral and anteroposterior dimensions. The anatomical features are clearly developed and demarcated. Decapitated heads from gestational day 21 fetuses under sterile conditions using a sharp BP blade # 4 were placed in sterile calcium, magnesium free HBSS. An incision was placed at the preauricular region in imaginary extension at 30 degrees to the crossection angle of the mouth and the outer canthus of the orbit. With a quick snip at the incision the three projections were separated from the superficial fascia and deep fascia. The condyle at the neck were snipped out and stored in sterile HBSS. The dissected mandibular condylar heads were incubated with 0.5%/0.01% trypsin-EDTA

for about 30 minutes for complete dissociation of the ground matrix. The mandibular condyles were then inverted on the sterile gel foam sponges soaked in 10% NBCS MEM and incubated at 37 °C and 5% CO_2 for one week. Thereafter the sponges were separated from the condyles and dissolved in 0.02% collagenase in HBSS for 15 minutes. To stop the trypsinisation action NBCS supplemented media was added. Cell count was done with Neubeurs Haemocytometer from 15-18 pairs of mandibular condyles. The cells were plated accordingly in 25cm^2 flasks and then passaged further to 75cm^2 flasks at 5%CO2 and 37 °C. This method was implemented to isolate mandibular condylar cells from all the animals.

2.2.3.1 Histological Verification of Ingrown cells in gel foam sponges

To verify visually the process of ingrown mandibular condylar fibroblasts, we processed the gel foam sponges with ingrown cells in Karnovsky fixative (4% paraformaldehyde, 2.5% glutaraldehyde in 0.1M Phosphate Buffer, 8% sucrose PH7.2-7.4) for plastic sectioning of the gel foams at 6μm thickness and counter stained it with eosin and haematoxylin to visualize the fibroblast like cells. The mandibular condyles were processed separately and in comparative morphology to the mandibular condyle from the adult Sprague Dawley rats bilaterally.

2.3 Cigarette Description and Cigarette Smoke Extract (CSE) Treatments

Unfiltered cigarette 2RI (2RI is the subsequent research cigarette designation equivalent of the 1RI research cigarette manufactured in 1974 in Kentucky Tobacco Research and Development center) were used in the present study. Reference cigarettes

physical charactersistics are described in the Table 1. Cigarette smoke extract was prepared according to apparatus designed by Janoff and Carp, 1978 for CSE preparation. The solution was considered to be 100% CSE and stored at -80° C and adjusted to a pH 7.2 before application in cultures at dilutions of 1, 5, 10 or 20%. Optical density for CSE was scanned on a broad scale wavelength of 190-1100nm spectrophotometrically. Whole 100% CSE from one cigarette was subjected to gas chromatographic analysis Varion 320MS TQ 3900 Gas Chromatograph to analyze nicotine content at Manitoba chemical analysis laboratory against set standard of nicotine prepared in serial dilutions from 1.0 M nicotine concentration. The specifications for the GC column were as follows, VF-5ms, 30m, 0.25mm, Df=0.25µm. The oven program was 110°C for 3 minutes; 25°C/min to 270°C. The injector was operated in splitless mode at 265°C.

2.4 Protein Extraction

Isolated fetal fibroblasts and type II AECs treated with different concentrations of CSE were washed with HBSS three times. Monolayers of cells were lifted from culture plates in trypsin. Trypsin enzymatic action was neutralized with NCS in MEM. The cells suspension was centrifuged at 1100 rpm for 10 minutes. The cell pellet was homogenized in modified RIPA buffer in the presence of protease inhibitor cocktail (1 complete mini tab /10ml of extraction solution), 50mM Tris HCl pH 7.4, 1%NP 40, 150mM NaCl, 1mM, EDTA, triton X100, Na_3VO_4 1mM and SDS and 1mM PMSF for elution of transmembrane proteins. The cells were sonicated three times using sonicator at a pulse of three for 30 seconds (Fisher scientific 550 sonic disemberator) and centrifuged at 15,000 rpm (MicromaxRF Thermo IEC Centrifuge) for 15min at 4° C.

Supernates were collected and stored at -80 ° C until samples were prepared for SDS gels.

2.4.1 Determination of protein concentration

For each CSE treated concentration for 24 hours, total protein was collected from three independent samples and the concentration of each biological replicate was determined by Bradfords protein determination method using the Bio Rad protein assay kit (Bio Rad, Missiauga, Ontario). The Bradford assay is a dye based colorimetric method of quantitation of proteins where acidic Coomassie dye binds to basic proteins thereby producing a change in color which is read spectrophotometrically at 590 nm absorbance. Protein samples were collected in highly concentrated state, BSA stock standards of 2mg/ml prepared from lyophilized Bio-Rad BSA extract and 1µl RIPA buffer added to each BSA standard. To each sample 200µl of Bradford protein assay dye reagent concentrate was added. Tubes were gently vortexed and incubated at room temperature for 5 minutes. The BSA standards were used at concentrations of 1 µg/ml, 5 µg/ml, 10 µg/ml, 15 µg/ml, 20 µg/ml, 25 µg/ml, and 30 µg/ml. The absorbance was measured at a 595nm and a BSA standard curve plotted using Softmax pro software.

2.4.2 SDS-PAGE Western blotting for Native Expression of IGF-1R

To detect the presence of high molecular weight protein IGF-1R endogenous β subunit (200/97kDa), we performed, under reducing conditions and also under non-reducing conditions. Precision prestained broad range high molecular mass standards was used as molecular mass markers. 50µg protein samples were boiled for 5 min in

presence of 4x reducing sample buffer diluted to 1:4 in unknown samples.(4x reducing buffer contained 0.5ml Tris HCl pH 8.8, 0.8ml glycerol, 1.6ml 10%SDS, 0.4ml β mercaptoethanol, 0.2ml 0.05%bromophenol blue). SDS PAGE was performed using Bio-Rad protean III apparatus and samples were passed through a 5% stacking (0.5M Tris HCl 6.8 2.5ml, 10% SDS 0.1ml, 40% Acrylamide Bis solution 37.5:1 1.25ml, 10% APS 30µl and Temed 15µl) and separated on a 7% resolving gel (1.5 M Tris HCl pH 8.8 2.5ml, 10% SDS, 40% AB, 10% APS 30µl and Temed 15µl). The choice of gel percentage was based on the molecular weight of the protein of interest. Protein electrophoresis was performed with the 1x tris-glycine buffer system (5x running buffer composition, Tris Base 15gm, Glycine 72gm, SDS 5gm, DD H_2O 1 liter) at a constant voltage of 100V, at 4°C for one hour and 30 minutes. The gel was transferred in transfer buffer (25Mm Tris, 192Mm Glycine, 20% methanol pH8.3) over night at 25V, to a 0.45 µm nitrocellulose membrane using Bio rad transblot electrophoretic transfer cell.

Coomassie brilliant blue solution containing (40% ethanol, 10%acetic acid, 1% coomassie brilliant blue) was used to visualize the fractionated proteins in the gels. The gels were heated in microwave for one minute and kept at 4 °C on a shaker for two hours. After two hours, gels were rinsed in dd H_2O and destained with 40% ethanol and 10% acetic acid and reaction terminated with rinses in dd H_2O upon maximum resolution. Gels were sandwiched between cellophane papers and dried on a gel drying apparatus for one hour.

For immunodetection of proteins of interest following transfer, ponceau staining solution was used to visualize proteins on NC membrane this is a confirmatory step for transfer before immunodetection. The membranes were immersed in the ponceau S

staining solution (0.1% ponceau S and 5% acetic acid) for 5 min. The NC membranes were rinsed subsequently with distilled water and immersed in TBST (10%Tween 20 10ml, 10x TBS 100ml 10x TBS 38gm NaCl, 12.1gm Tris Base pH 7.5 for 500ml, dd H_2O 1000ml) to remove the stain. Inert Ponceau does not react with any of the subsequent steps of immunoblotting. Blocking procedure was carried out at two hours at room temperature in 1x TBST and 5% skim milk powder. The blots were incubated O/N at 4°C in a 1:1000 dilution of rabbit polyclonal antibody (C-20) raised against IGF-IR beta subunit (Santa Cruz Biotechnology, Inc Santa Cruz Ca.). Membranes were washed in 1x TBST for five times each for five minutes and incubated for one hour in 1:10000 dilution goat antirabbit HRP conjugated IgG (Bio Rad, Missiauga, Ontario Inc.) Following three washes color development was performed using a chemiluminesce substrate kit according to the manufacturers instructions. Membranes were exposed to Kodak Omat film for different time periods, each exposure time was evaluated with a subsequent doubling of exposure time. Multiple independent western blots were performed. Alfa Ease software was used to acquire the integrated density values of the exposed films. For reverifying uniform loading the same blots were probed for house keeping genes with antibodies to β actin at 1:5000 dilution mouse monoclonal Abcam for one hour at room temperature with three 10 minutes washing and 1:10000 goat anti mouse Bio Rad for one hour with subsequent three 10 minute washes and one minute exposure of the membrane to ECL.

2.4.3 Densitometric Analysis

The images of the ECL exposed nitrocellulose membranes on X-Ray films were captured by Alpha Ease software. The density of the bands was measured as an integrated density value in pixels. The band densities determined from the film were acquired from separate time points. The ratio of the two was calculated to normalize the interpretation. This value was indicative of a linear relationship since the band intensity of signal at one time point doubles as a function of double exposure times. The comparison verified the reliability of the detection system. The values obtained from different blot density of IGF-1R protein bands was standardized to the density of loading control house keeping genes β actin.

2.5 IGF-1 Treatment

Fetal type II AECs and lung fibroblasts in culture conditions were subjected to IGF-I (Sigma Chemical St.Louis, MO) treatments for short exposures of 10 minutes. This short period was chosen based on the short half life of IGF-1 which is 10 minutes. Cells were subjected to two different concentrations of IGF-1 treatments 50ng/ml and 100ng/ml at each time point for phosphorylation studies in lung fibroblasts. For type II AECs, IGF-1 dosage was optimized to 200 ng/ml for 15 minutes. In the case of proliferation assays only the fetal lung fibroblasts were used and those cells were exposed to CSE at 1, 5 and 10% with combined addition of 50 and 100ng/ml of IGF-I for 24 hours. All experiments were run in triplicates for statistical validation.

2.6 Lysates for Autophosphorylation studies

Modified RIPA buffer was prepared with addition of Sodium Orthovanadate (Na_3VO_4) to preserve phosphates from degradation by the phosphatases. Sodium deoxycholate an ionic reagent known to inactivate kinases was not added. Cold lysis buffer was used to harvest the cells from cultures and subjected to Bradford protein estimation as described above.

2.6.1 Western Blotting to detect autophosphorylated proteins

Western blotting was performed under reducing conditions. The molecular weight of antibody against the IGF-1R tyrosine domain was 95kDa. SDS-PAGE was run under reducing conditions and specifically targeted antibody to the phosphorylated tyrosine domains 1135/1136 of the IGF-1R beta subunit was applied. Following the transfer of the protein on to NC membranes overnight at 25 Volts, 4°C, membranes were blocked in 5% BSA in TBST at RT for two hours following which they were incubated with 1:1000 dilution optimized for primary rabbit monoclonal antibody overnight at 4 °C. Following which the membranes were washed for one hour 10 minutes in TBST in 100% Tween 20 according to the manufacturer's instructions. Goat Anti-rabbit IgG conjugated secondary antibody was used to identify the primary antibody binding sites. Membranes were washed six times with TBST supplemented with 100% Tween 20. The blots were exposed to ECL chemiluniscence for one minute before exposing the Kodak Omat films. Densitometric analysis was performed for the same to look for the phosphorylated subunits. The blots were rinsed thoroughly to eliminate the ECL and stripped in a stripping buffer (Restore Pierce) for 30 minutes at 37 °C. Successful

stripping was confirmed by absence of signal during re-incubation with ECL. Blots were incubated with the same secondary antibody to confirm the absence of primary antibody signals. For the native expression of proteins polyclonal IGF-1R antibody against the C terminal subunit of the endogenous β receptor was used. The blots were rewashed thoroughly and blocked in 5% skim milk for two hours at room temperature and incubated overnight at 4°C in 1:1000 dilution with rabbit polyclonal primary antibody against endogenous non phosphorylated β subunit IGF-1R beta subunit. Following 3x TBST washes for each 10 minutes in TBST the blots were incubated in goat anti rabbit IgG conjugated HRP secondary antibody for one hour at room temperature subjected to TBST three 10 minutes washes for each and incubated in ECL for film exposure. The results were interpreted through densitometry scans for the independent blots and statistically analyzed through Duncan's Multiple Range software.

2.7 Immunohistochemistry (IHC)

IHC was performed to confirm our in vitro results and specifically examined IGF-1R alpha subunit for lung sections fixed in neutral formalin and embedded in paraffin. 6μm lung sections were deparaffinized in xylene and rehydrated in decreasing concentrations of alcohol (100%, 70%, 50% and H_2O, for five minutes each), followed by quenching the endogenous dehydrogenase activity in 0.3% hydrogen peroxide in methanol, the sections were washed three times in 1x PBS for five minutes each and were blocked in normal goat blocking serum for one hour. Negative controls were incubated in absence of primary antibody while other sections were incubated with 1:100 dilution of IGF-IR alpha subunit antibody overnight at 4 °C. Sections were

incubated with biotinylated secondary antibody for one hour followed by three washes in 1xPBS. Immunoreactive sites were detected with DAB immunohistochemistry substrate incubation for one minute. DAB (3,3'-diaminobenzidine) is oxidized in the presence of peroxidase and hydrogen peroxide resulting in the deposition of a brown, alcohol-insoluble precipitate at the site of enzymatic activity. This was followed by counter staining with haematoxylin and mounted with permanent mounting medium for prolonged records. IHC was performed on lungs from fetuses of gestation day 21, and postnatal day 7, day 8 and day 9 lung tissues. Mouse kidney was used as positive control and negative controls by omitting the primary antibodies.

2.8 Cell Viability Trypan Blue

Trypan Blue is a dye exclusion procedure for viewing viable cell. This method is based on the principle that live (viable) cells do not take up certain dyes, whereas dead (non-viable) cells do. Staining facilitates the visualization of cell morphology. A Cell suspension is prepared in 0.3 ml HBSS with 0.5 ml of 0.4% trypan blue and 0.2 ml of cell suspension. Cell count, each square of Haemocytometer with cover slip in place represents a total volume of 0.1 mm^3 or 10^{-4} cm^3. Since 1 cm^3 is equivalent to approximately 1ml, the subsequent cell concentration per ml and total number of cells is determined using the following calculations. Cells per ml= average count per square x dilution factor x10^4 (count 10 squares). Total cells= cells/ml x original volume from which cell sample is removed. Cell viability (%) =total viable cells (unstained)/total cells (stained and unstained) x 100. In the present context we counted all ten fields per sample to estimate the cell numbers.

2.9 Crystal Violet Assay

Crystal violet assay is based on the principle that only DNA of viable cell takes up the stain. The methanol soluble dye is released in methanol and samples were read spectrophotometrically at an O.D. of 590 nm. Cells were used in the log phase at 80% confluence and serum starved for 24 hours before the treatment with the CSE and IGF-1. CSE was dissolved in culture media at a range of 1-20% CSE. Optimum concentration range was determined both for CSE and IGFs and optimum seeding curves generated for a 24 hour time point with 3000 cells plated per well. CSE was prepared and dissolved in culture media with IGF-1 at concentrations 50 and 100ng/ml. Plates were left undisturbed for 24 hours in 5% CO_2 at 37 °C and 100% humidity. At about 80% confluence cells were serum starved for 24 hours before CSE or IGF-1 application. After 24 hours of treatment, culture media were discarded and plates were incubated with 100µl crystal violet stain at 0.4% concentration for 10 minutes. The samples were gentle rinsed at 30 degree angulation to running tap water to avoid lifting of cells. Plates were placed upside down on paper towel to remove any remaining water. When the plates were semi dried 200µl of 100% methanol at room temperature was added for 20-30 minutes to remove the dye bound to DNA. Absorbance was recorded at 590 nm through Pro Max spectrophotometer plate reader. Data was collected from multiple and independently tested 96 well plates.

2.10 MTS Formazan Assay

MTS is a colorimetric assay to determine the cellular viability. Promega cell titre 96 aqueous one solution reagent kit was used which contains a novel compound [3-(4, 5-

dimethylthiazol-2yl)-5-(3-carboxymethoxyphenyl)-2-(4-sulfophenyl)-2H-tetrazolium, inner salt, MTS] and an electron coupling reagent (phenazineethosulphate, PES). The MTS tetrazolium compound (Owens reagent) is bioreduced by viable cells into a colored. The absorbance was read spectrophotometrically at 490nm. Formazan product is soluble in tissue culture medium. The reaction is accomplished by conversion of NADPH to NADH produced by mitochondrial dehydrogenase enzymes of the metabolically active cells. Assay was performed according to the manufaturers directions.

2.11 Morphological studies

Cell morphology was evaluated following CSE treatment under ELWD 0.3 Nikon Phase contrast microscope at objectives (4x at a scale of 4500μm), (10x at a scale of 2000μm), (20x at a scale of 1000μm) and (40x at a scale of 500μm) specific to this Nikon Phase Contrast microscope.

2.12 Statistical Analysis

Data were analysed between the groups by Duncan's Multiple Range Test. Analysis were validated by analysis of variance.

Rationale

Rationale for this project is based on what is known thereby moving on to elucidate the unknown. *In utero* development as a whole is a complex process of developing hard and soft tissues. Among the different organ systems respiratory system is a complex process involving 40 different cell types through four different stages of embryonic development. The structure remains unique in its ability to grow throughout and instantly ready to function at the time of birth. Growing fetus receives dual supply of nourishment through its own circulation and amniotic fluid. Detrimental exposure of fetus to genotoxins in cigarette smoke through maternal route may cause sufficient damage to the growing embryo. Enough evidence indicates maternal smoking as a primary cause for fetal growth restriction and potential respiratory ailments along with involvement of hormones on negative effects on fetal development (Kapoor et al., 2005). However, among the various hormones involved there has been little speculation over fetal IGF axis involved during maternal smoking. Thus this project, through an *in vitro* molecular study, is the first to fill the plausible gaps in research of fetal IGF axis involved through maternal smoking at the cellular level. So far *in-vivo* studies have not established sufficient evidence to suggest IGF axis involvement during maternal smoking (Ermis et al., 2004). Presently we studied the effect of cigarette smoke extract on IGF axis in two specific cell types of the fetal rat lung type II AECs and lung fibroblasts. Within the lung, type II Alveoloepithelial cells (AECs) are of critical importance as they produce surfactant which maintains alveolar patency at maximum end expiration. Due to the intricate regulatory interactions between the type II AECs and lung fibroblasts we have also examined CSE effects on these latter cells. On the

contrary, the effects of CSE on developing cells from the craniofacial structures are also considered to be affected. There has been much speculation on the effects of maternal smoking on intrauterine growth retardation or failure of development of fetus as a whole but little attention is given to effects of maternal smoking on maxillo-facial structures such as mandibular condylar units of TMJ structures during fetal development. Numerous studies have suggested a link between maternal smoking and facial cleft and palate defects (Chung et al., 2000; Shi et al., 2007). Facial defects with abnormal dentitions can alter the facial joint functionality as a complex. Therefore the role of mandibular condyle in development has not been extensively probed. Mandibular condyle combines two principal functions, namely articulation and growth within the covering fibrocartilage. The intimate association of these two roles may make the effect of maternal smoking induced pathological process on TMJ more complex during intra-uterine development. The resultant deformity is harder to interpret unless these functions were anatomically and physiologically distinct. Malformation or damage to the condyle may cause deformity of the mandible by direct impairment of the mechanisms for compensatory growth and adjustment between the tooth-bearing jaw and the skull (Poswillo and Robinson, 1992). The cytotoxic effects of maternal smoking on these regions remains an area of extensive research. Future radiographic cephalometric studies on assessing a pattern of maxillo-facial changes in children born to maternal smoking can help us assess their maxillo-mandibular relations in growth and development. Thus, within the developing embryo we assessed the hard and soft tissues affected by cigarette smoke extract based on the known facts in an attempt to find the missing links.

Hypothesis, Objectives, Aims

We hypothesized that

(a) IGF-1R is expressed differentially during different stages of lung development.

(b) Cigarette smoke exposure affects IGF-1R protein expression differentially in cells from developing soft (lung epithelial-mesenchymal) and hard tissues (mandibular condylar cartilage) of the rat fetus.

Objectives

The present *in vitro* study examines the effects of cigarette smoke extract (CSE) on IGF-1R in developing fetal rat hard and soft tissues.

Aims

Specific Aim # 1. To study IGF-1 receptor protein expression in lung fibroblasts from pre and post natal rat lungs.

Specific Aim # 2. (a). To isolate type II AECs and lung fibroblasts from gestational day 21 fetal rat litters and distinguish IGF-1R protein expression in CSE exposed both lung fibroblasts and type II epithelial cells.

(b). To study receptor activation in lung fibroblasts and type II AECs from gestational day 21 lung cells.

(c). To study the effect of CSE on IGF-1R expression in cells from gestational day 21 embryonic mandibular condylar cartilage.

(d). To study the receptor expression in CSE exposed postnatal day one rat lung fibroblast.

3.0 Results

3.1 Results for Gestational Profile of IGF-1R

3.1.1 IGF-1R Protein expression in pre and postnatal rat lung development

IGF-1Rβ expression from western blots is shown in Figure 5. Bands were observed in homogenate from cells isolated from lungs of rats aged, day one (Figure 5. A), day 3 (Figure 5. B), gestational day 21, day 7, day 8 and day 9 (Figure 5. C). Bands were detected corresponding to 97kDa molecular mass. Corresponding to 42kDa bands were detected against antibody to β actin loading control. Hela cell lysates served as positive controls and mouse liver extract as negative controls. Immunogenic reaction to antibody for IGF-1R was detected in all ages starting from gestational day 21 and postnatal day 1, 3, 7, 8 and 9 from lung fibroblasts. The receptor expression was increased significantly ($p<0.05$) in new born rat lung fibroblasts compared to gestational day 21 and day 3, 7, 8 or 9 with ($p<0.05$). Significantly reduced receptor expression ($p<0.05$) at day 3 or 9 cell cultures relative to other age groups was observed as shown in figure 5 E.

3.12 Immunohistochemistry

Gestational day 21, day 7, day 8 and day 9 lung sections region (Figure 5 F) showed immunoreactivity to antibody against IGF-1R alpha subunit. Kidney sections served as positive controls. Immunoreactivity was detected positively in positive controls in kidney sections and lung specimens (Figures 5F. a, c, e, g, i). Primary

antibody was omitted for the negative controls (Figures 5 F. b, d, f, h, j). Immunoreactivity in kidneys to antibody against IGF-1R was seen as positive DAB staining at the peripheral cortical regions (Figure 5 F a). In gestational day 21 lung sections positive reaction to the IGF-1R antibody was seen in the mesenchymal regions (Figure 5 F c). The dense mesenchymal region displayed less differentiated alveoli at this gestational age. Animal lung sections from day 7 old displayed positive reaction to IGF-1R antibody in the well developed alveolar regions and appeared to be confined to the alveolar epithelium (Figure 5 F e). Positive reaction was also detected in the bronchial epithelium of the lung sections in day 8 and 9 lung sections (Figure 5 F. g, i).

3.2 CSE Spectrophotometric Scan and Gas Chromatographic analysis for nicotine.

To ensure consistency, optical density of the CSE was measured at a wavelengths of 190-1100nm. Absorbance of 1.0-1.2 was considered standard for standard minimum essential medium at 550-580nm wavelength. 100% CSE was compared to standard studies on medium which displayed absorbance of 1.0-1.2 at 300-320nm absorbance. Consolidated scan for 100% CSE as compared to plain standard minimum essential media is shown in figure 6. Gas Chromatograph analysis determined 30μg/ml nicotine content in whole CSE. Treatment with 1% CSE is 0.028 puffs/ml of smoke in plain culture medium. Therefore 75ng/ml of nicotine was applied at 1% CSE treatment.

3.3 Studies on gestational day 21 fetal rat lung fibroblasts

3.3.1 Primary cell cultures from gestational day 21 lung fibroblasts exposed to CSE

Primary cell cultures from fetal pulmonary lungs were used in these studies. Fibroblast cells were grown in 10% newborn calf serum as explained in detail in

methods section. Primary lung fibroblasts isolated from gestational day 21 fetal rat lungs are shown in Figure 7 (a) grown in monolayers attached to the tissue culture flasks. Cultured cells were grown to 80% confluence and serum starved for 24 hours (Figure 7 a). These cells appear spindle like in appearance and grow parallel to one another in a circular pattern. Post 24 hours of serum deprivation, primary lung fibroblasts were treated with CSE at dilutions from 1-20% (Figures 7. b, c, d, e, and f). At 1, 5, 10% CSE (Figure 7. b, c, d) concentrations the gross phenotypic morphology of these lung fibroblasts under phase contrast microscope was similar to the phenotype of cells in control group. However at 20% CSE (Figure 7. e) concentrations the cells were observed as floating colonies with few cells remaining attached to the tissue culture flasks. After 48 hours of incubation with 20% CSE (Figure 7. f) few cells with more debris remaining on tissue culture flasks were observed. Lung fibroblast cells exposed to hydrogen peroxide at a concentration of 200μM served as negative controls (Figure 7. g) show no fibroblasts attached to the tissue culture flasks. All images were captured at 10x magnification from a phase contrast microscope. Nuclear changes in membrane continuity, cell shrinkage, blebbing features were observed at higher magnifications (images not shown).

3.3.2 Effects of CSE on cell numbers

The effects of CSE on isolated fetal rat lung fibroblast numbers are shown in (Figure 8). Cell numbers for gestational day 21 fetal rat lung fibroblasts in untreated samples were estimated at $6x10^6$ cells/ml. Exposure to 1% CSE did not significantly

alter the mean cell numbers. In contrast, exposure to 10% or 20% CSE significantly reduced ($p<0.05$) the mean cell numbers in culture.

3.3.3 Effects of CSE on cell viability

Viability as measured by trypan blue exclusion (Figure 9) was significantly reduced ($p<0.05$) in samples of isolated fetal rat lung fibroblasts exposed to 5%, 10% or 20% CSE compared to the control samples. Similarly samples treated with 5%, 10% or 20% CSE were significantly reduced compared with samples exposed to 1% CSE.

3.3.4 Effects of CSE on proliferative capacity

Exposure to 5%, 10% or 20% CSE significantly reduced ($p<0.05$) proliferative capacity as determined by crystal violet assay (Figure 10) relative to the control group. Similarly 5%, 10% or 20% CSE significantly reduced ($p<0.05$) proliferation compared to the cells exposed to 1% CSE.

3.3.5 Effects of combined IGF-1 with CSE on proliferative capacity.

The combined effects of various concentrations of CSE plus 50ng/ml or 100ng/ml IGF-1 on proliferative capacity were determined by crystal violet assay as shown in (Figure 11). IGF alone did not significantly alter proliferative capacity compared to the control samples. Again as observed previously (Figure 10) CSE (10 or 20%) significantly decreased proliferative capacity compared to the control samples. The addition of IGF-1 did not alter the pattern of reduced proliferative capacity induced by exposure to increasing concentrations of CSE. Similarly no significant differences were

observed in proliferative capacity observed by crystal violet assay in cells exposed to 100ng/ml IGF-1 compared to the control samples (Figure 11). Exposure of the isolated fetal rat lung fibroblasts to increasing concentrations of CSE with 100ng/ml IGF-1 signficantly reduced ($p<0.05$) proliferative capacity in a dose-dependent manner except at 10% CSE. Generally this pattern was not significantly altered by the addition of 100ng/ml of IGF-1 to the gestational day 21 lung fibroblasts.

3.3.6 Effects of CSE on cellular metabolic activity

MTS assay which measures the metabolic activity of the mitochondria was measured in gestational day 21 fetal rat lung fibroblasts incubated in serum contained CSE at 1, 5, 10 or 20% concentrations for 24 hours (Figure 12) at 490nm absorbance spectrophotometrically. In serum contained CSE group, maximum MTS activity at 8 hour was recorded in controls, 1%, 5%, 10% or 20% CSE. The activity was significantly decreased ($p<0.05$) after exposures to 5, 10 or 20% CSE compared to controls ($p<0.05$). Hydrogen peroxide at 200μM concentration was incubated with lung fibroblasts to serve as a negative control.

3.3.7 Effects of combined IGF-1 with CSE on cellular metabolic activity.

The combined effects of various concentrations of CSE plus 50ng/ml or 100ng/ml IGF-1 on metabolic activity were determined by MTS assay as shown in (Figure 13). After 24 hours IGF-1 alone at concentrations of 50 or 100ng/ml significantly increased metabolic activity compared to the control samples. Again as observed previously (Figure 12) CSE significantly decreased metabolic activity

compared to the control samples. The addition of IGF-1 did not alter the pattern of reduced MTS activity induced by exposure to increasing concentrations of CSE or in combination with IGF-1 at 50 or 100ng/ml. However, significant increase was observed in metabolic activity in cells exposed to 10% CSE with 100ng/ml IGF-1 compared to the 10% CSE alone (Figure 13).

3.3.8 Effects of CSE on protein yield

In preparation for Western blot analysis of protein concentrations for cultures of gestational day 21 fetal rat lung fibroblasts were determined. Control lung fibroblast samples contained an average of 6.02 $\mu g/10^6$ cells, samples exposed to 1% CSE contained 8.71 $\mu g /10^6$cells, samples exposed to 5% CSE contained 5.99 $\mu g/10^6$cells while exposure to 10% CSE contained 5.20 $\mu g/10^6$cells from three independent replicates.

.

3.3.9 Effect of CSE on IGF-1R β protein expression.

Western blot analysis was performed using gestational day 21 fetal rat lung fibroblasts to assess IGF-1Rβ expression upon cigarette smoke extract exposure. Fibroblasts were exposed at 1, 5, or 10% CSE concentrations. Bands corresponding to 97kDa were detected (Figure 14). The blots were normalized against β actin house-keeping gene for assessing uniform loading. Bands were detected corresponding to 42 kDa molecular mass (Figure 14). Significant differences ($p<0.05$) in receptor expression were observed at 1, 5 or 10% CSE concentrations compared to controls (Figure 14). Hela cell lysate served as a positive control and mouse liver extract as a negative control.

3.3.10 Effect of CSE on Autophosphorylation of IGF-1R β

CSE treated samples were treated with IGF-1 ligand at 50 or 100ng/ml concentrations for 10 minutes (Figure 15). Bands were detected corresponding to the 95 kDa molecular mass marker of the 1135/36 autophosphorylated subunit of the IGF-1R β. Bands suggestive of complete autophosphorylation were observed in positive controls, 5 or 10% CSE with 100ng/ml IGF-1 and 1 or 5% CSE with 50ng/ml IGF-1, partial bands were seen in negative controls, 1% with 100ng/ml IGF-1 and 10% CSE with 50ng/ml IGF-1 as shown in (Figure 26 A). IGF-1R β expression observed bands corresponding to 97kDa molecular mass with varying degrees of density as shown in (Figure 13 B). The samples were normalized against β actin house keeping gene to assess uniform loading (Figure 16 C) where in bands corresponded to the 42kDa molecular mass marker. Significant differences ($p<0.05$) were detected (Figure 27) at 10% CSE with 100ng/ml IGF-1, 5% CSE with 50ng/ml IGF-1 and 10% CSE with 50ng/ml IGF-1 relative to the positive control.

3.4 Studies on gestational day 21 fetal rat lung Type II AECs

3.4.1 Primary cell cultures from gestational day 21 lung type II AECs exposed to CSE.

Primary cell cultures from fetal pulmonary lung were used in these studies. Type II AECs cells were grown in 10% stripped newborn calf serum as explained in detail in methods section. Primary lung type II AECs isolated from gestational day 21 fetal rat lungs are shown in Figure 17 (a) grown in monolayers attached to the tissue culture flasks in colonies. The images in Figure 17 (a, b) were captured post 24 hours of type II

cell cultures. Cultured cells were grown to 80% confluence and serum starved for 24 hours (Figure 17 c). These cells appear cuboidal in appearance and grow in clustered colonies. Post 24 hours of serum deprivation, primary lung type II AECs were treated with CSE at dilutions from 1-20% (Figures 17 d, e, f, g). At 1, 5, 10% CSE (Figure 17 d, e, f) concentrations the gross phenotypic morphology of these type II AECs under phase contrast microscope was similar to the phenotype of cells in control group. In CSE treated cells frequency of cell detachment was higher compared to lung fibroblasts treated for the same concentrations. However at 20% CSE (Figure 17 e) concentrations the cells were observed as floating colonies with few cells remaining attached to the tissue culture flasks.

3.4.2 Effect of CSE on cell numbers

Cell numbers for gestational day 21 fetal rat lung Type II AECs in control samples were estimated (Figure 18) at $6x10^{5}$ cells/ml. After 12 hours of response to CSE there was a significant increase ($p<0.05$) in cell numbers at 5% CSE (Figure 18) compared to the control samples ($p<0.05$). However at 24 hours (Figure 18) cell numbers were significantly reduced ($p<0.05$) after exposure to 1, 5, 10 or 20% CSE compared to the controls.

3.4.3 Effect of CSE on cell viability

Type II AECs viability was assessed by trypan blue exclusion assay. After 12 hours of exposure to CSE, viability (Figure 19) was significantly reduced ($p<0.05$) in isolated fetal rat lung Type II AECs exposed to 20% CSE compared to the control

samples. Similarly at 24 hours (Figure 19) cells treated with 1, 5, 10 or 20% CSE were significantly reduced ($p<0.05$) compared with control samples.

3.4.4 Effects of CSE on proliferative capacity

Exposure to 5%, 10% or 20% CSE significantly reduced ($p<0.05$) proliferative capacity as determined by crystal violet assay (Figure 20) relative to the control group in serum- starved group. However, CSE exposed cells with serum showed no significant differences compared to the control groups (Figure 20).

3.4.5 Effects of CSE on cellular metabolic activity

MTS activity was recorded in gestational day 21 lung type II AECs treated with or without serum conditions plus CSE at 1, 5, 10 or 20% concentrations for 24 hours (Figure 21). In serum containing CSE group, maximum MTS activity at 24 hours was recorded, in controls, 1%, 5%, 10% or 20% CSE. The activity was increased in cells exposed to 1 5, 10% CSE compared to controls ($p<0.05$). Hydrogen peroxide at 100μM concentration in lung Type II AECs served as a negative control. In serum starved CSE exposed group, maximum MTS activity at 24 hours was detected. The activity decreased at 20% CSE compared to the controls ($p<0.05$).

3.4.6 Effects of CSE on protein yield

In preparation for Western blot analysis of protein concentrations for cultures of gestational day 21 fetal rat lung type II AECs were determined. Control samples contained an average of 1.02 $\mu g/10^5$cells, samples exposed to 1% CSE contained

1.34μg/10^5cells, samples exposed to 5%CSE contained 1 μg/10^5cells while exposure to 10% CSE contained 0.77 μg/10^5cells from three independent samples.

3.4.7 Effect of CSE on IGF-1R β protein expression.

Western blot analysis was performed using gestational day 21 fetal rat lung type II AECs and to assess IGF-1Rβ expression upon cigarette smoke exposures. Type II AECs were exposed at 1, 5, or 10% CSE concentrations. Bands corresponding to 97kDa were detected (Figure 22). The blots were normalized against β actin house keeping gene for assessing uniform loading. Bands were detected corresponding to 42kDa molecular mass (Figure 22). Significant differences ($p<0.05$) in receptor expression were detected after exposure to 5 or 10% CSE compared to controls (Figure 22). Hela cell lysate served as a positive control and mouse liver extract as a negative control.

3.4.8 Effect of CSE on Autophosphorylation of IGF-1R β

Cells were treated with IGF-1 ligand at 200 ng/ml concentrations for 15 minutes (Figure 23 A). Bands were detected corresponding to 95kDa molecular mass of the 1135/36 subunit of the IGF-1R β subunit. Bands suggestive of autophosphorylation were seen in positive controls, 1, 5 or 10% CSE with 200ng/ml IGF-1. Total receptor expression (Figure 23 B) was detected corresponding to the 97kDa molecular mass with varying degrees of density. The samples were normalized against β actin house-keeping gene to assess uniform loading (Figure 23 C). Bands were seen corresponding to the 42kDa molecular mass. Significant increase ($p<0.05$) in autophosphorylation (Figure 23) occurred in cell samples exposed to at 1% CSE with 200ng/ml IGF-1 compared to the

positive and treatment control. Partial autophosphorylation was seen at 5% CSE with 200ng/ml IGF-1 and 10% CSE with 200ng/ml IGF-1 relative to the control samples.

3.5 Studies on day one rat lung fibroblasts

3.5.1 Primary cell cultures from postnatal day one lung fibroblasts exposed to CSE.

Primary cell cultures from lungs from day one rats were used in these studies. Fibroblast cells were grown in 10% newborn calf serum as explained in detail in methods section. Primary lung fibroblasts isolated from day one rat lungs are shown in Figure 24 (a) grown in monolayers attached to the tissue culture flasks. Cultured cells were grown to 80% confluence and serum starved for 24 hours (Figure 24 a). These cells appear spindle like in appearance and grow parallel to one another in a circular pattern. Post 24 hours of serum deprivation, primary lung fibroblasts were treated with CSE at dilutions from 0.1-50% (Figures 24 b, c, d, e, f, g). At 0.1, 0.01, 1, 10% CSE (Figure 24 b, c, d, e) concentrations the gross phenotypic morphology of these lung fibroblasts under phase contrast microscope was similar to the phenotype of cells in control group. However at 25% or 50% CSE (Figure 24 f, g) concentrations the cells were observed as floating colonies with few cells remaining attached to the tissue culture flasks.

3.5.2 Effects of CSE on cell numbers

The effects of CSE on isolated day one rat lung fibroblasts are shown in Figure 25. Cell numbers in untreated samples were estimated at $8x10^6$cells/ml. Exposure to 1, 5, 10 or 20% CSE significantly reduced ($p<0.05$) the mean cell numbers compared to the untreated samples.

3.5.3 Effects of CSE on cell viability

Viability as measured by trypan blue exclusion was significantly reduced ($p<0.05$) in samples of isolated day one rat lung fibroblasts exposed to 20% CSE compared to the control samples (Figure 26). However at 1, 5, or 10% CSE viability was similar to control values.

3.5.4 Effects of combined IGF-1 with CSE on proliferative capacity

The combined effects of various concentrations of CSE plus 50ng/ml or 100ng/ml IGF-1 on proliferative capacity were determined by crystal violet assay as shown in Figure 27. IGF-1 (50ng/ml or 100ng/ml) significantly increased ($p<0.05$) proliferative capacity compared to the control samples. CSE significantly increased ($p<0.05$) proliferative capacity compared to the control samples ($p<0.05$) at 1, 5, 10 or 20% CSE. The addition of IGF-1 did not alter the pattern of proliferative capacity induced by combined exposure to increasing concentrations of CSE. Generally this pattern was not significantly altered by the addition of 100ng/ml of IGF-1 to the day one rat lung fibroblasts.

3.5.5 Effects of CSE on cellular metabolic activity

MTS activity was observed in day one rat lung fibroblasts treated with and without serum conditioned with CSE at 1, 5, or 10% concentrations for 24 hours (Figure 28). In serum-contained CSE group, maximum MTS activity at four hours was observed, in controls, 1%, 5%, or 10% CSE. The MTS activity was significantly increased ($p<0.05$) in 1, 5 or 10% CSE compared to controls. In the serum-starved CSE-exposed

group, maximum MTS activity was observed also at four hours. The MTS activity increased significantly ($p<0.05$) at 5 or 10 % CSE compared to the controls. Hydrogen peroxide at 100μM was incubated with lung fibroblasts to serve as a negative control.

3.5.6 Effects of CSE on protein yield

In preparation for Western blot analysis of protein concentrations from cell cultures of day one rat lung fibroblasts were determined. Control samples contained an average of 2.95 $\mu g/10^6$cells, samples exposed to 1% CSE contained 2.91 $\mu g/10^6$cells, samples exposed to 5% CSE contained 2.54$\mu g/10^6$cells, exposure to 10% CSE contained 2.21 $\mu g/10^6$cells while exposure to 20% CSE contained 2.91$\mu g/10^6$cells from three independent samples.

3.5.7 Effect of CSE on IGF-1R β protein expression.

Western blot analysis was performed using day one rat lung fibroblasts to assess IGF-1Rβ expression upon cigarette smoke extract exposure. Fibroblasts were exposed at 1, 5, 10% or 20% CSE concentrations (Figure 29). Bands corresponding to 97kDa were detected (Figure 29). The blots were normalized against β actin house-keeping gene for assessing uniform loading. These bands corresponded to 42kDa molecular mass (Figure 29). Significant differences ($p<0.05$) were found at 1, 5, 10 or 20% CSE conditions compared to controls (Figure 29). Hela cell lysate served as positive control and mouse liver extract as negative control.

3.6 Studies on gestational day 21 fetal rat mandibular condylar fibroblasts

3.6.1 Developmental mandibular condylar histology

Fetal rat mandibular condylar histology at gestational day 21 was studied. Condyle of the mandible during this period of growth is a fragile soft structure. Histological sections through the mandibular condylar head from gestational day 21 fetal rat stained in eosin and haematoxylin are shown in the figure 30 a 4x magnification. Figure 30 a^1. shows proliferating zone, figure 30 a.^{2} cartilage like cells. Fibroblast like cells were grown in gel foam sponges as described in methods section. Fibroblast like cells grown in gel foam sponges shown in figures 30 b^1. (fibroblast like cells) and figure 30 b^2. (gel foam threads). In subsequent sections primary fibroblast cells isolated from mandibular condyles were used for experiments. Mandibular condylar fibroblast cells were grown in 10% newborn calf serum as explained in detail in methods section. Primary mandibular condylar fibroblasts isolated from gestational day 21 fetal rat are shown in figure 30 grown in monolayers attached to the tissue culture flasks in colonies at 0 hour (c) of plating, 5 hours (d), 48 hours confluence (e), and 1week cultures (f).

3.6.2 Primary cell cultures from mandibular condylar fibroblasts exposed to CSE

Cultured cells were grown to 80% confluence and serum starved for 24 hours (Figure 31 a). These cells appear spindle shaped and grow in parallel, elongated circular patterns. Post 24 hours of serum deprivation, primary mandibular condylar fibroblasts were treated with CSE at dilutions from 1-20% (Figures 31 b, c, d, e,) for 24 hours. Subsequent (Figure 31 g, h, i, j, k, l, m, n) images of mandibular condylar fibroblasts treated with IGF-1 in combination with CSE at 1, 5, 10 or 20% CSE concentration with

50 or 100ng/ml IGF-1 show morphological features similar to as described above in CSE treated conditions alone.

3.6.3 Effects of CSE on cell numbers

The effects of CSE on isolated gestational day 21 fetal rat mandibular condylar fibroblasts are shown in (Figure 32). Cell numbers in control samples were estimated at $6x10^5$cells/ml. Exposure to 1, 5 or 10% CSE did not significantly alter the mean cell numbers. In contrast, exposure to 20% CSE significantly reduced ($p<0.05$) the mean cell numbers in culture.

3.6.4 Effects of CSE on cell viability

Viability as measured by trypan blue exclusion (Figure 33) was significantly reduced ($p<0.05$) in samples exposed to 20% CSE compared to the control samples. However samples treated with 1, 5, or 10% CSE were comparable to the control values.

3.6.5 Effects of combined IGF-1 with CSE on proliferative capacity

The combined effects of various concentrations of CSE plus 50ng/ml or 100ng/ml IGF-1 on proliferative capacity were determined in serum starved state by crystal violet assay as shown in figure 34. IGF-1 at 50ng/ml alone did not significantly alter proliferative capacity compared to the control samples. CSE significantly increased ($p<0.05$) proliferative capacity compared to the control samples at 10 or 20% CSE The addition of IGF-1 did not alter the pattern of reduced proliferative capacity in combination with increasing concentrations of CSE. Significant increase ($p<0.05$) was

observed in proliferative capacity observed by crystal violet assay in cells exposed to 100ng/ml IGF-1 compared to the control samples (Figure 34). Addition of 50 or 100ng/ml of IGF-1 to 10 or 20% CSE concentrations significantly increased ($p<0.05$) proliferation compared to the controls.

3.6.6 Effects of CSE on proliferative capacity

In serum-contained CSE exposed cells proliferative activity was detected, in controls, 1%, 5%, 10% or 20% CSE exposed as shown in figure 35. The activity was decreased significantly ($p<0.05$) in 5, 10 or 20% CSE exposed cells compared to controls ($p<0.05$). Hydrogen peroxide at 200μM was incubated with mandibular condylar fibroblasts to serve as a negative control.

3.6.7 Effects of combined IGF-1 with CSE on cellular metabolic activity

The combined effects of various concentrations of CSE plus 50ng/ml or 100ng/ml IGF-1 on metabolic activity were determined by MTS assay as shown in Figure 36 at three or nine hours of incubation after exposure to CSE for 24 hours. At three hours MTS activity was significantly decreased ($p<0.05$) in cells exposed to 50ng/ml, 100ng/ml, 1%, 10%, 20%, 20% with 50ng/ml or 10% with 100ng/ml CSE compared to the controls were observed. At nine hours exposure to 20% CSE with or without 50ng/ml IGF-1 cells displayed significantly reduced ($p<0.05$) MTS activity compared to the control values.

3.6.8 Effects of CSE on protein yield

In preparation for Western blot analysis of protein concentrations from cell cultures of gestational day 21 fetal rat mandibular condylar fibroblasts were determined. Control samples contained an average of 3.57 $\mu g/10^6$cells, samples exposed to 1% CSE contained 3.44$\mu g/10^6$cells, samples exposed to 5% CSE contained 4.13$\mu g/10^6$cells, exposure to 10% CSE contained 4.27 $\mu g/10^6$cells while exposure to 20% CSE contained 3.10 $\mu g/10^6$cells from three independent samples.

3.6.9 Effect of CSE on IGF-1R β protein expression.

Western blot analysis was performed using gestational day 21 fetal rat mandibular condylar fibroblasts to assess IGF-1Rβ expression upon cigarette smoke extract exposures. Fetal mandibular condylar fibroblasts were exposed at 1, 5, 10 or 20% CSE concentrations. Bands corresponding to 97kDa were detected (Figure 37). The blots were normalized against β actin house-keeping genes for assessing uniform loading. These bands were detected corresponding to 42kDa molecular mass (Figure 37). Receptor expression was not altered in response to CSE (Figure 37). Hela cell lysate served as a positive control and mouse liver extract as a negative control.

FIGURES AND TABLES

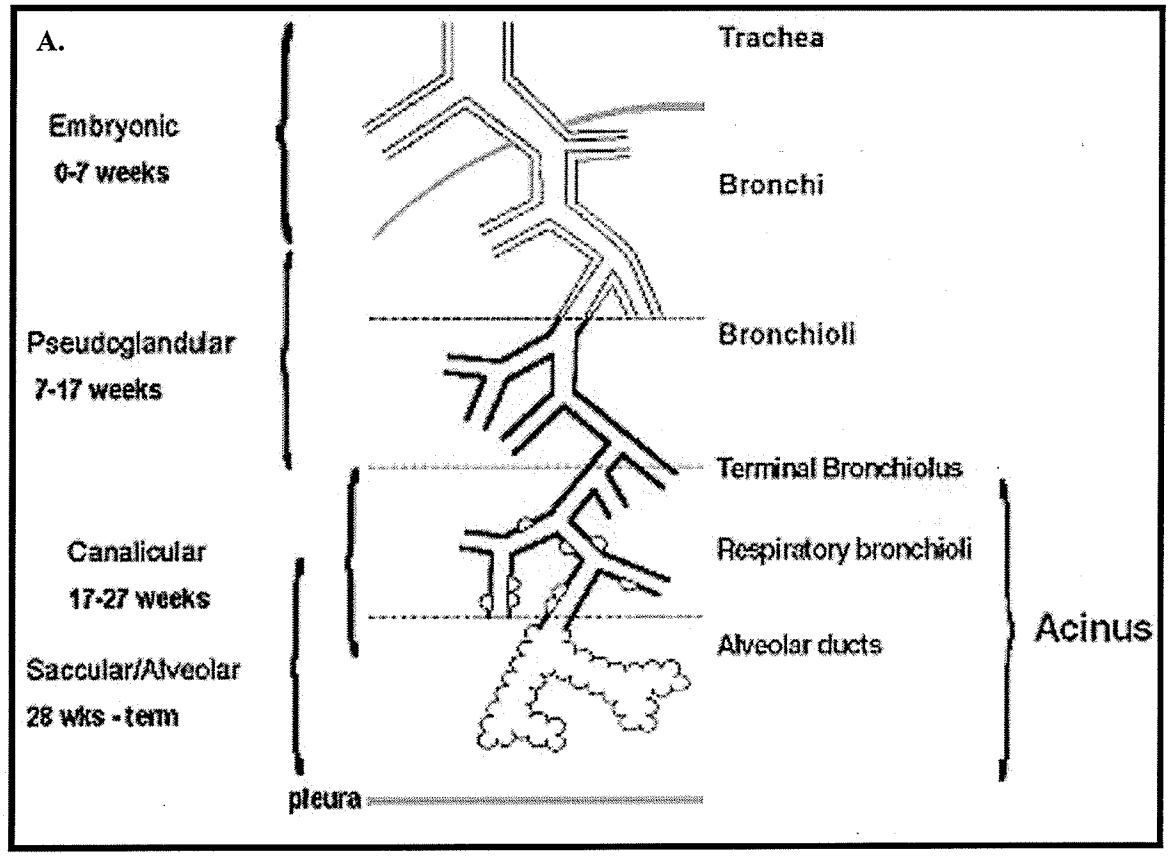

Figure 1: A. Airway development. The figure represents the four stages of lung development (a)Embryonic, (b) Pseudoglandular, (c) Canalicular, (d) Saccular/alveolar in humans. *Adapted from (Hislop A. 2002).*

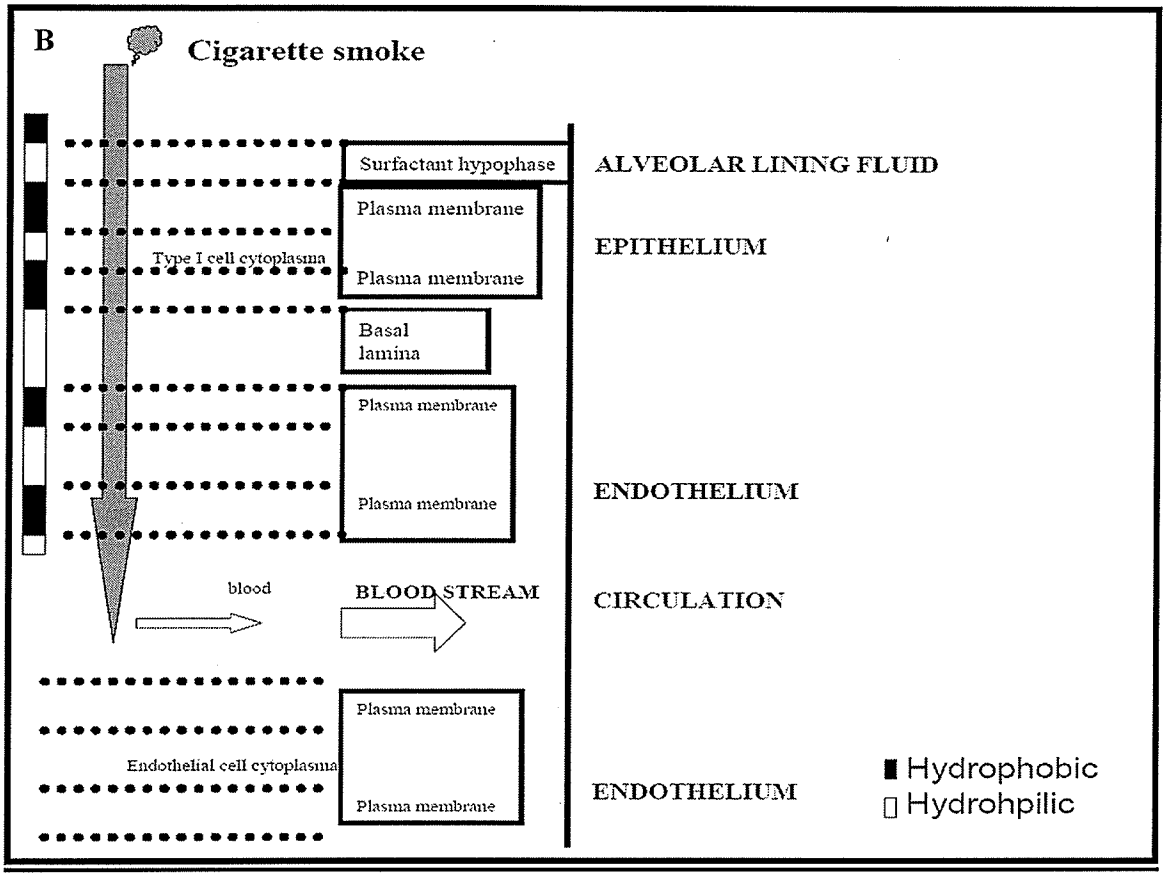

Figure 1. B. Paths and barriers for cigarette smoke passage in the human body. This figure shows the paths via which the cigarette smoke reaches the circulation and tissues. On the way to the alveoli tar and particles precipitate changing the composition of cigarette smoke. After the passage through the upper respiratory system, cigarette smoke reaches one of the most complex biological barriers separating the environment from the internal system. The filtrating layers between the alveolar lumen and blood are shown in the figure above. Cigarette smoke chemicals have to pass at least nine layers with alternating hydrophilic and hydrophobic character. Cigarette smoke might pass the lung-blood barrier by free diffusion (gases) or via cellular transport mechanisms for water, ion, macromolecules or other chemicals. The chemical character (hydrophilic/hydrophobic) of the pictured layers are shown in the picture above
(Figures adapted from Scott and Wang 2005).

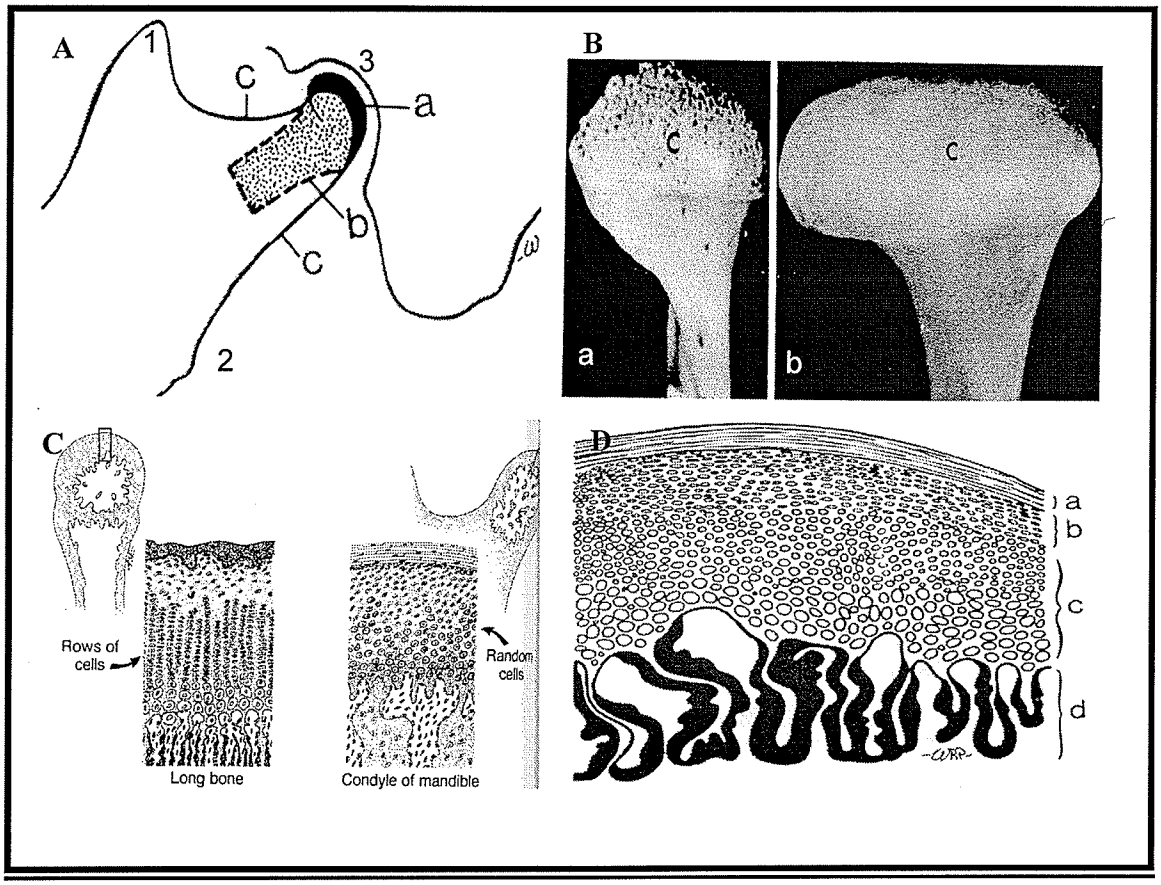

Figure 2: A. Mandibular condylar macroscopic features. Condylar cartilage proliferates in an upward and backward direction (a), mandibular condyle, medullary core of the endochondral bone (b), mandibular neck and periosteal-endosteal bone formation (c), (1) coronoid of the mandible ,(2) angle of the mandible, (3) Glenoid fossa of the temporal bone.

B. Comparison of younger 6 years old condyle (a) and an adult condyle (b). Note the increase in the lateral dimension.

C. Cartilage comparsion long bone and the mandibular condyle. There is a lack of palisading and thick perichondrium in the condyle.

D. Microscopic features of the mandibular condyle. The condylar cartilage has a fibrous covering (a) that overlays a region of rapidly proliferating prechondroblasts (b). In area c, the cells have become chondroblasts that mature in the deeper part of the zone. Each cell undergoes hypertrophy, and a limited deposition of inter-cellular matrix occurs. Near zone d, the matrix calicifies, and cartilage resorption with subsequent bone deposition begins along the posterosuperior moving interface between c and d.
(Figures 2A, D Adapted from TMJ Ed Laskin 1992. Figures 2 B, C Adapted from Oral histology and development Ed James K.Avery 1994.)

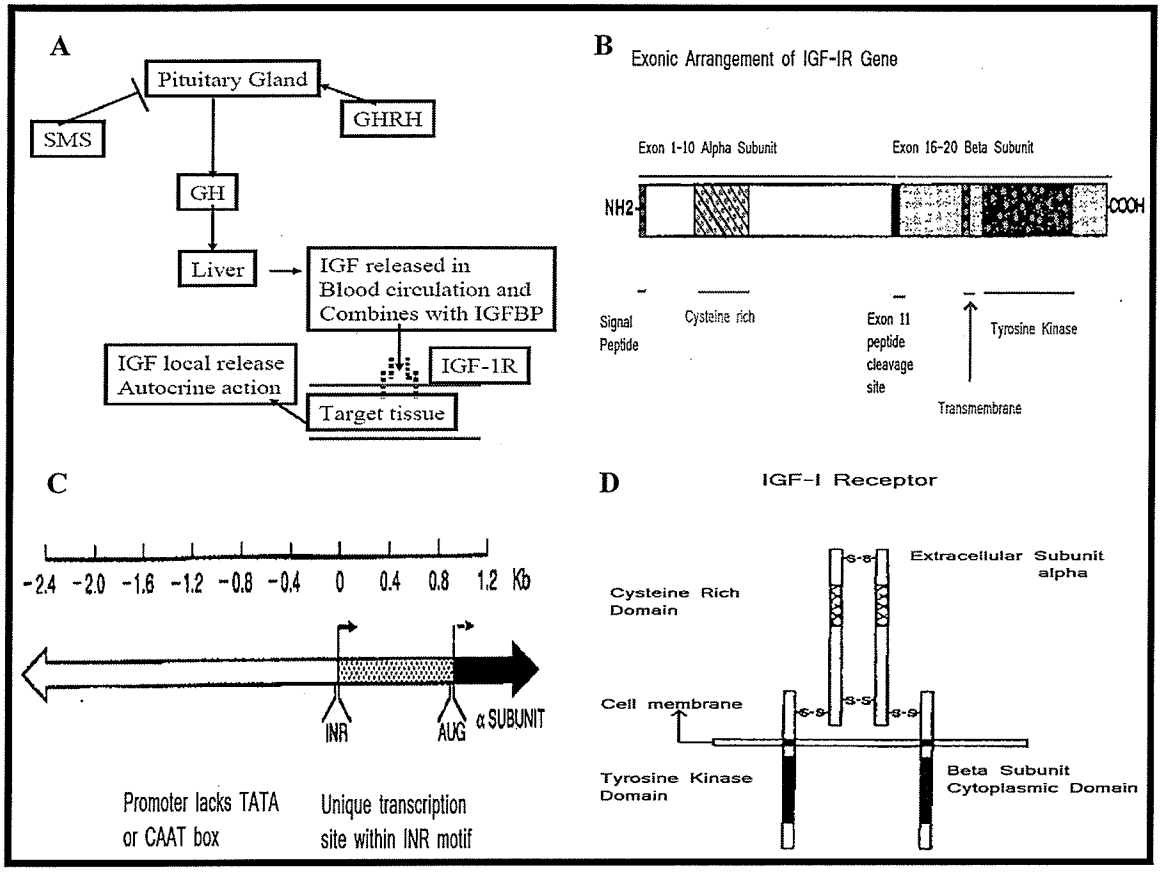

Figure 3: A. IGF-Axis Summary IGFs source (liver), mode of transport of IGFs complexed with binding proteins. The growth hormone–insulin–like growth factor (GH–IGF) axis. GH secretion is regulated by hypothalamus, pituitary interaction. The hypothalamus produces and secretes growth hormone–releasing factor (GRF) and the hormone somatostatin (SMS) into the blood vessels linking the hypothalamus and pituitary. GRF stimulates GH synthesis and secretion, and SMS inhibits GH secretion. GH, secreted into the general circulation, in turn stimulates the synthesis and secretion of the growth–stimulating hormone insulin–like growth factor 1 (IGF–1) release from liver into the blood circulation. IGF ligands circulate complexed with binding proteins and mediate their effects through the IGF-1 receptors. *(Adapted Nature publishing group 2004).*

B. IGF-1R precursor unit with exonic arrangement of IGF-1R. Illustrates the different functional domains at the alpha and beta subunits.

C. IGF-1R promoter region with no TATA /CAAT motifs.

D. IGF-1R Structure representing the mature heterotetrameric receptor with two alpha subunits, and beta subunits with tyrosine kinase domains. *(Adapted Le Roith et al 1995).*

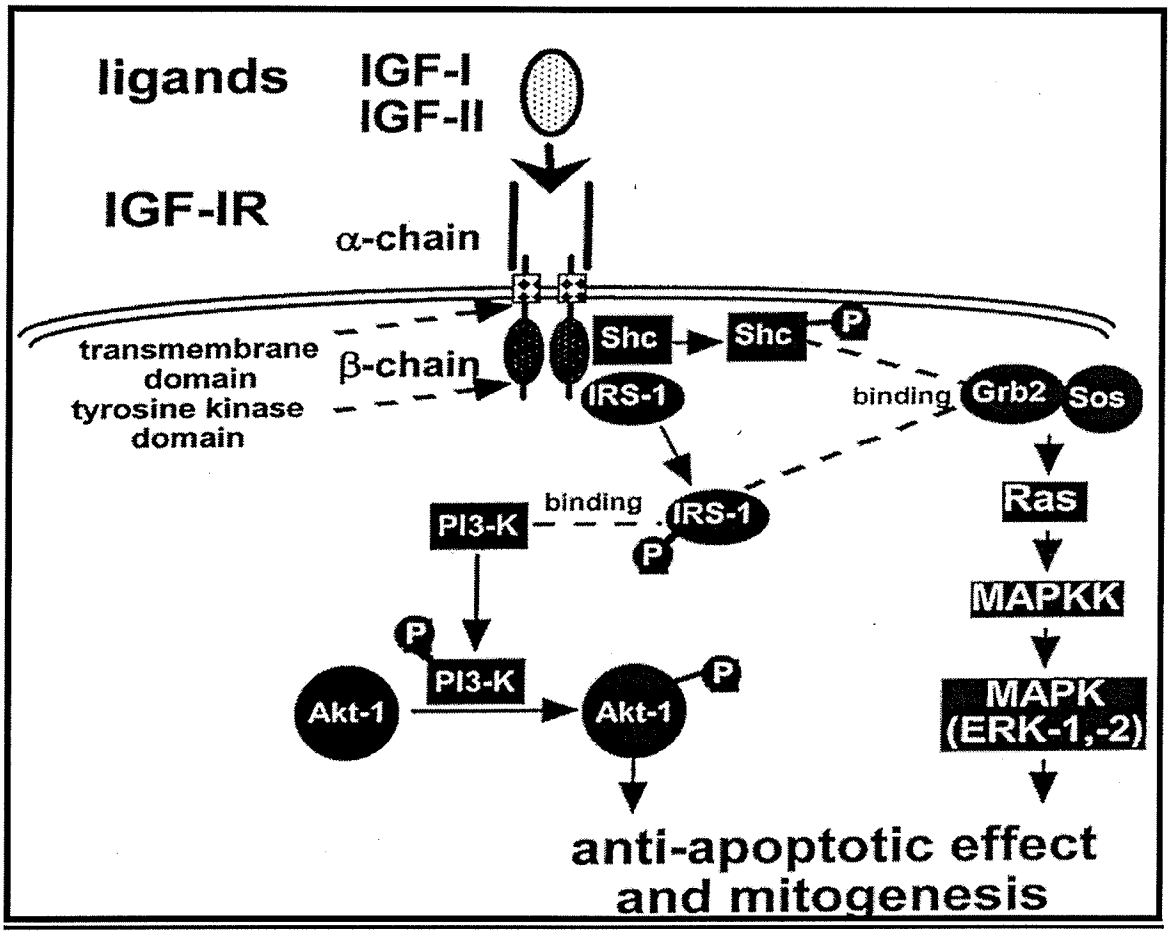

Figure 4: IGF-1R mediated signal transduction. IGF-1R with extracellular alpha subunit, beta subunit with transmembrane and tyrosine kinase domains. IGF-1 or -2 ligands bind to the extracellular subunit and IGF-1R turns on its signal transduction mechanism resulting in anti-apoptotic effect and mitogenesis through MAPKinase and PI3-K pathways *(Adapted from Biology of IGF-1 Novartis foundation).*

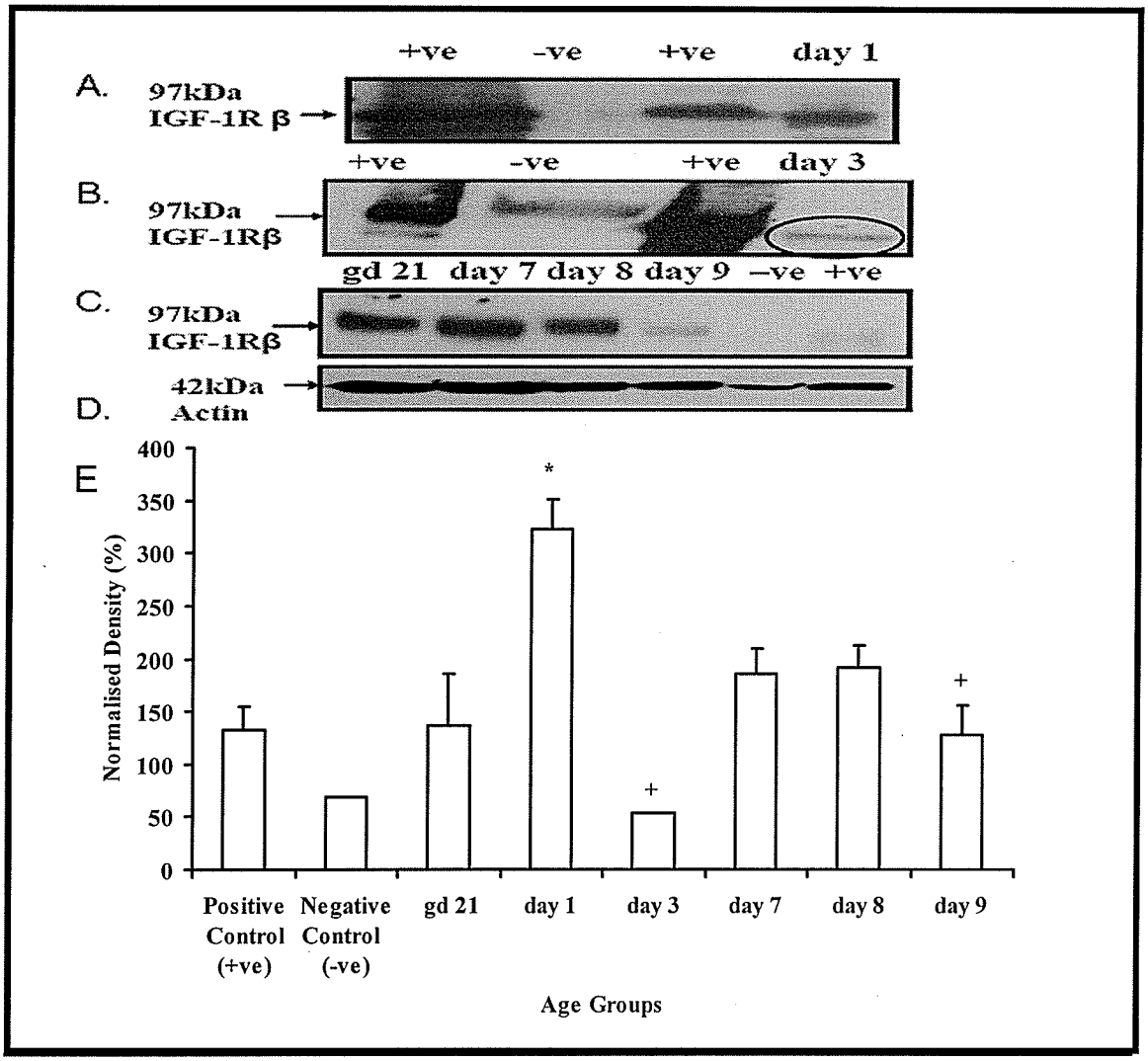

Figure 5: IGF-1R protein expression at different stages of rat lung development through Western blotting.

A. IGF-1Rβ expression from isolated rat lung fibroblasts from day one
B. IGF-1Rβ expression from isolated rat lung fibroblasts postnatal day three
C. IGF-1Rβ expression from isolated rat lung fibroblasts gestational day (gd) 21, day 7, day 8 or day 9 aged.
D. Protein loading normalized to actin house-keeping protein expression.
E. Quantitation of IGF-1R expression in pre and post natal age groups of fetal rat lungs. The receptor expression was increased significantly ($p<0.05$) in postnatal day one rat lung fibroblasts compared to gestational day 21, and postnatal day 3, 7, 8, or 9 aged rats. Significantly reduced receptor expression (*/+ $p<0.05$) in postnatal day 3 or 9 in cell cultures relative to other age groups was observed (+ve, positive control; -ve negative control).

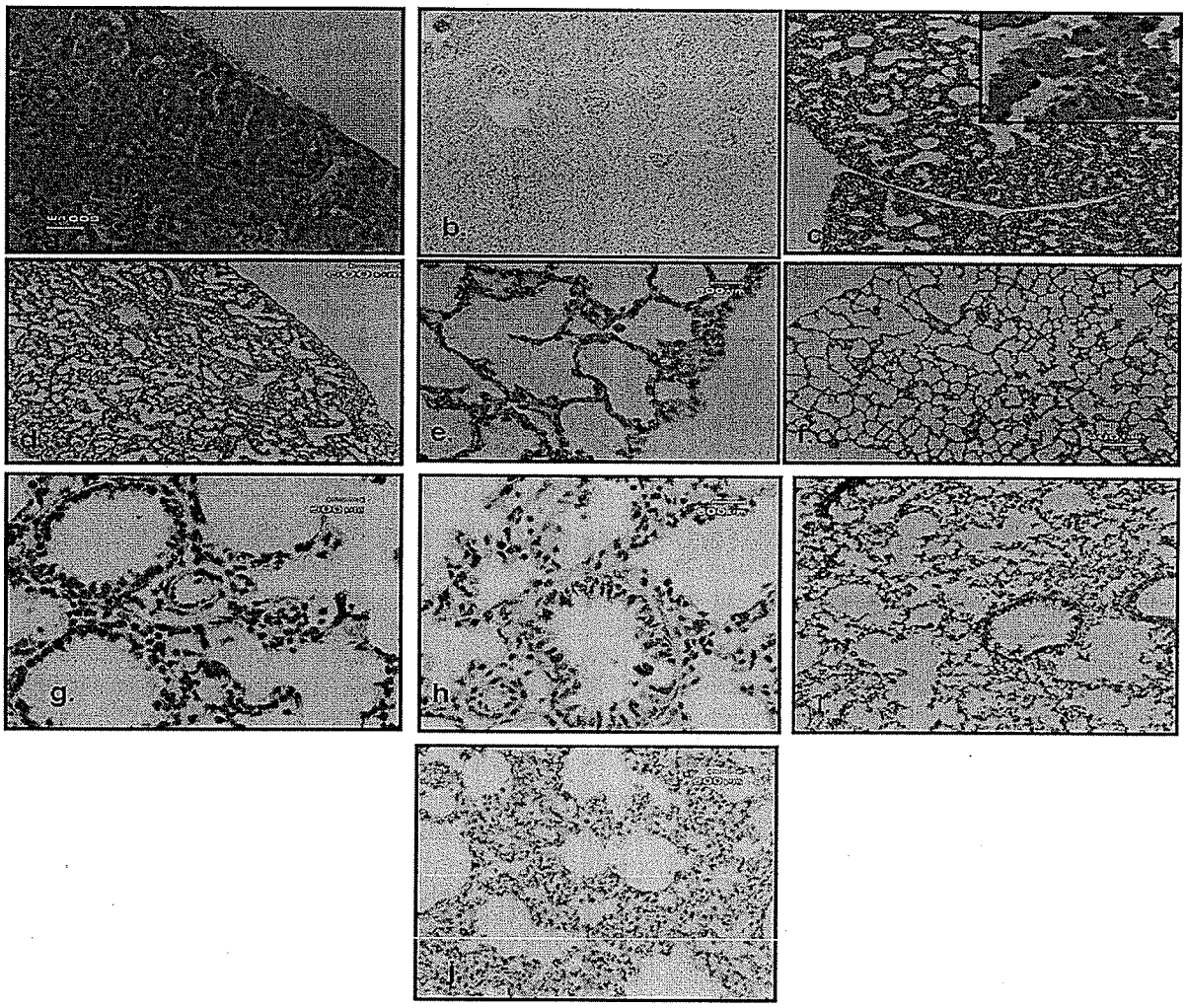

Figure 5: Immunohistochemical analysis of IGF-1R α during rat lung development.

F. (a) Kidney positive control, (b) Kidney negative control primary antibody omitted, (c) Prenatal gestational age day 21 (+ve reaction) (d) Prenatal gestational age day 21; primary antibody omitted (-ve reaction), (e) Postnatal age day 7 lung section with positive reaction, (f) Postnatal age day 7 lung section with primary antibody omitted served as negative control, (g) Postnatal age day 8 lung section with positive reaction to IGF-1R antibody in the bronchiolar region, (h) postnatal age day 8 lung section with primary antibody omitted as negative control, (i) Postnatal age day 9 lung section with positive reaction to IGF-1R in the bronchiolar region, (j) Postnatal age day 9 lung section with primary antibody omitted as negative control, (Scale bar 600μm); (-ve negative; +ve positive).

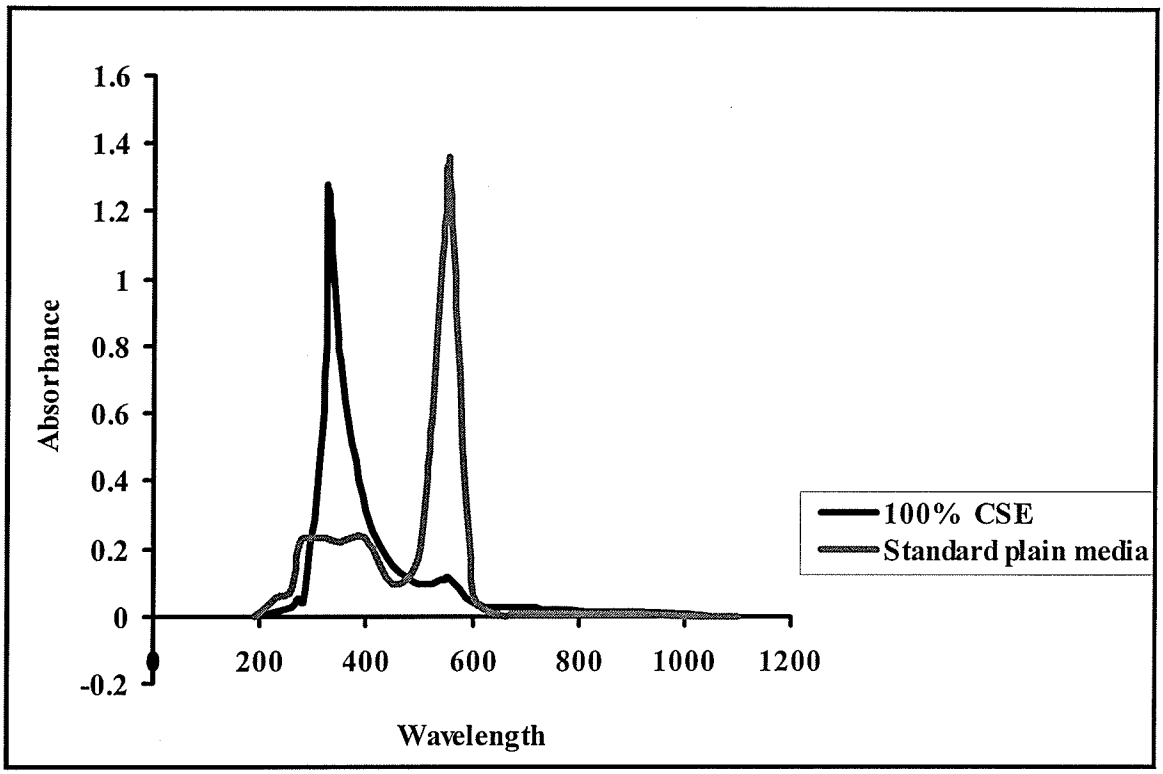

Figure 6: Spectrophotometric scan of CSE on a broad range scale of 190-1100nm wavelength. Wavelength for plain media recorded at 550nm and 100% CSE at 350nm. The peaks show relatively equivalent absorbances at two different wavelengths for 100% CSE and plain media.

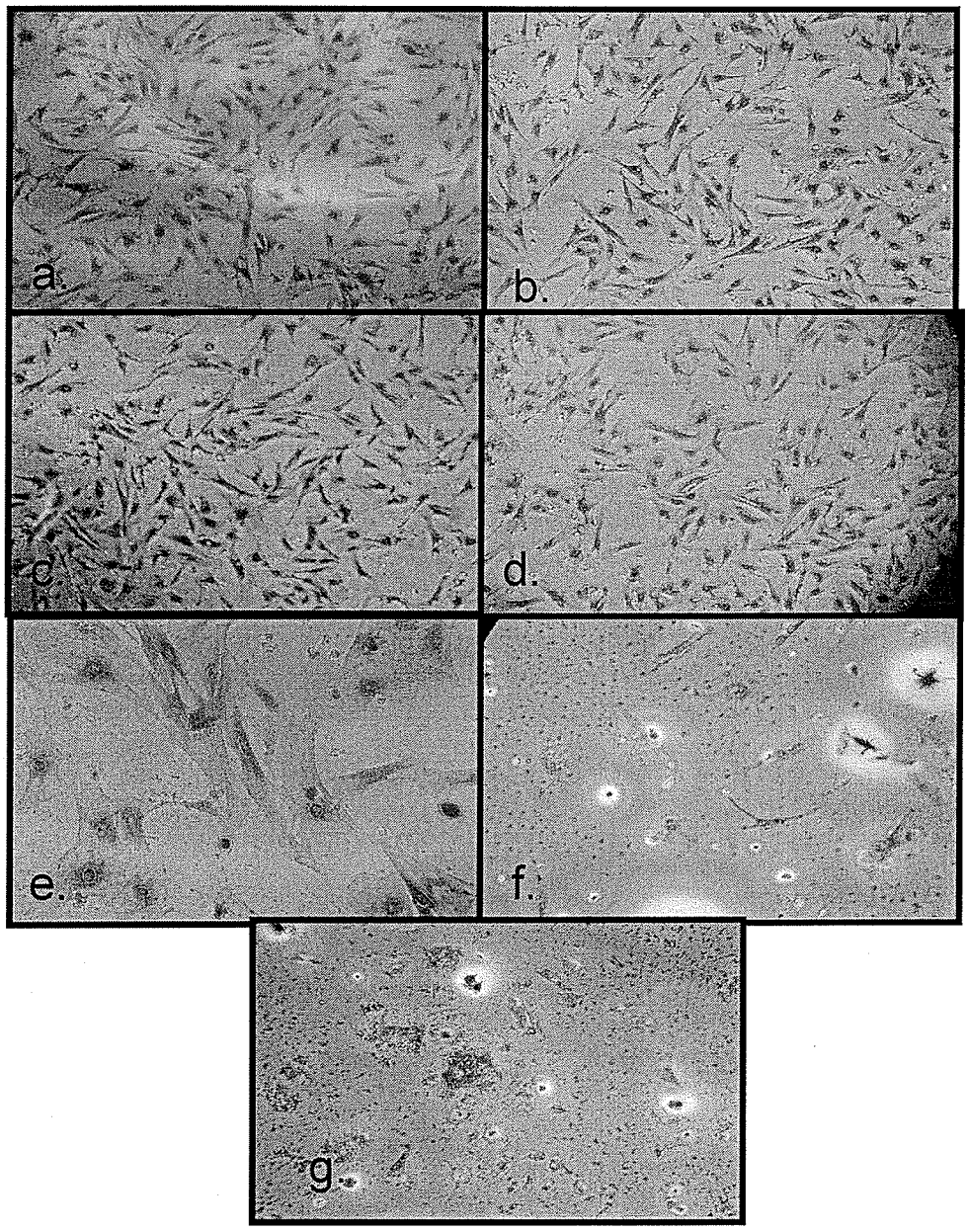

<u>Figure 7:</u> Lung fibroblasts from gestational day 21 fetal rat in response to 24 hour CSE exposures. Phase contrast microscopy 10x magnification.

(a) Treatment Control.
(b) Lung fibroblasts to 1% CSE exposures
(c) Lung fibroblasts 5% CSE exposures.
(d) Lung fibroblasts 10% CSE exposures.
(e) Lung fibroblasts 20% CSE exposures.
(f) Lung fibroblasts 20% CSE 48 hours of CSE exposures.
(g) Lung fibroblasts to H2O2 exposures negative control.

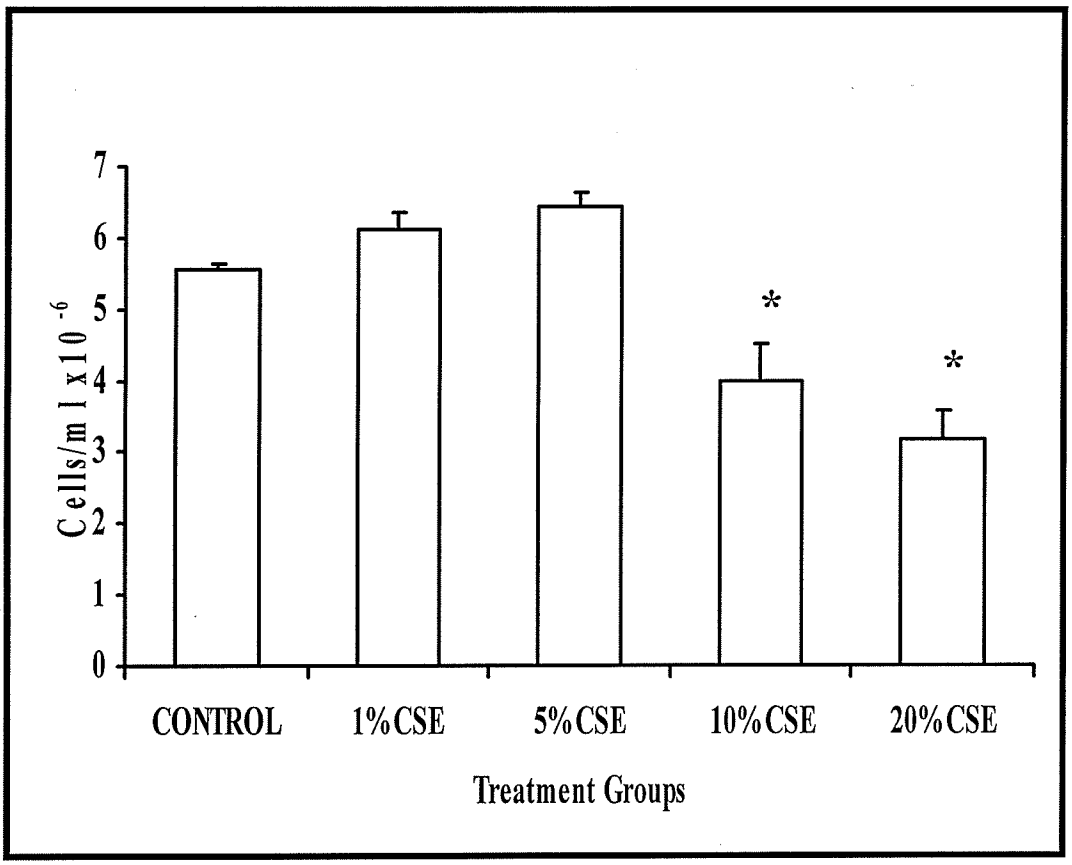

Figure 8: Effects of CSE on cell numbers from gestational day 21 fetal rat lung fibroblasts. Cell count for 24 hours at 1, 5, 10 or 20% CSE concentrations. Statistically significant differences at 10% or 20% CSE relative to the control group are illustrated (* $p<0.05$). Data collected from 2 independent experiments (with 5 measurements per treatment for each condition, n=10) were combined and are represented as +/-S.D.

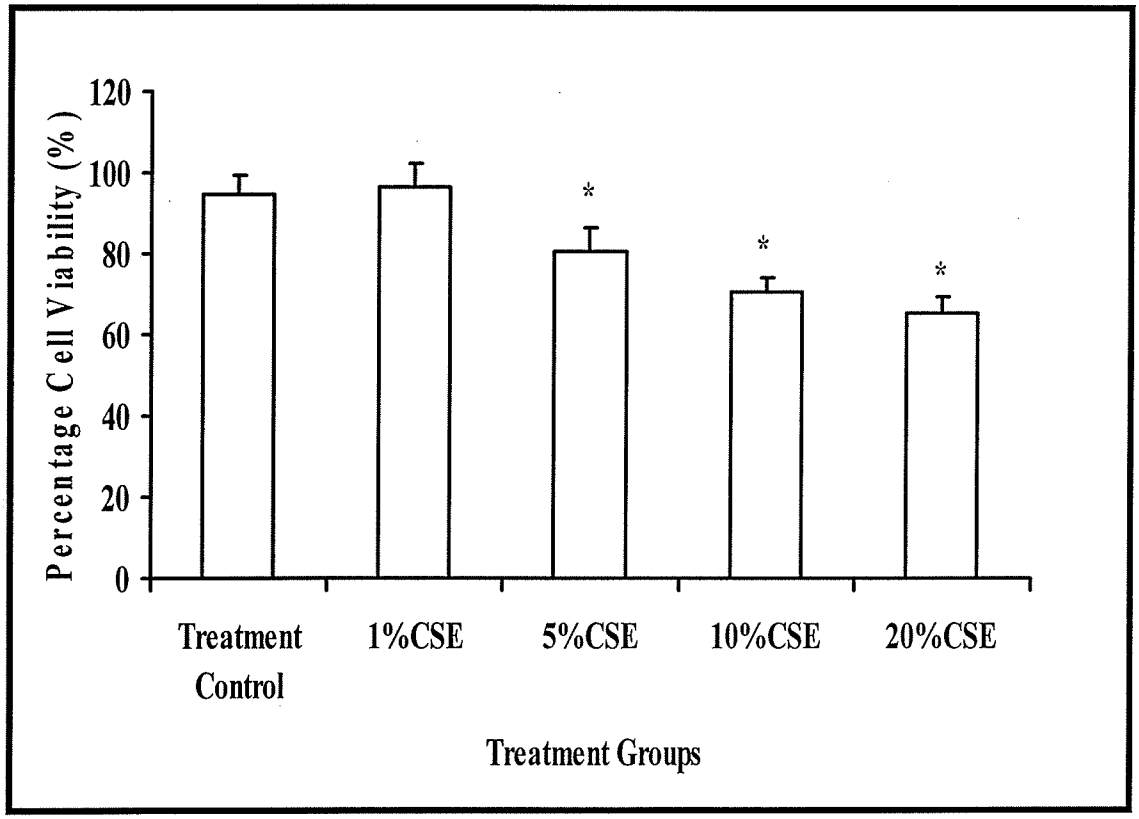

Figure 9: Effects of CSE on cell viability from gestational day 21 fetal rat lung fibroblasts. Trypan Blue Exclusion by gestational day 21 fetal rat lung fibroblasts exposed to CSE. At 24 hours (*) indicates significant difference ($p<0.05$) at 5, 10 or 20% CSE relative to the treatment controls. Data collected from 2 independent experiments (with 5 measurements per treatment for each condition, n=10) were combined and are represented as +/-S.D.

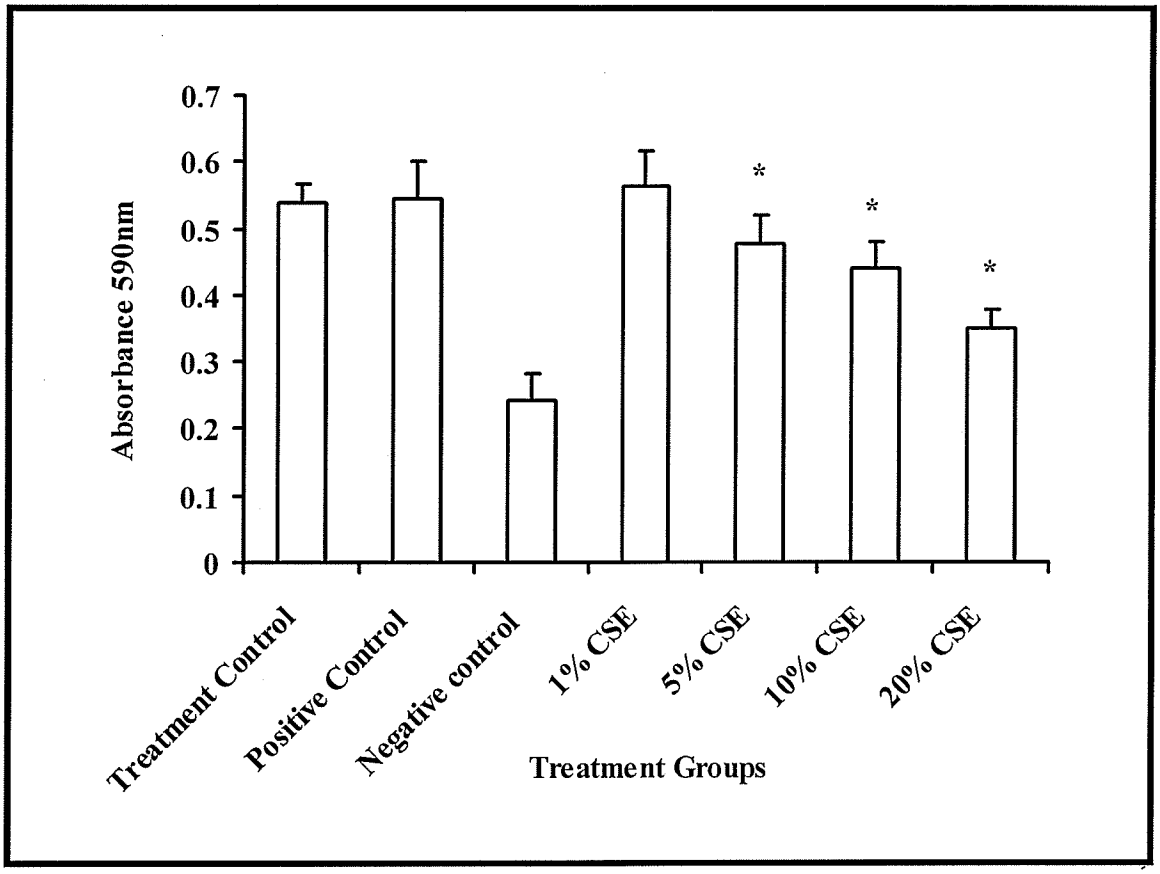

Figure 10: Effects of CSE on proliferative capacity from gestational day 21 fetal rat lung fibroblasts. Crystal violet assay to assess proliferative effect of CSE on gestational day 21 fetal rat lung fibroblasts. 24 hours serum treated group were considered as positive controls. Serum free groups were treated with 1,5,10 or 20% CSE. Hydrogen peroxide 200μM was used to induce oxidative stress and served as negative control for recording proliferative activity. Significant difference at 5, 10 or 20% CSE (* $p<0.05$) compared to the control group. Data collected from 3 independent experiments (with 8 measurements per treatment for each condition, n=24) were combined and are represented as +/-S.D.

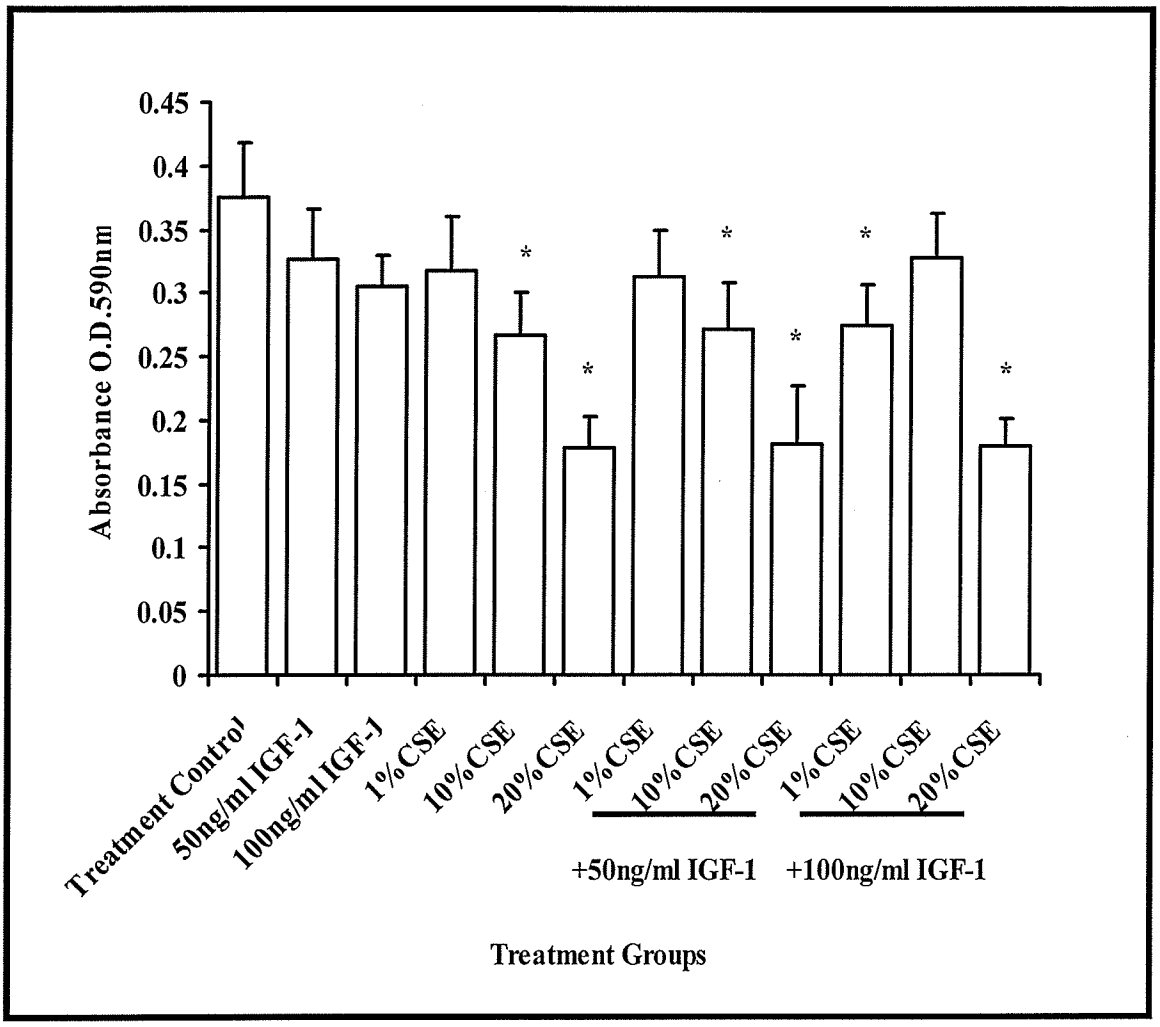

Figure 11: Effects of combined IGF-1 with CSE on proliferative capacity from gestational day 21 fetal rat lung fibroblasts. Crystal violet assay to assess combined effect of CSE/IGF-1 on 21 gestational fetal rat lung fibroblasts. 24 hour serum starved groups were treated with 1, 10 or 20% CSE with or without 50 or 100ng/ml IGF-1. Significant difference at 10%, 20%, 10% or 20% CSE with 50ng/ml, 1% or 20% CSE with 100ng/ml compared to the treatment control samples (*$p<0.05$). Data collected from 3 independent experiments (with 8 measurements per treatment for each condition, n=24) were combined and are represented as +/-S.D.

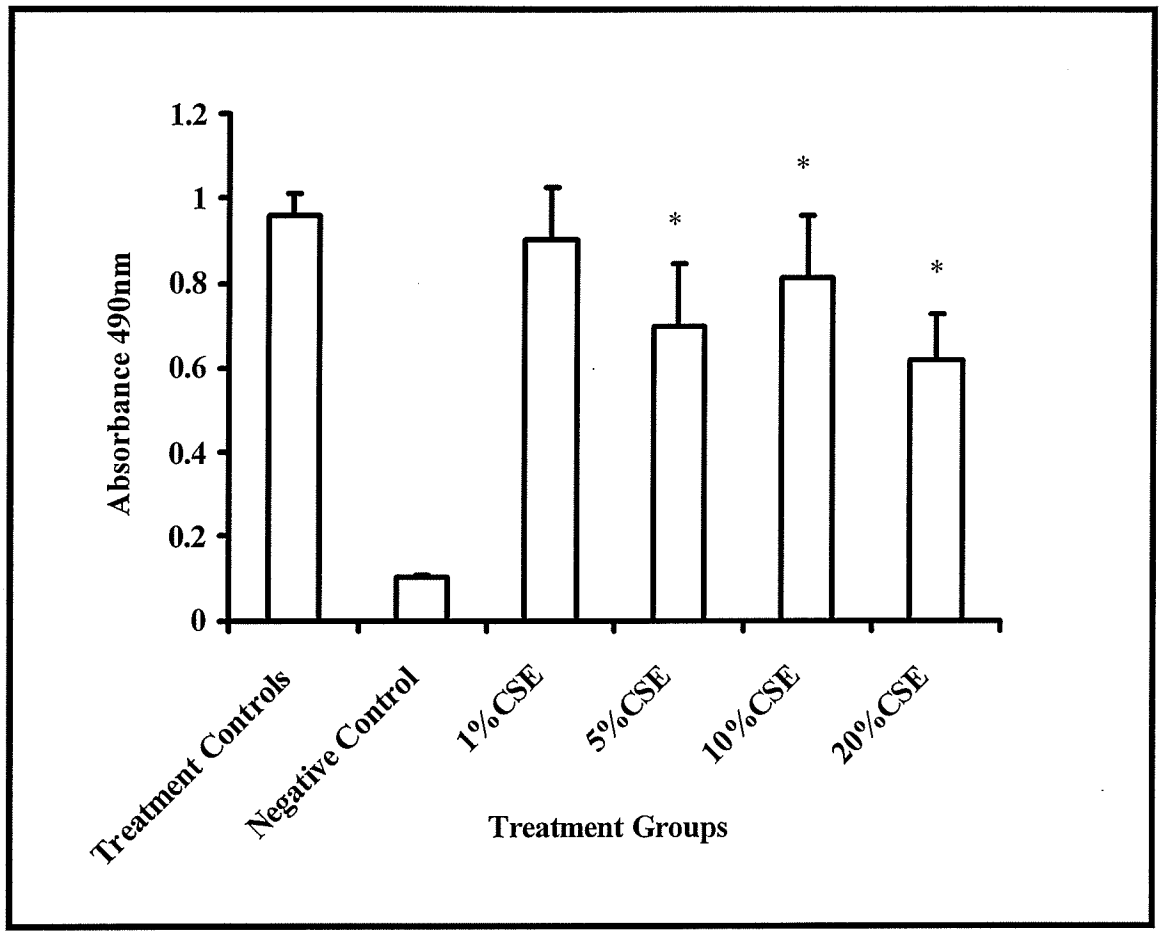

Figure 12: Effects of CSE on cellular metabolic activity from gestational day 21 fetal rat lung fibroblasts. MTS activity in gestational day 21 fetal rat lung fibroblasts exposed to CSE after 24 hour treatment. Maximum activity recorded for serum treated group at 8 hour incubation with significant difference (* $p<0.05$) at 5, 10 or 20% CSE relative to the control samples. Lung fibroblasts treated with hydrogen per oxide served as negative control. Data collected from 3 independent experiments (with 8 measurements per treatment for each condition, n=24) were combined and are represented as +/-S.D.

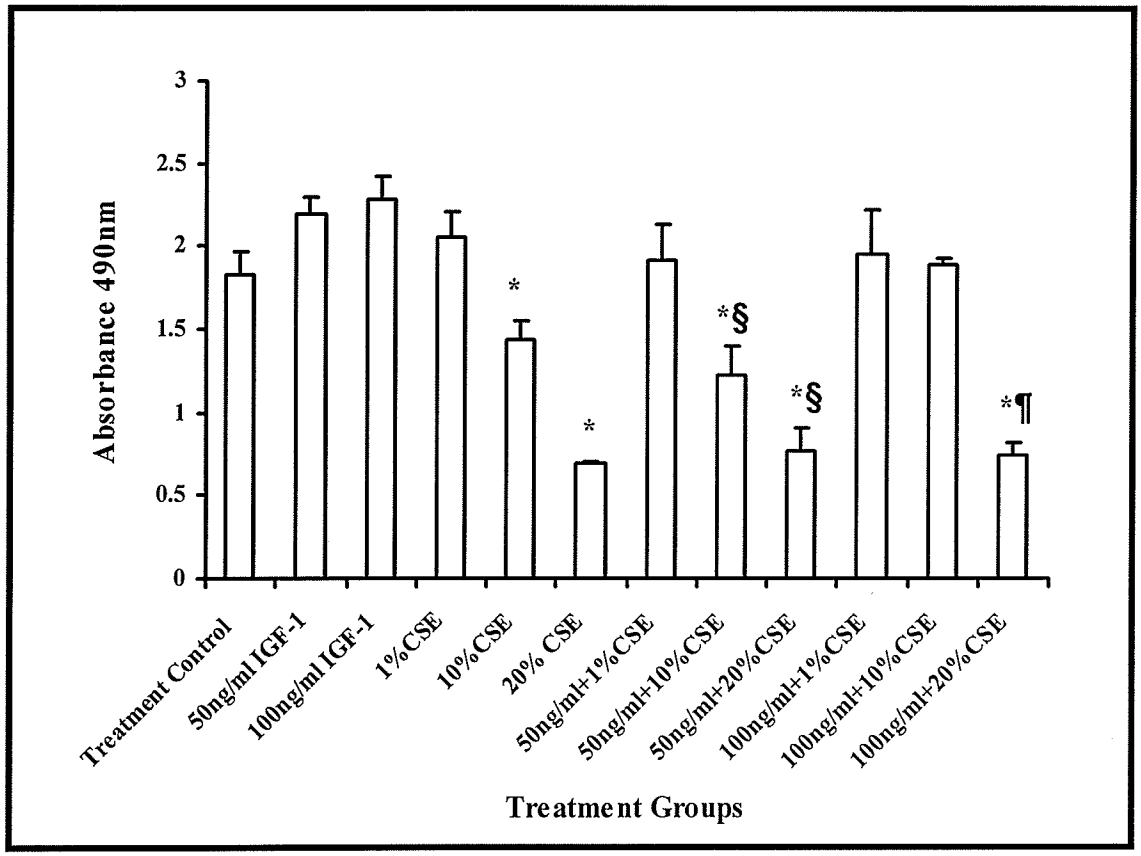

Figure 13: Effects of combined IGF-1 with CSE on cellular metabolic activity from gestational day 21 fetal rat lung fibroblasts. MTS activity in gestational day 21 fetal rat lung fibroblasts exposed to 24 hour CSE treatments. Maximum activity for serum free group at 24 hour incubation with significant difference (* $p<0.05$) at 10%, 20% CSE with or without 50ng/ml compared to controls. (¶ $p<0.05$) at 100ng/ml with 20% CSE compared to 100ng/ml and (§, $p<0.05$) at 10% or 20% CSE with 50ng/ml compared to 50ng/ml. For serum starved state maximum activity recorded at 4 hours with ($p<0.05$) with significant differences at 10 or 20% CSE relative to control samples. Data collected from 3 independent experiments (with 8 measurements per treatment for each condition, n=24) were combined and are represented as +/-S.D.

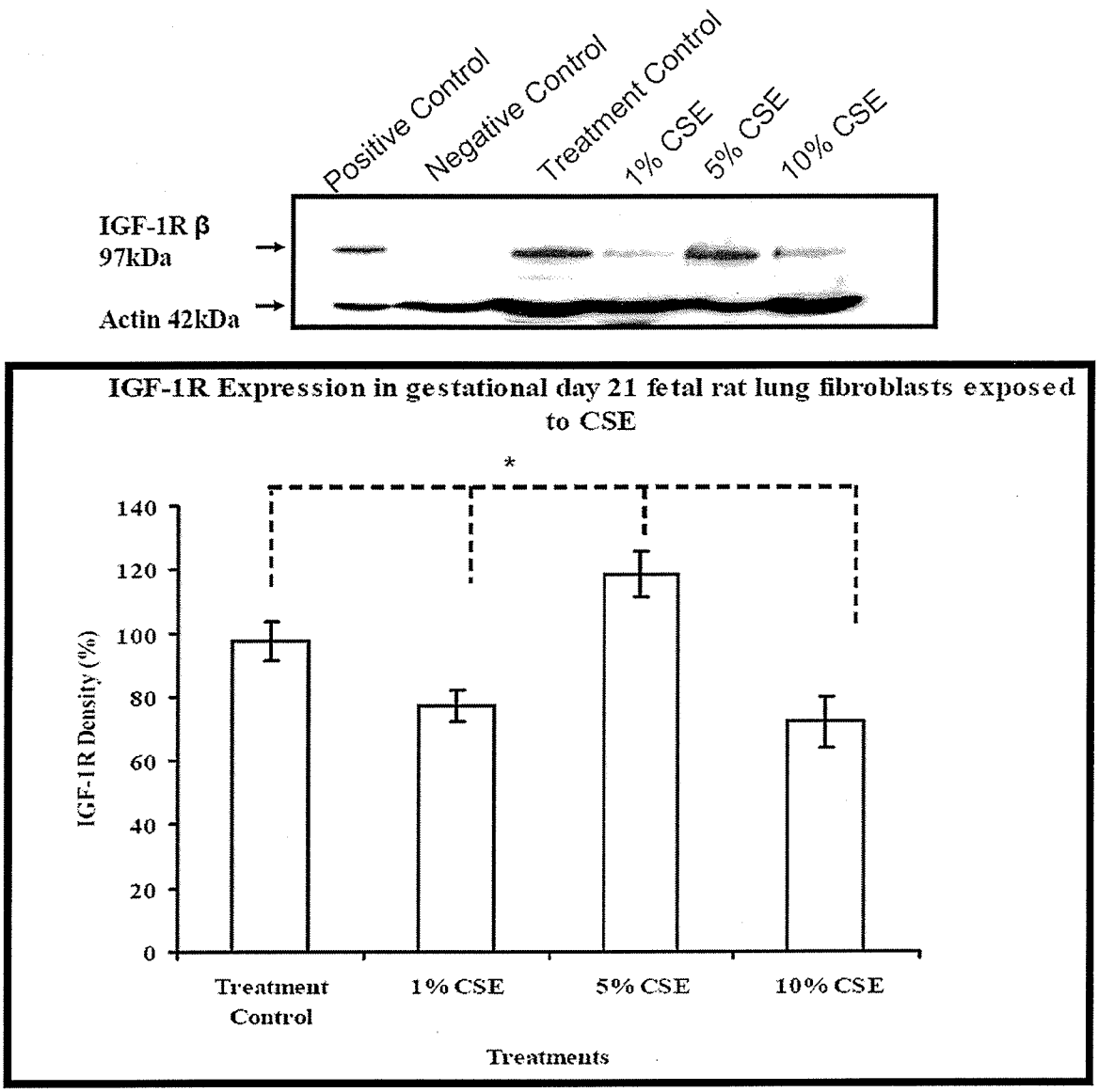

Figure 14: Effect of CSE on IGF-1R β protein expression from 21 gestational day fetal rat lung fibroblasts. Representative Western blot showing IGF-1Rβ expression in lung fibroblasts treated with 1, 5, or 10% CSE for 24 hour time period. Hela cell lysates were positive controls and mouse liver extract as negative control controls. Antibody against actin was used to assess uniform loading of 50μg of samples per lane. Densitometric quantitation of IGF-1Rβ native expression for 24 hour time point in fetal rat lung fibroblasts exposed at 1, 5, or 10% CSE concentrations. (*) Indicates ($p<0.05$) significant differences at 1, 5, or 10% CSE relative to the controls. Statistical representation of +/-S.E from 4 independent blots from two independent experiments.

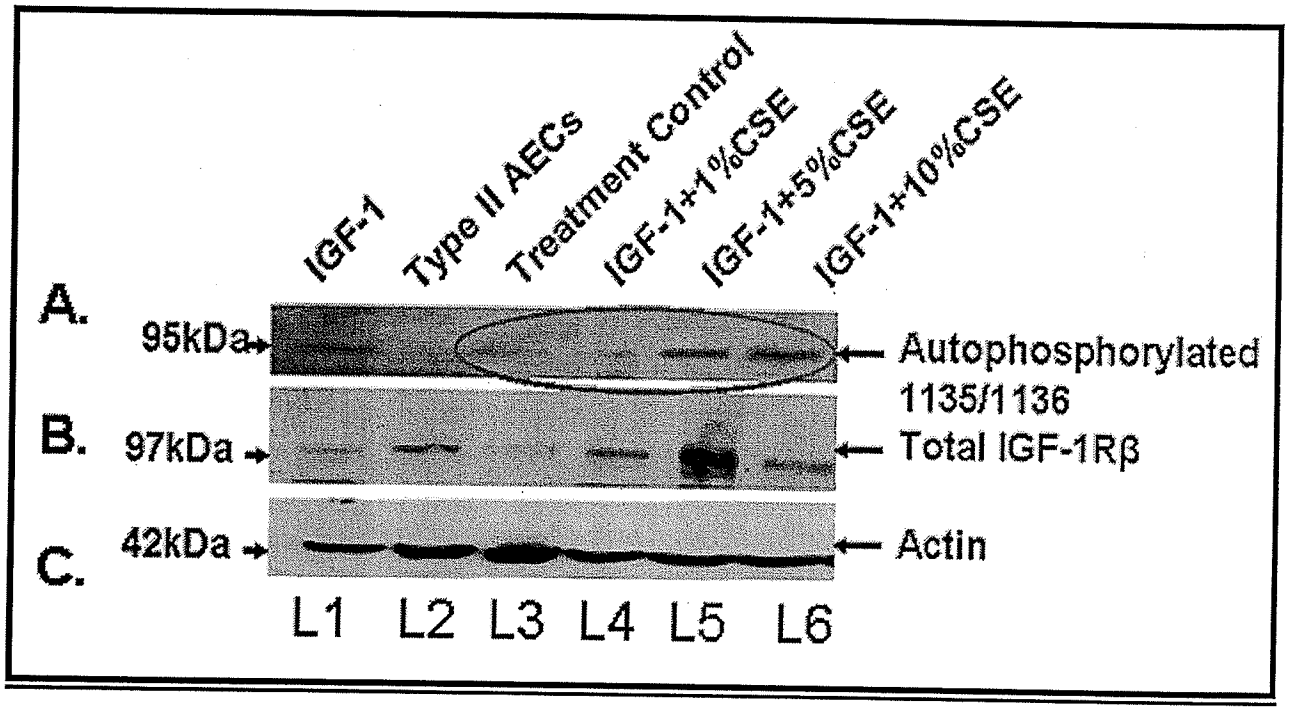

Figure 15: Effect of CSE on Autophosphorylation of IGF-1R β from gestational day 21 fetal rat lung fibroblasts Western blot representative of autophosphorylated IGF-1R β subunit at 1135/1136 subunit in lung fibroblasts from gestational day 21 rat lungs. Cells treated with or without IGF-1 served as positive and negative controls.

A. Represents autophosphorylated expression in different groups.
B. Represents native IGF-1 receptor expression.
C. Represents loading control assessed with antibody against house keeping gene beta actin.(L, lane) L1, Positive control, L2, Negative control, L3 Treatment control, L 4,5,6, 1%, 5% or 10% CSE with 100ng/ml.

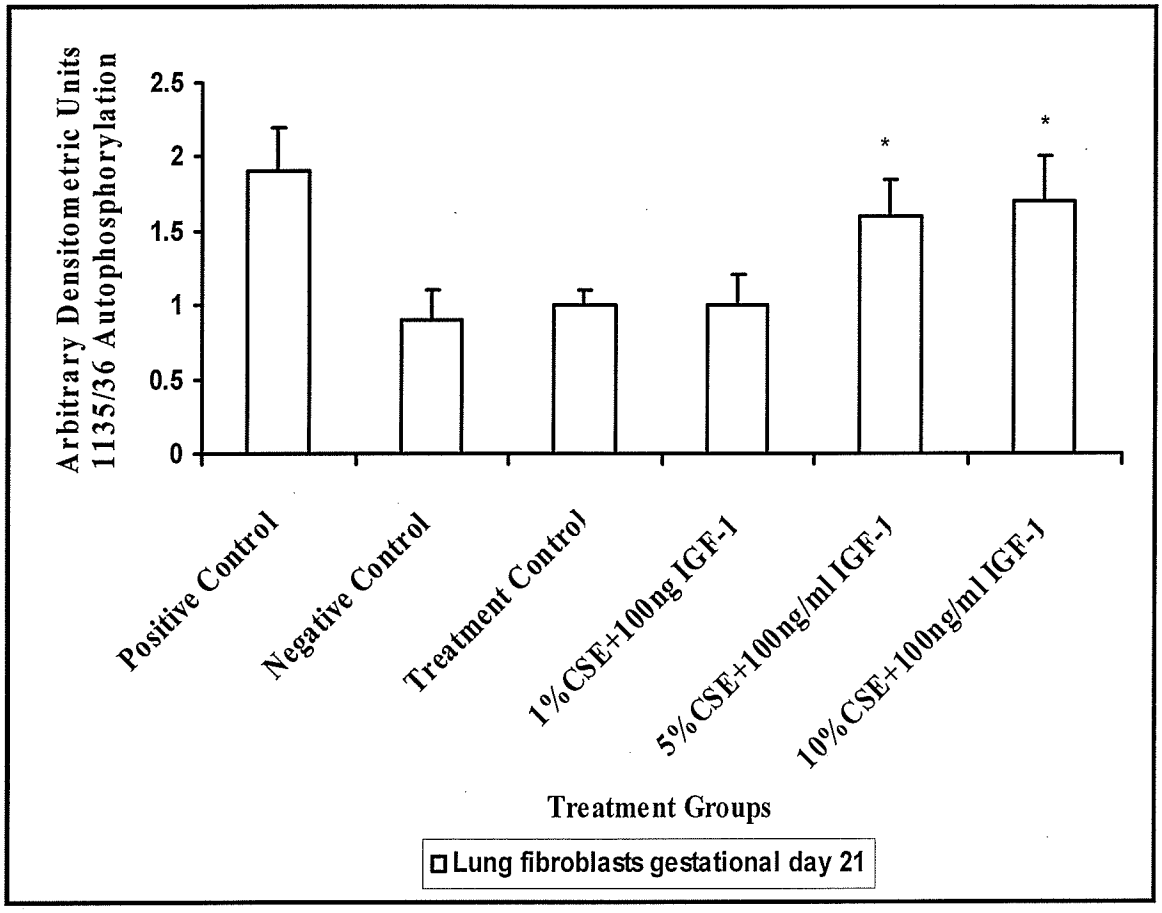

Figure 16: Effect of CSE on Autophosphorylation of IGF-1R β from gestational day 21 fetal rat lung fibroblasts Representative blot for autophosphorylated expression of IGF-1R in fetal rat lung fibroblasts exposed to CSE. Cells treated with or without IGF-1 served as positive and negative control. Data indicates (*) ($p<0.05$) at 5 or 10% CSE with100ng/ml IGF-1 relative to the treatment control. Statistical representation of +/-S.E from 3 independent blots.

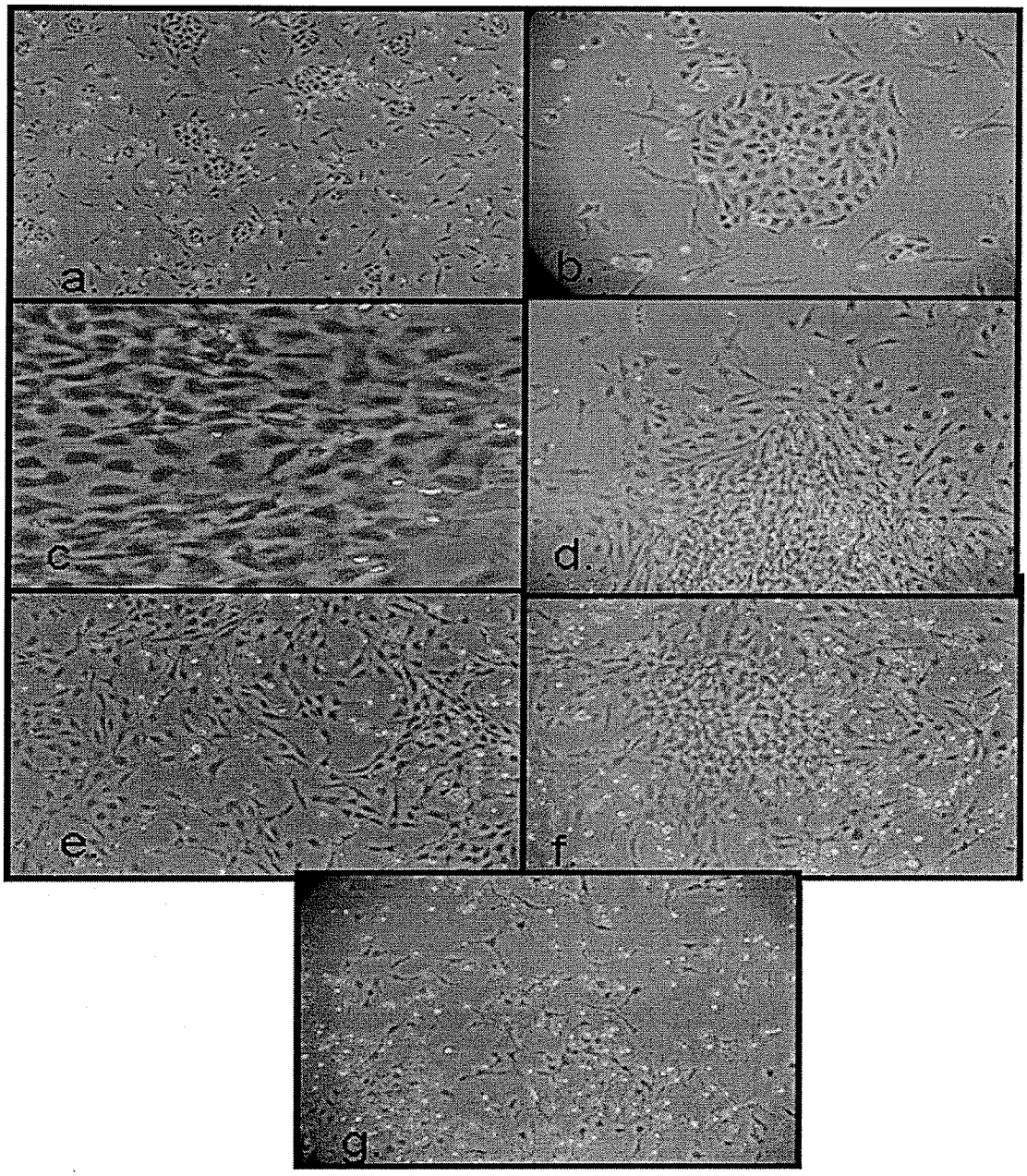

<u>Figure 17:</u> Lung Type II AECs from gestational day 21 fetal rat in response to CSE exposures after 24 hours. Images at 4x magnification through phase contrast microscope.

(a, b). Type II AECs growing in colonies in interaction with fibroblasts.
(c). Treatment Controls
(d). Type II AECs in response to 1% CSE,
(e). Type II AECs in response to 5% CSE, (f) 10% CSE and (g) 20% CSE.

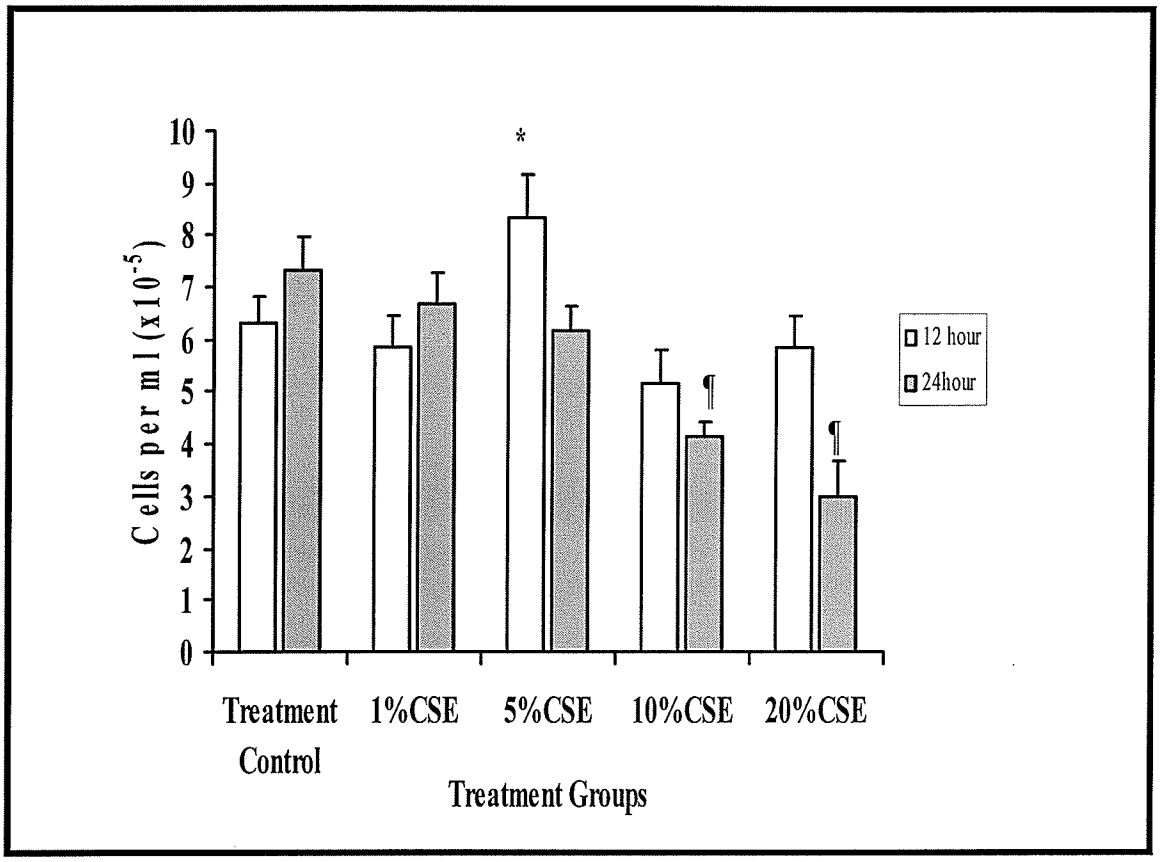

Figure 18: Effect of CSE on cell numbers from gestational day 21 fetal rat lung type II AECs. Cell numbers for fetal Type II AECs upon CSE exposure for 12 or 24 hours. At 12 hour time point (*) indicates ($p<0.05$) compared to the control groups. At 24 hour time point (¶) indicates ($p<0.05$) at 10 or 20% CSE compared to the control samples. Data collected from 2 independent experiments (with 5 measurements per treatment for each condition, n=10) were combined and are represented as +/-S.D.

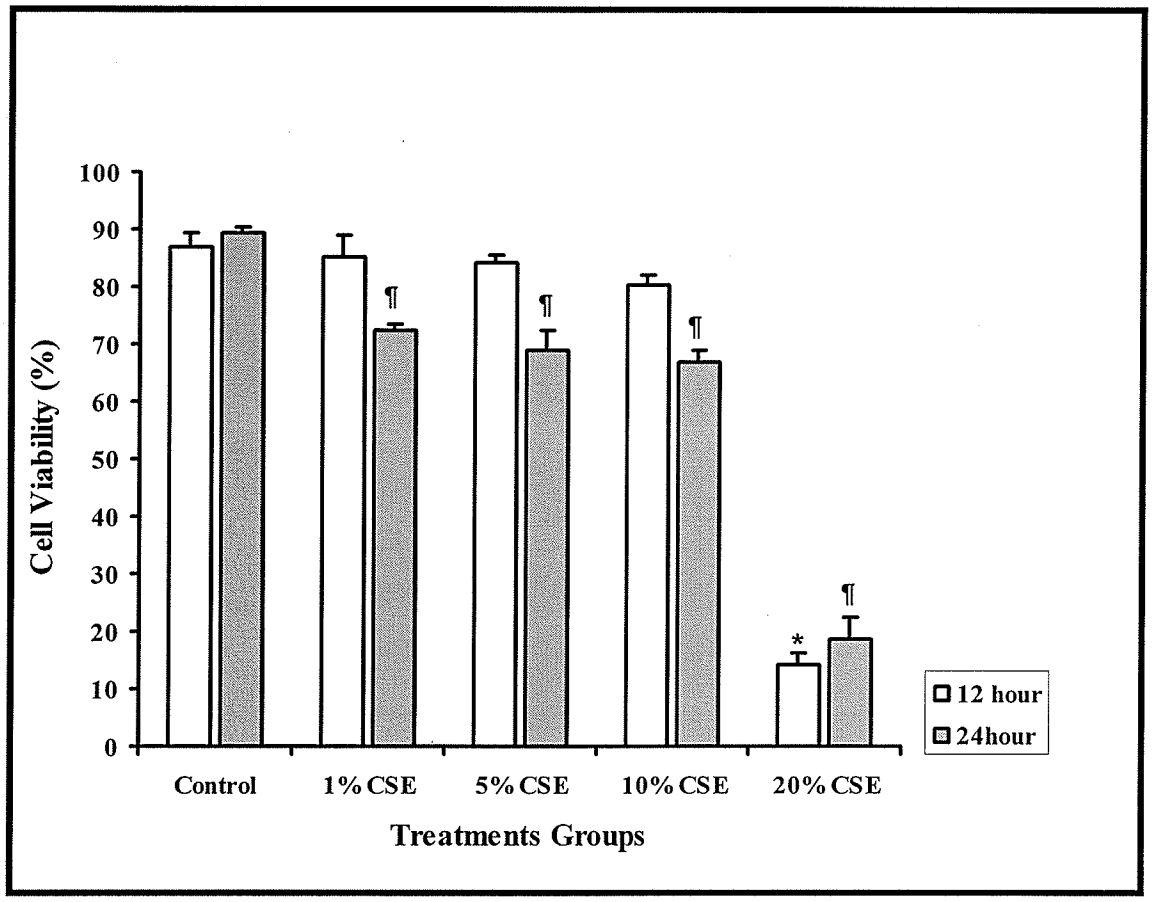

Figure 19: Effect of CSE on cell viability from gestational day 21 fetal rat lung type II AECs. Cell viability determined by Trypan blue exclusion of fetal rat Type II AECs upon CSE exposure for 12 or 24 hours. At 12 hour time point (*) indicates ($p<0.05$)at 20% CSE relative to the control groups. At 24 hour time point (¶) indicates ($p<0.05$) at 1, 5, 10, or 20% CSE relative to the control groups. Data collected from 2 independent experiments (with 5 measurements per treatment for each condition, n=10) were combined and are represented as +/-S.D.

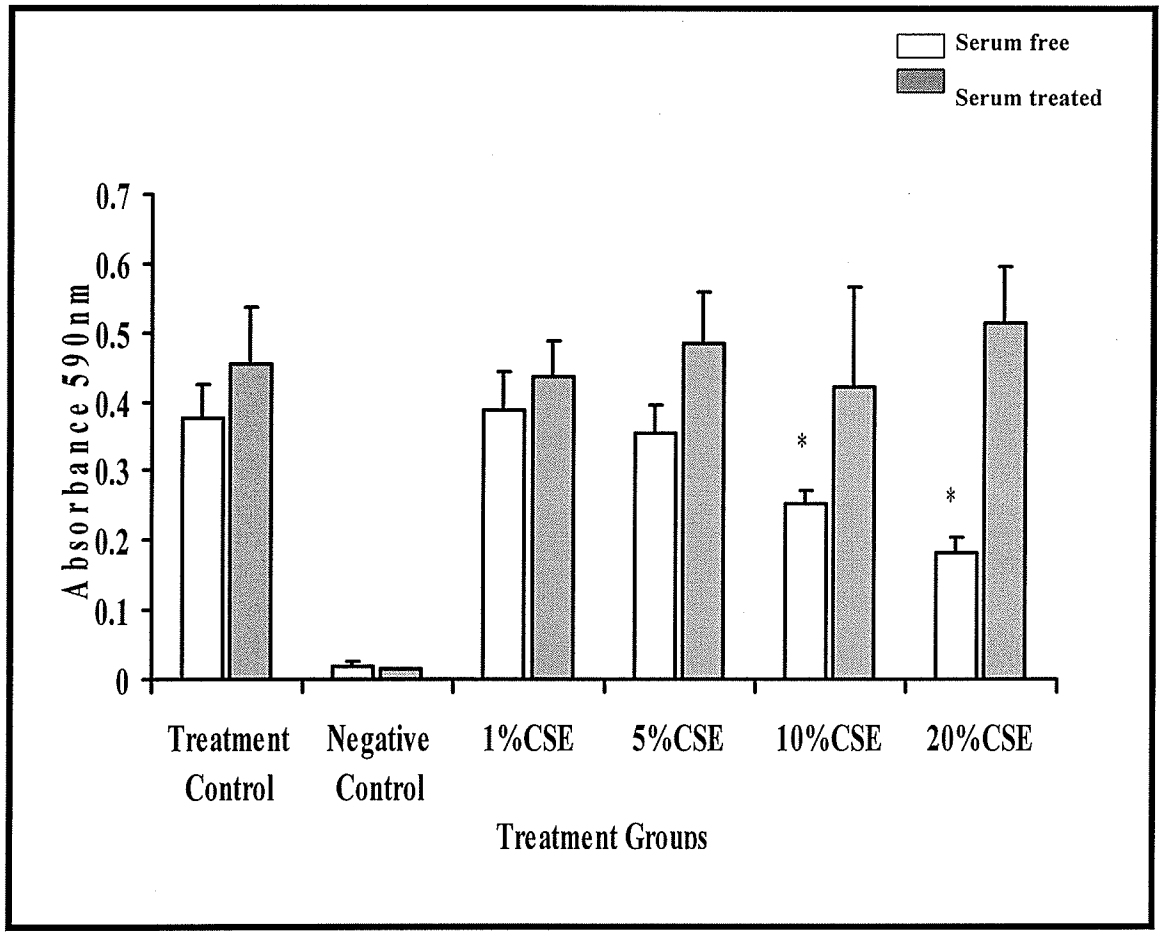

Figure 20: Effects of CSE on proliferative capacity from gestational day 21 fetal rat lung type II AECs. Crystal violet proliferation assay to assess the effect of CSE on serum starved and serum contained Type II AECs proliferation for 24 hour time point. Significant difference ($p<0.05$) at 10 or 20% CSE relative to the control samples in serum starved groups. Hydrogen peroxide served as negative control. Data collected from 3 independent experiments (with 8 measurements per treatment for each condition, n=24) were combined and are represented as +/-S.D.

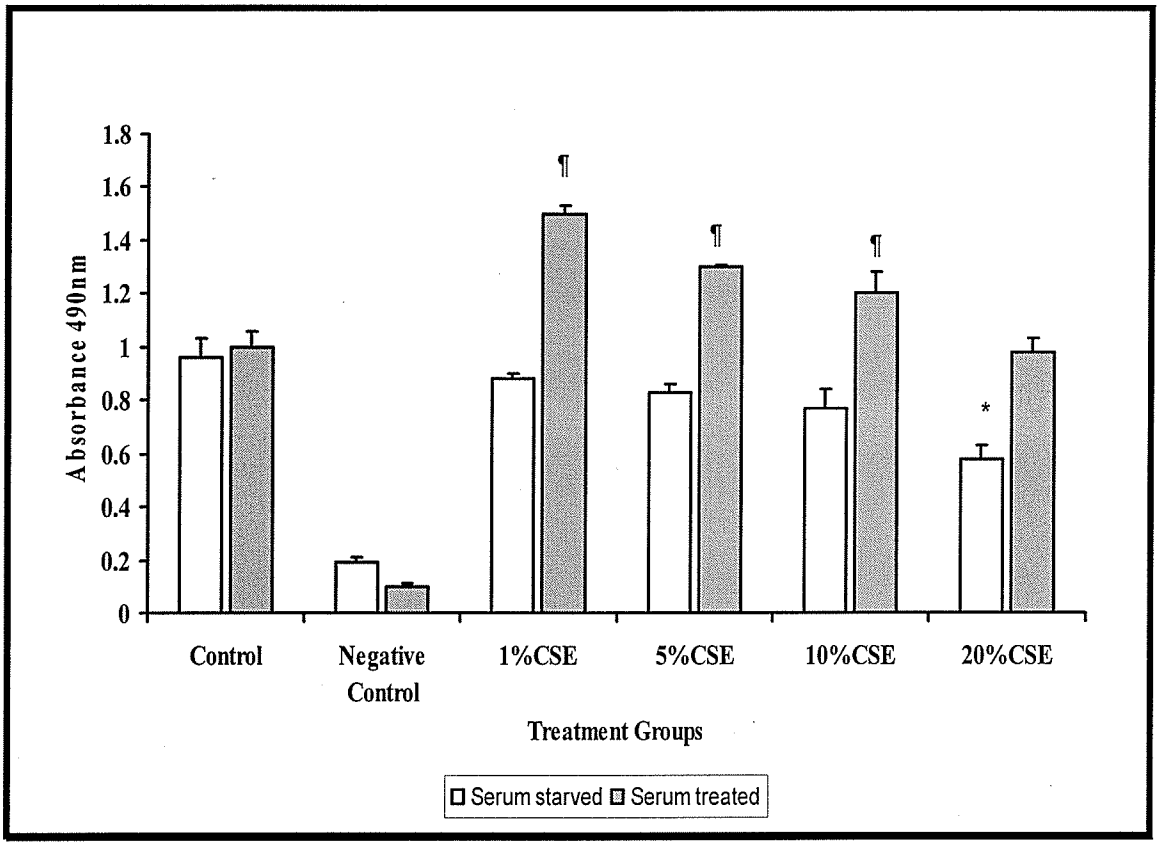

Figure 21: Effects of CSE on cellular metabolic activity from gestational day 21 fetal rat lung type II AECs. MTS activity in serum starved and serum contained Type II AECs exposed to 24 hour CSE treatments.In serum contained CSE treated groups at 24 hour point of incubation (¶) indicates significant differences ($p<0.05$) recorded at 1,5,or 10% CSE compared to the controls. In serum starved CSE treated group at 24 hour time point (*) indicates significant differences ($p<0.05$) at 20% CSE relative to the controls. Data collected from 3 independent experiments (with 8 measurements per treatment for each condition, n=24) were combined and are represented as +/-S.D.

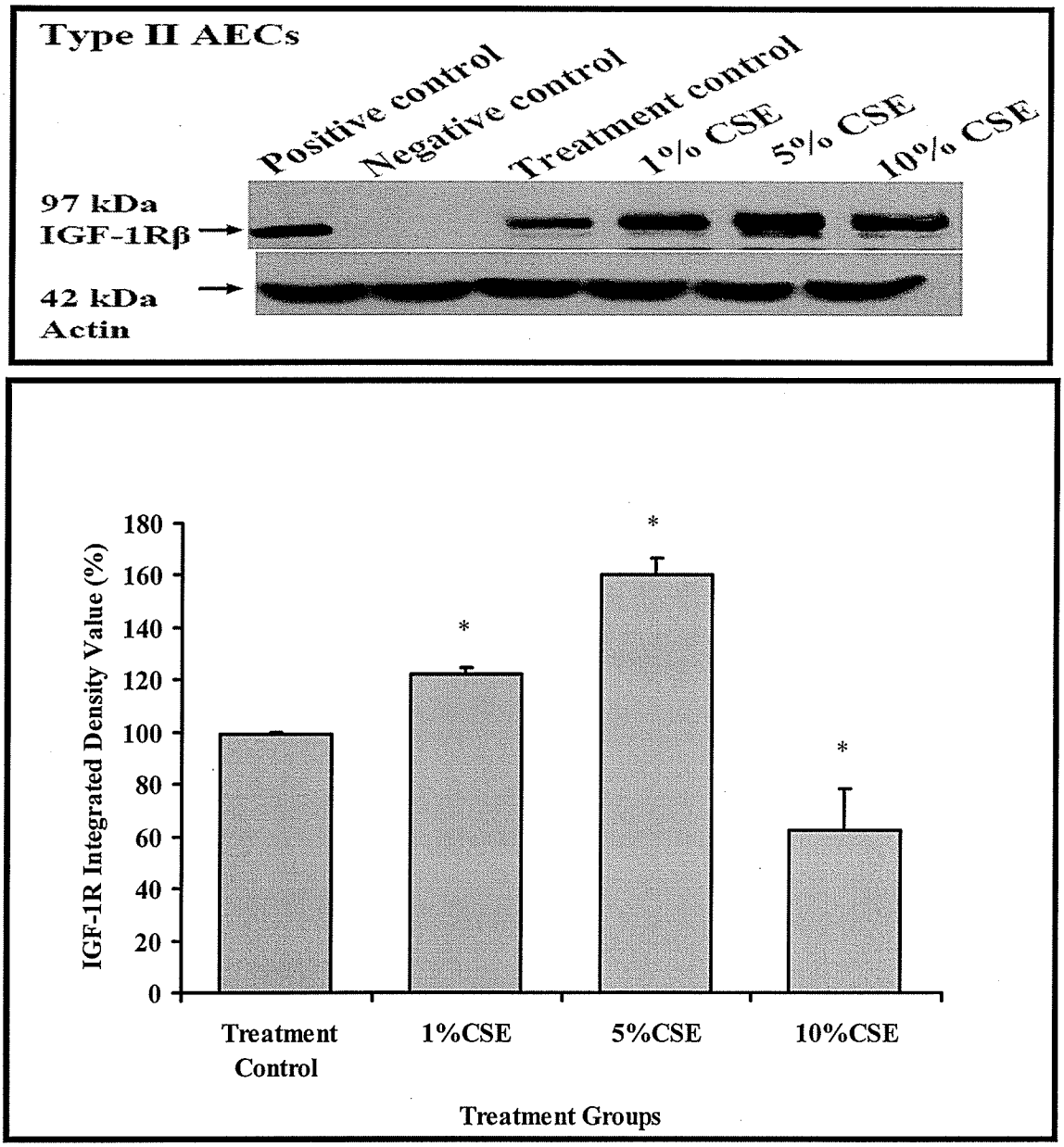

Figure 22: Effects of CSE on IGF-1Rβ from gestational day 21 fetal rat lung type II AECs. Representative Western blot showing IGF-1R expression in Type II AECs treated with 1, 5, or 10% CSE concentrations for 24 hour time period. Hela cells lysate served as positive control and mouse liver extract as negative control. Densitometric quantitation of IGF-1R expression in Type II AECs exposed to CSE. Type II AECs were treated with 1, 5, or 10% CSE dilutions. (*) Indicates ($p<0.05$) at 5 or 10% CSE compared to the controls. Statistical representation of +/-S.E from 4 independent blots from 2 independent experiments.

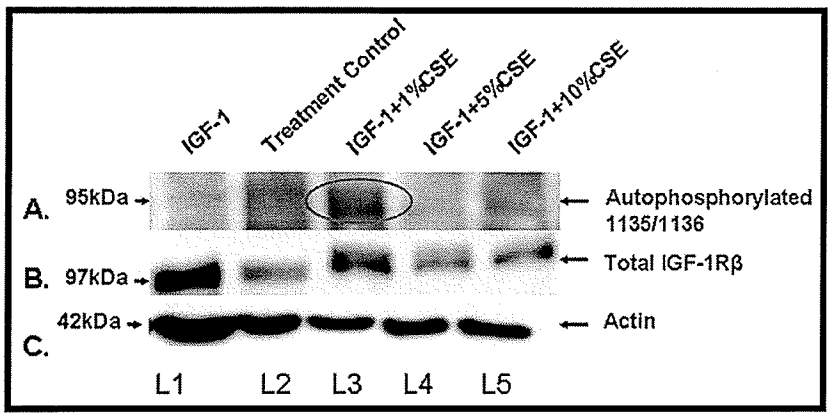

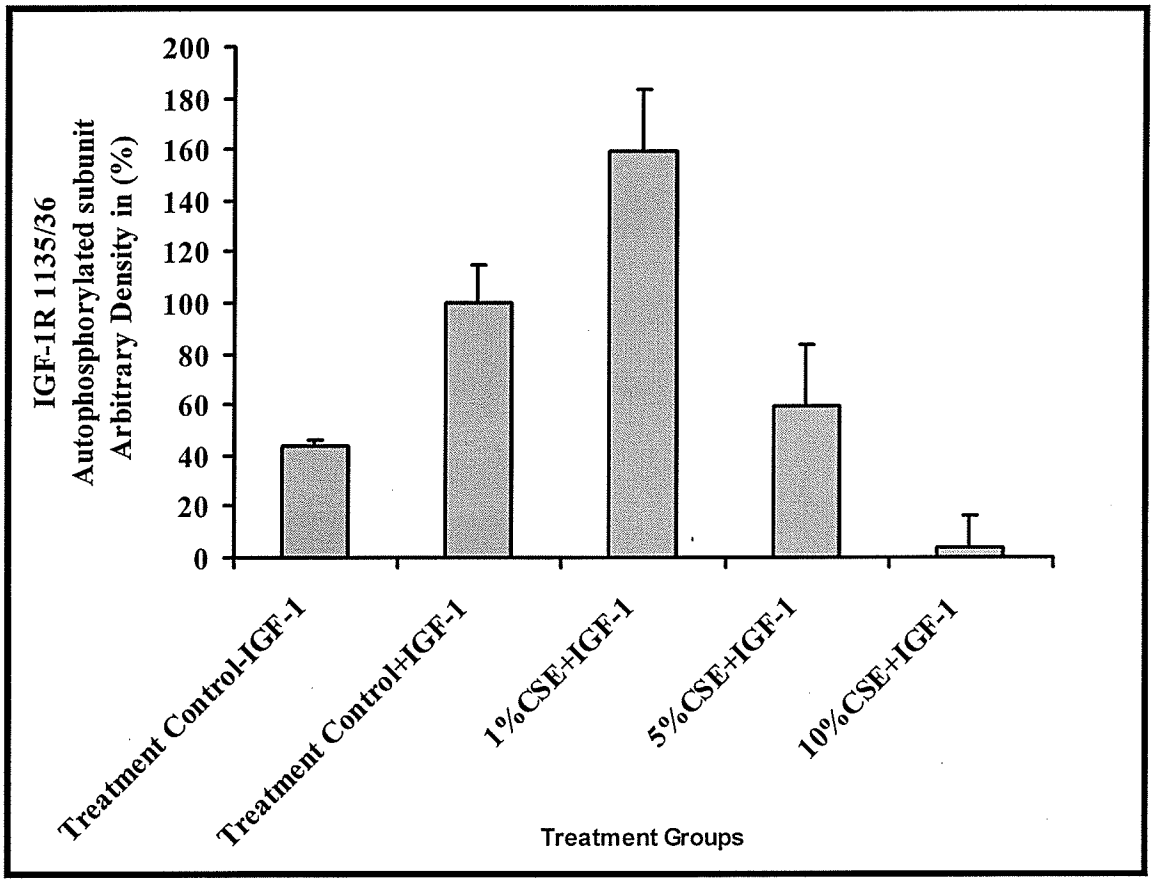

Figure 23: Effect of CSE on Autophosphorylation of IGF-1R β from gestational day 21 fetal rat lung type II AECs. Representative Western blot for autophosphorylated IGF-1R beta receptor at 1135/36 subunits in Type II AECs. Type II AECs stimulated with IG-1 at 200ng/ml served as positive controls. Type II AECs treated with 24 hour CSE concentrations were stimulated with IGF-1 at 200ng/ml. L1 Negative control without IGF-1, L2 Controls with IGF-1 200ng/ml, L3, L4, L5 1, 5 or 10% CSE with IGF-1 at 200ng/ml. (A) Autophosphorylated receptor expression, (B) Native receptor expression, (C) Loading control assessed with beta actin house keeping gene.

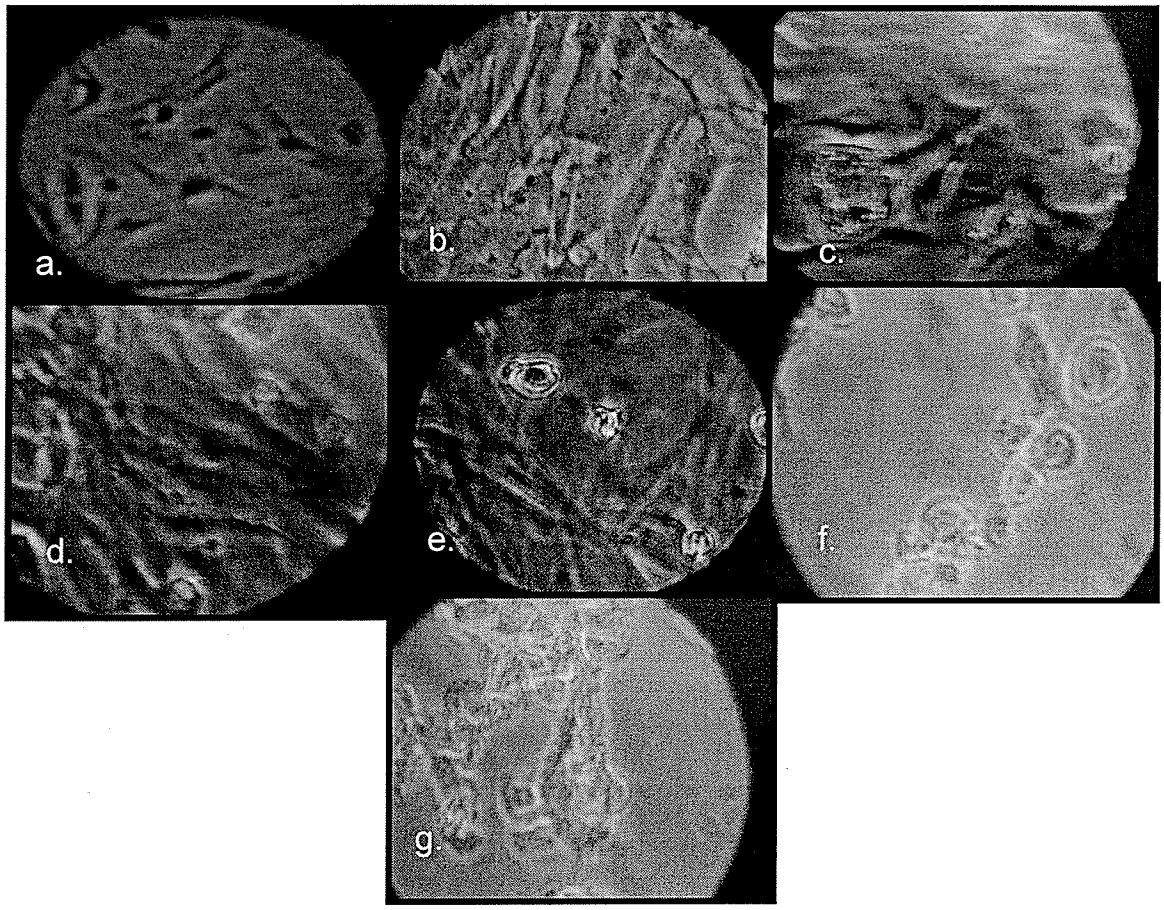

Figure 24: Postnatal day one lung fibroblasts cells in response to 24 hour CSE exposures: (a) Treatment Control, (b) 0.1% CSE, (c) 0.01%, (d) 1% CSE, (e) 10% CSE, (f) 25% CSE, (g) 50% CSE. Images at 10x magnification through phase contrast microscope.

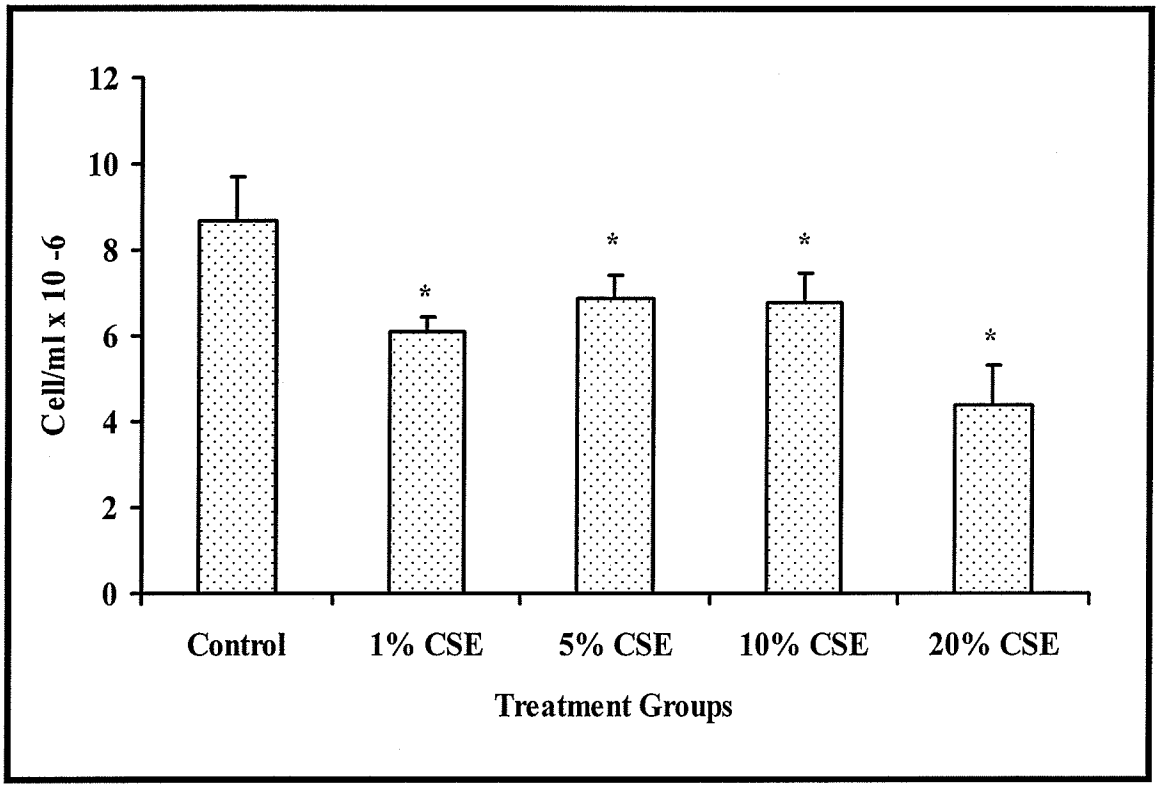

Figure 25: Effects of CSE on cell numbers from postnatal day one rat lung fibroblasts Cell numbers for day one rat lung fibroblast upon CSE exposure for 24 hours. At 24 hour time point (*) indicates ($p<0.05$) in 1,5,10 or 20% CSE compared to the control groups. Data collected from 2 independent experiments (with 5 measurements per treatment for each condition, n=10) were combined and are represented as +/-S.D.

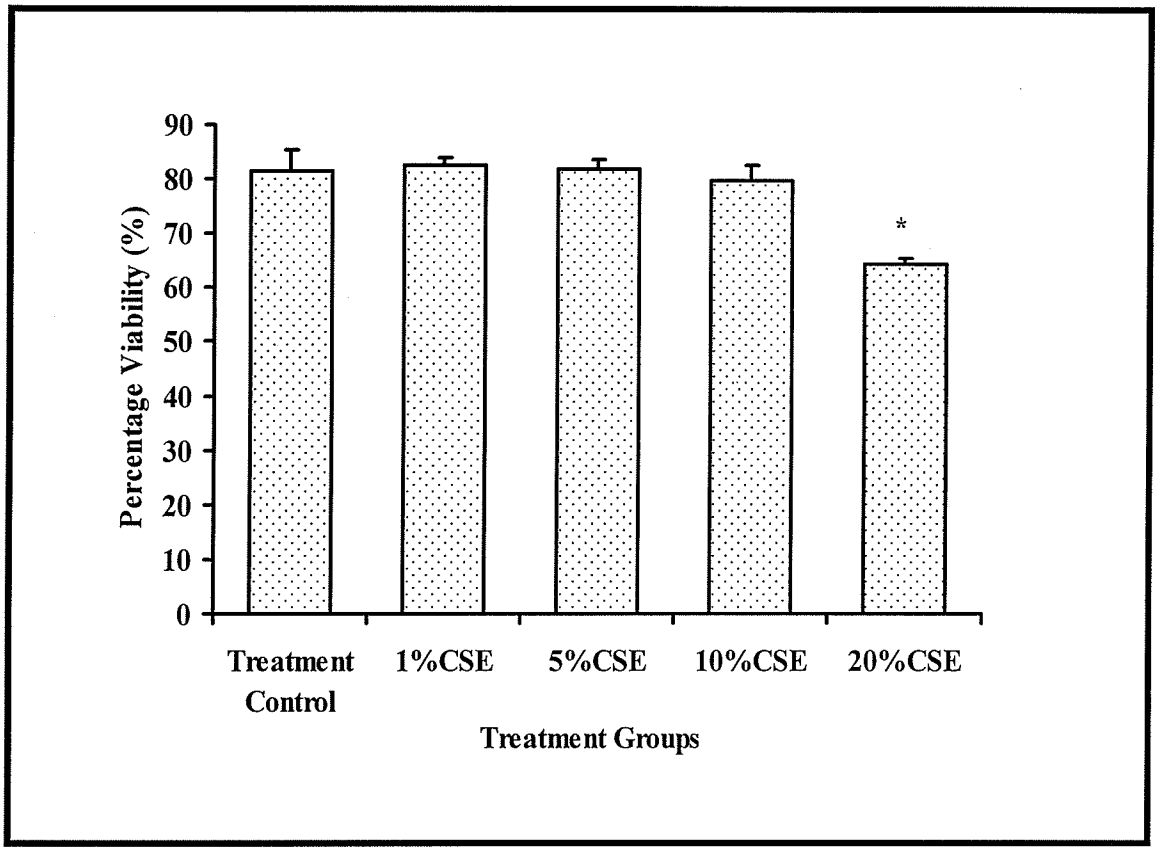

Figure 26: Effects of CSE on cell viability from postnatal day one rat lung fibroblasts Trypan Blue Exclusion by day one rat lung fibroblasts exposed to CSE. At 24 hours (*) indicates significant difference ($p<0.05$) at 20% CSE relative to the controls. Data collected from 2 independent experiments (with 5 measurements per treatment for each condition, n=10) were combined and are represented as +/-S.D.

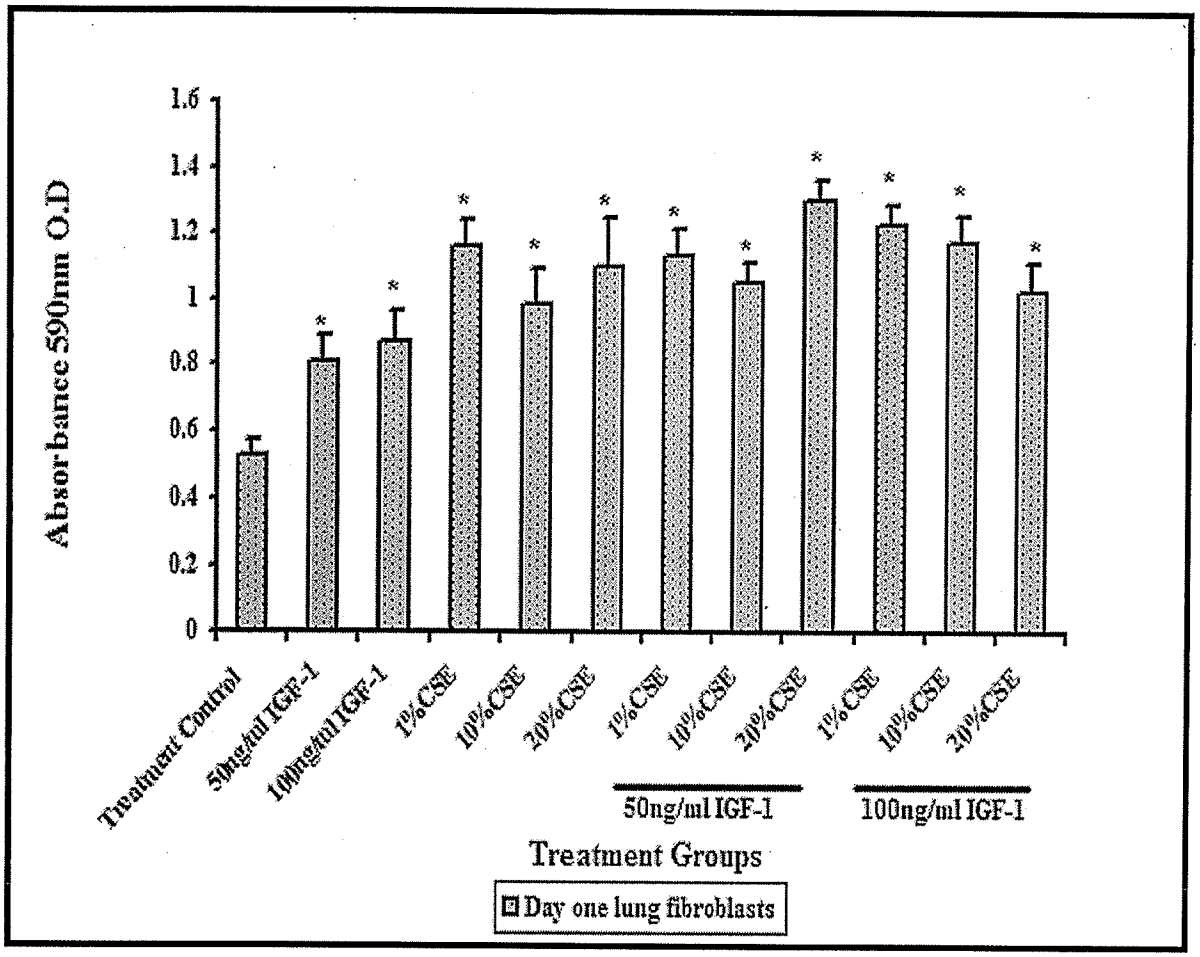

Figure 27: Effects of combined IGF-1 with CSE on proliferative capacity from postnatal day one rat lung fibroblasts Crystal violet assay to assess proliferative effect of CSE on day one rat lung fibroblasts for 24 hour. Serum starved groups were treated with 1,5,10 or20% CSE with or without IGF-1 at 50 or 100ng/ml. (*) Indicates significant difference at 50ng/ml, 100ng/ml IGF-1, 1, 5, 10 or 20% CSE with or without IGF-1 at 50 or 100ng/ml ($p<0.05$) compared to the control group. Data collected from 3 independent experiments (with 8 measurements per treatment for each condition, n=24) were combined and are represented as +/-S.D.

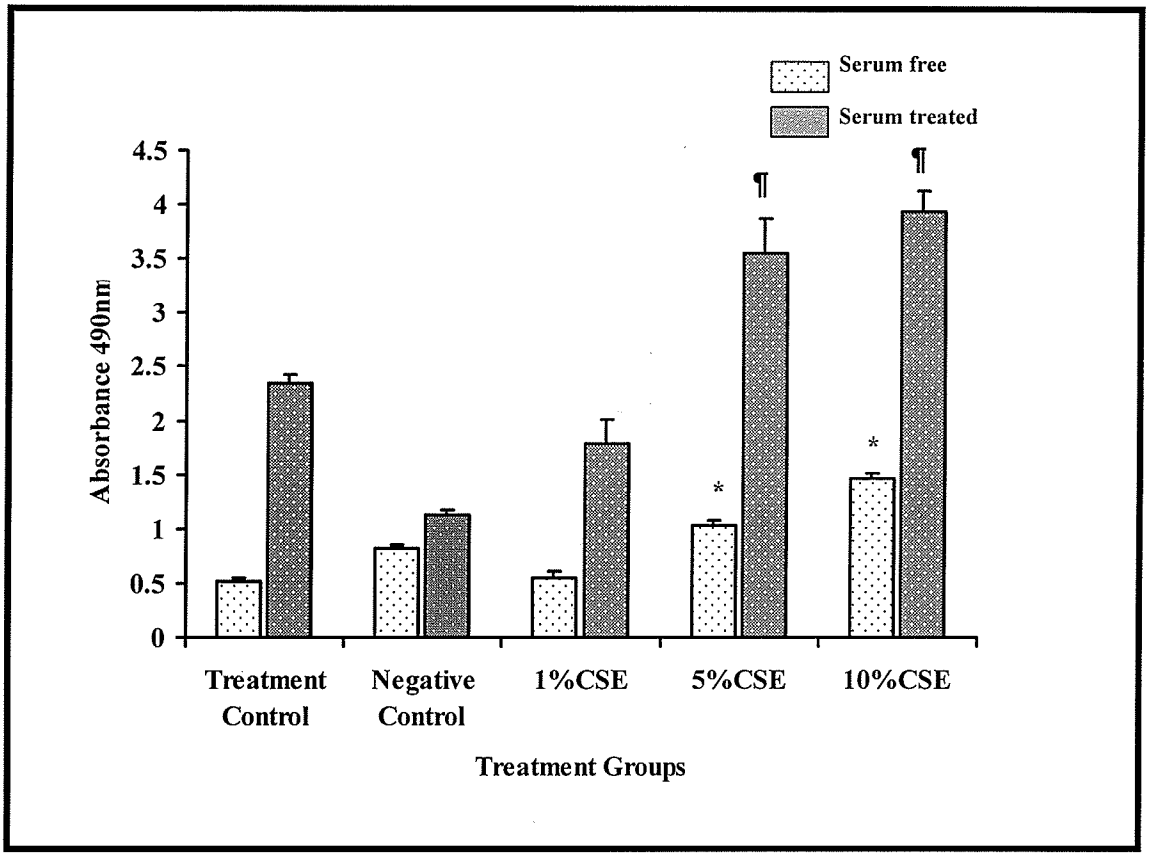

Figure 28: Effects of CSE on cellular metabolic activity from postnatal day one rat lung fibroblasts MTS Activity recorded in day one rat lung fibroblasts exposed to 24 hour CSE. Maximum activity recorded for serum contained at 4 hour incubation with significant difference ($p<0.05$) at 5 or 10% CSE relative to the control samples. For serum starved state maximum activity recorded at 4 hours with ($p<0.05$) with significant differences at 5 or 10% CSE relative to control samples. Lung fibroblasts treated with hydrogen per oxide served as negative control. (* for serum starved, ¶ for serum contained). Data collected from 3 independent experiments (with 8 measurements per treatment for each condition, n=24) were combined and are represented as +/-S.D.

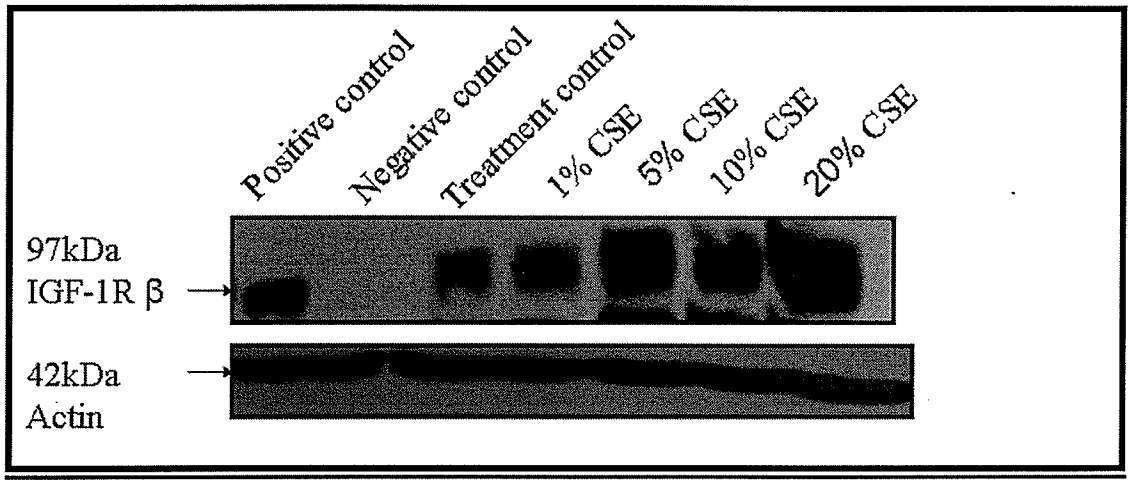

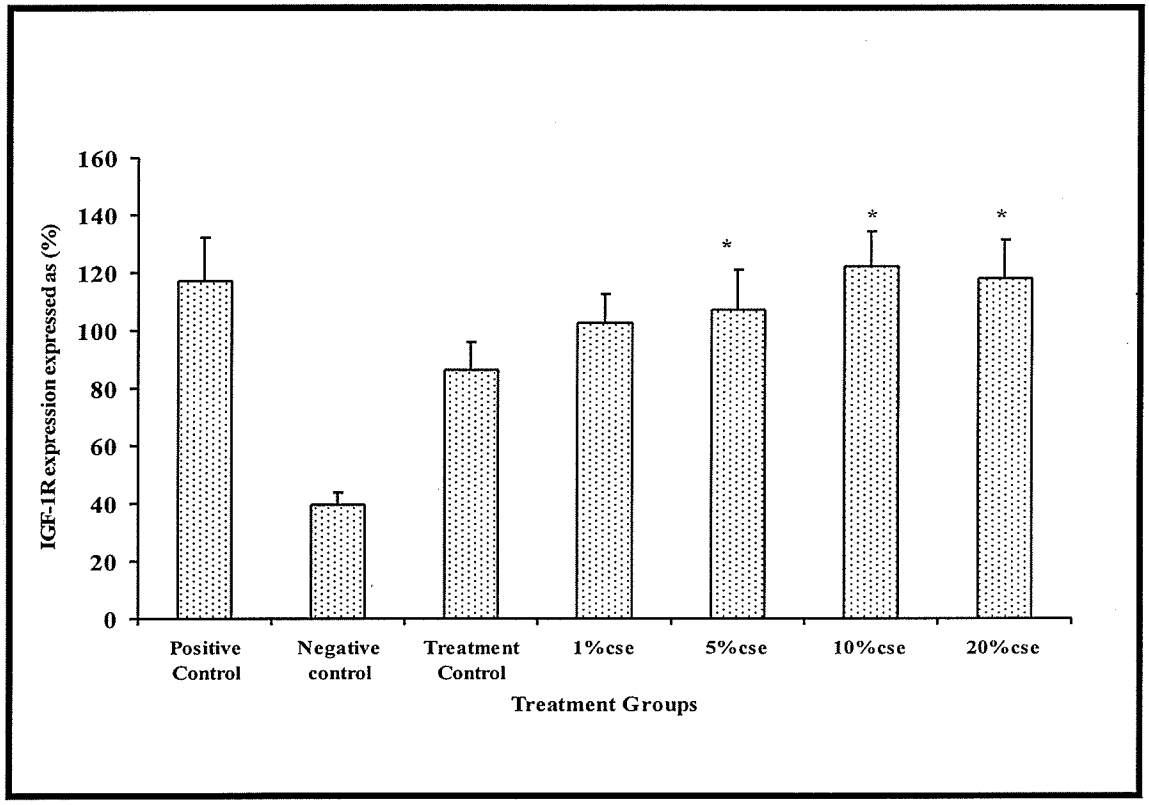

Figure 29: Effect of CSE on IGF-1R β protein expression in postnatal day one rat lung fibroblasts Western blot for native IGF-1R expression. Representative Western blot showing IGF-1Rβ expression in day one rat lung fibroblasts treated with 1, 5, 10, or 20% CSE for 24 hour time period. Hela cell lysates were (+ve) controls and mouse liver extract as negative control (-ve) controls. Antibody against actin was used to assess uniform loading of 50μg of samples per lane. Densitometric quantitation of IGF-1Rβ native expression for 24 hour time point in day one rat lung fibroblasts exposed at 1%, 5%, 10% or 20% CSE concentrations. (*) Indicates ($p<0.05$) significant differences at 5%, 10% or 20% CSE compared to the controls. Statistical representation of +/-SE from 3 independent blots.

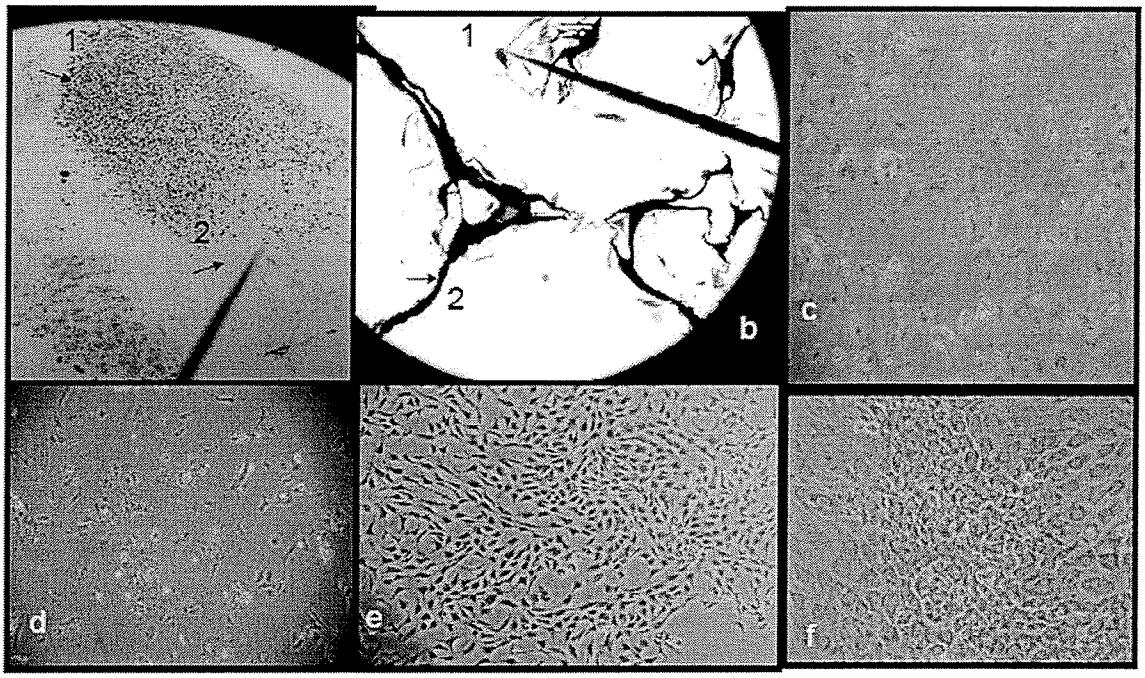

Figure 30: Histological features of rat mandibular condyle

(a) Mandibular condyle from gestational day 21 fetal rat (4x).
(b) Fibroblast like cells grown in gel foam sponges (10x). Figure a[1]. Proliferating zone, a.[2] cartilage like cells, b1. Fibroblast like cells, b[2]. gel foam threads.

Mandibular condylar fibroblasts cells from gestational day 21 fetal rat in cell cultures with changing phenotypes

(c) 0 hour cells in culture
(d) 5 hours in cell cultures
(e) 48 hours confluent cells with spindle shaped morphology
(f) Cuboidal shaped cartilage like cells at one week.

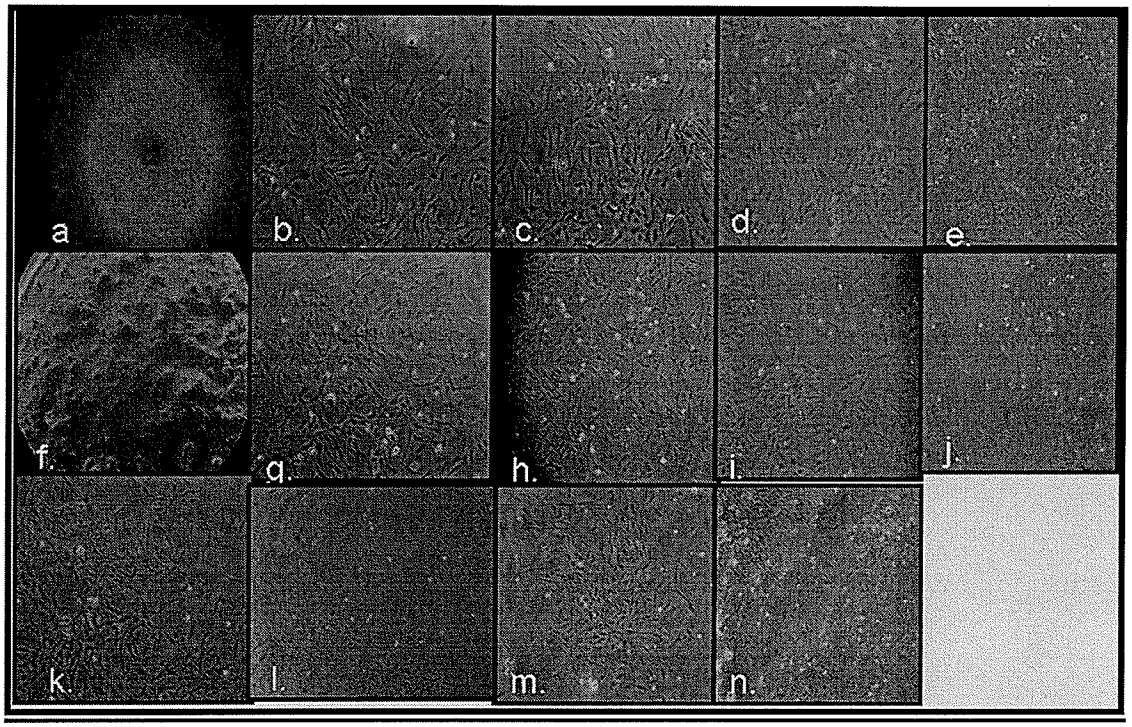

Figure 31: Mandibular condylar fibroblasts cells in response to 24 hour CSE exposures: Phase contrast microscopy for cells treated with CSE at concentrations from 1-20% CSE with IGF-1 at 50 or 100ng/ml concentrations.(4x magnification).
a). treatment control,
b). 1% CSE,
c). 5% CSE,
d). 10% CSE,
e). 20% CSE,
f). hydrogen per oxide treatment
g). 1%CSE with 50ng/ml IGF-1
h). 5% CSE with 50ng/ml IGF-1
i). 10% with 50ng/ml IGF-1
j). 20% with 50ng/ml IGF-1
k). 1% with 100ng/ml IGF-1
l). 5% with 100ng/ml IGF-1
m). 10% with 100ng/ml IGF-1
n). 20% with 100ng/ml IGF-1.

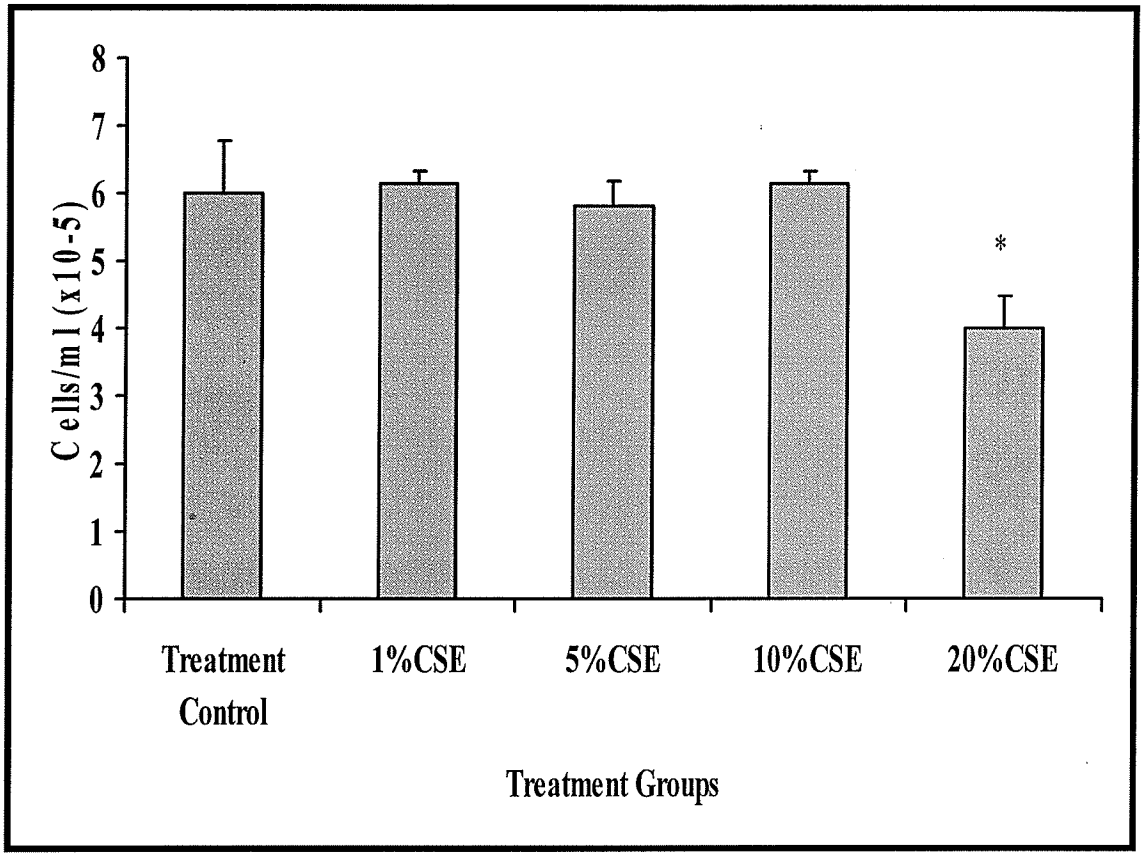

Figure 32: Effects of CSE on cell numbers from gestational day 21 fetal rat mandibular condylar fibroblasts Cell numbers for gestational day 21 fetal rat mandibular condylar fibroblasts upon CSE exposure for 24 hours at 1, 5, 10 or 20% CSE concentrations. ($p<0.05$) at 20% CSE relative to the control group. Data collected from 2 independent experiments (with 5 measurements per treatment for each condition, n=10) were combined and are represented as +/-S.D.

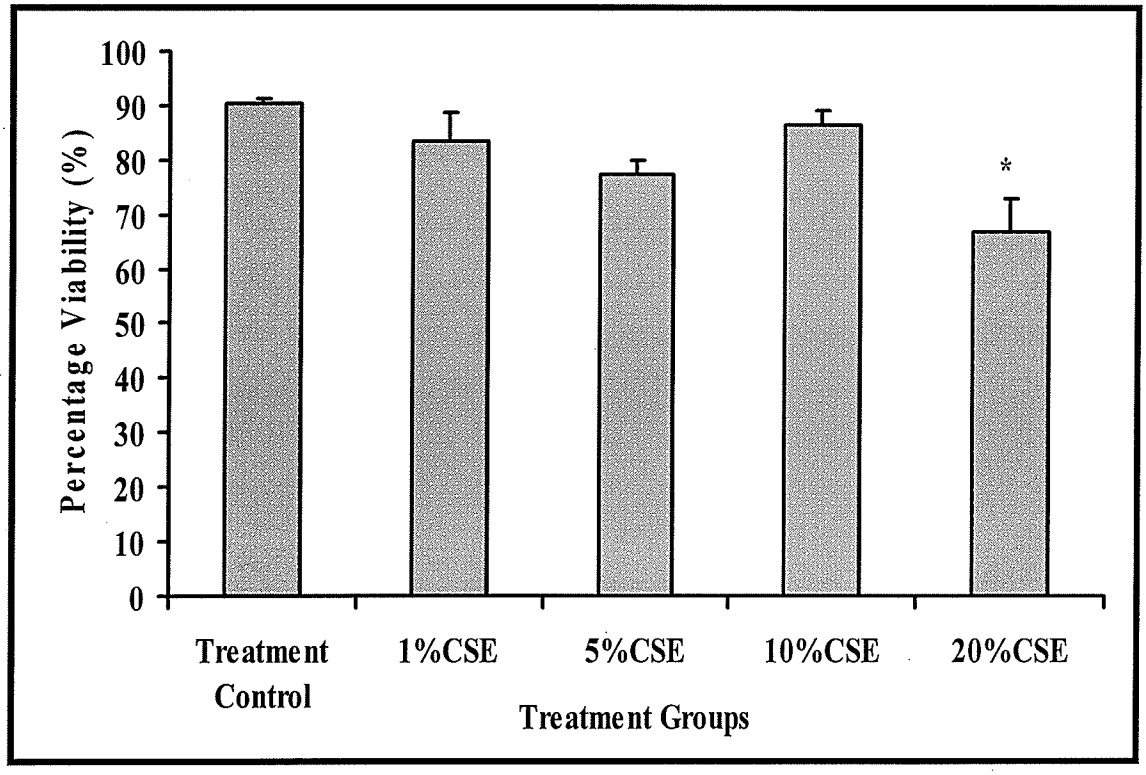

Figure 33: Effects of CSE on cell viability from gestational day 21 fetal rat mandibular condylar fibroblasts Trypan Blue Exclusion by gestational day 21 fetal rat mandibular condylar fibroblasts exposed to CSE. At 24 hours (*) indicates significant difference ($p<0.05$) at 20% CSE relative to the controls. Data collected from 2 independent experiments (with 5 measurements per treatment for each condition, n=10) were combined and are represented as +/-S.D.

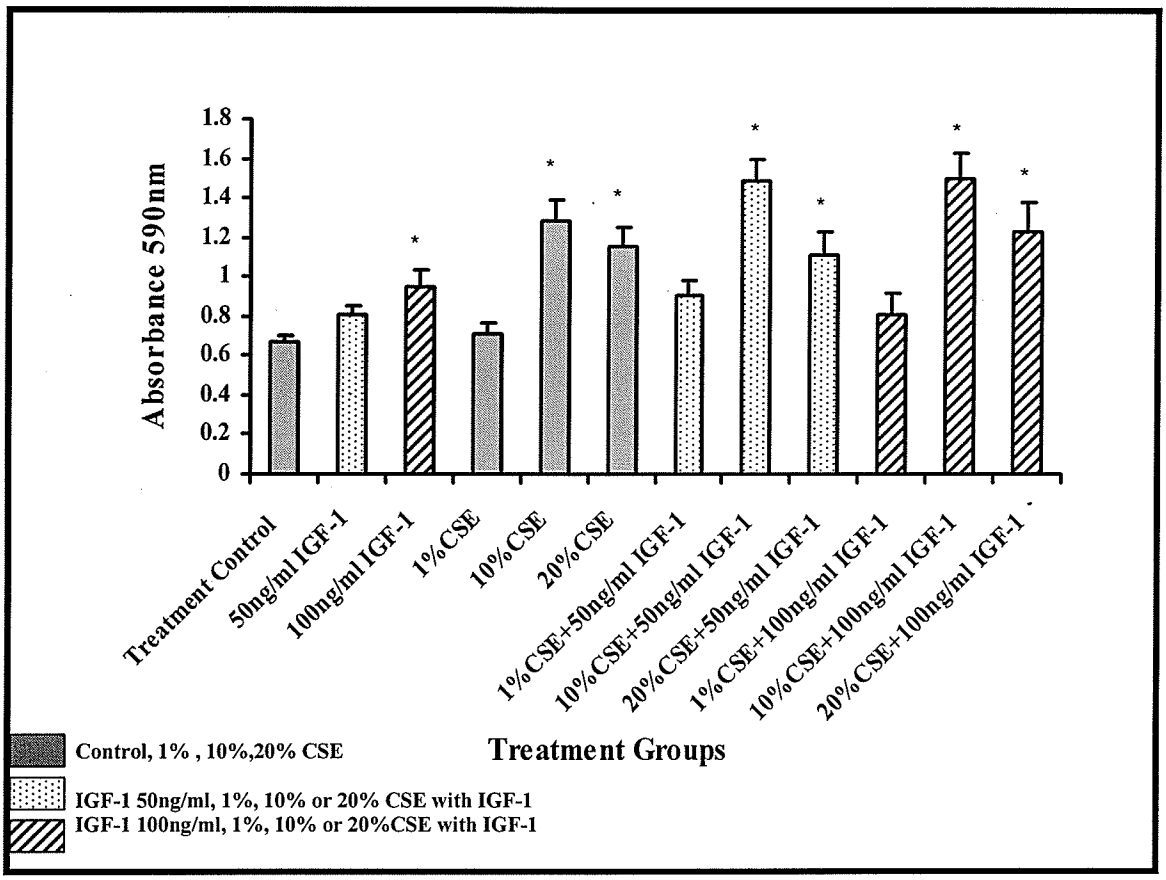

Figure 34: Effects of combined IGF-1 with CSE on proliferative capacity from gestational day 21 fetal rat mandibular condylar fibroblasts Combined effect of CSE/IGF-1 on gestational day 21 fetal mandibular condylar fibroblasts for 24 hours. Serum starved groups were treated with 1, 10 or 20% CSE with or without 50 or 100ng/ml IGF-1. (*) Indicates ($p<0.05$) significant difference at 100ng/ml, 10%, 20%, 10% or 20% CSE with 50ng/ml, 1% or 20% CSE with 100ng/ml compared to the control samples. Data collected from 3 independent experiments (with 8 measurements per treatment for each condition, n=24) were combined and are represented as +/-S.D.

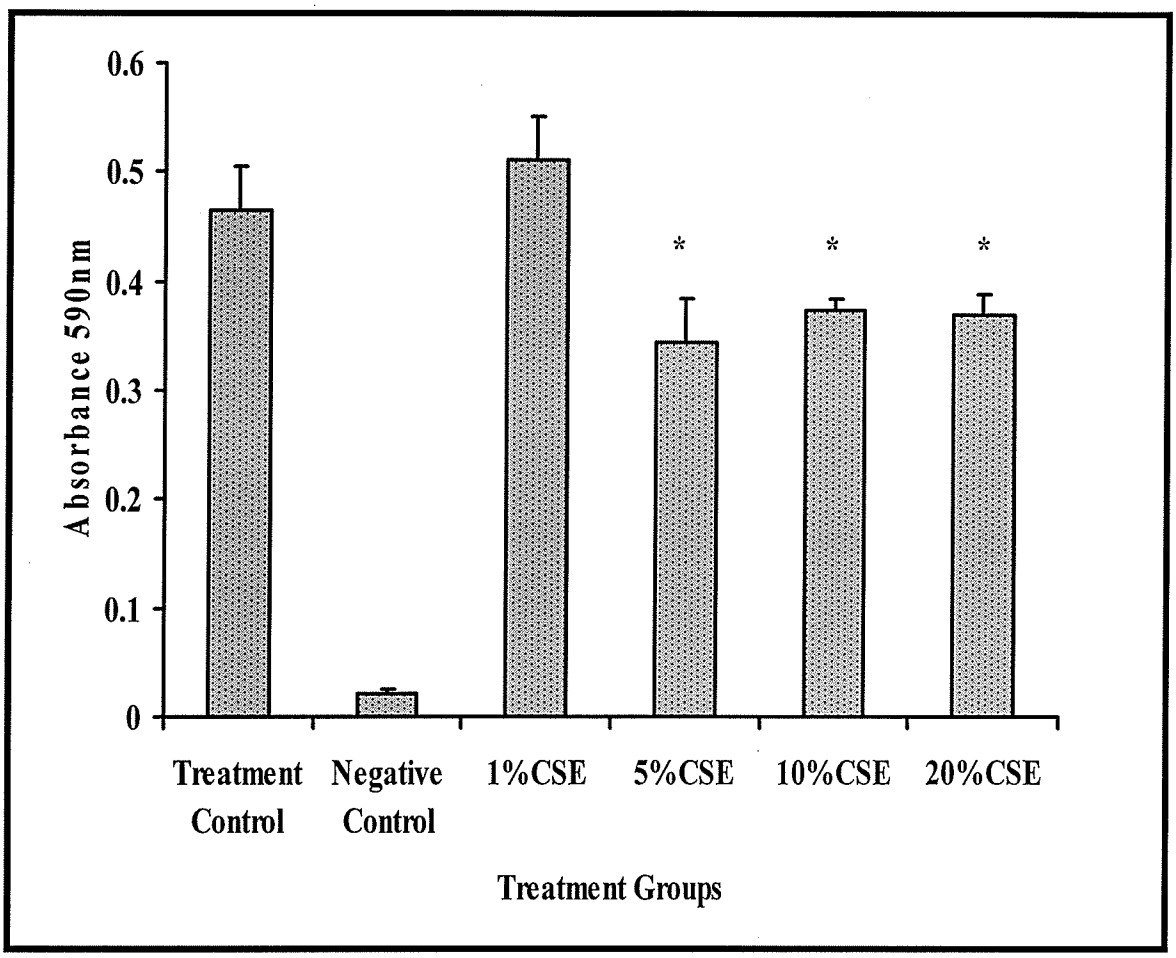

Figure 35: Effects of CSE on proliferative capacity from gestational day 21 fetal rat mandibular condylar fibroblasts Crystal violet assay to assess proliferative effect of CSE on gestational day 21 fetal rat mandibular condylar fibroblasts for 24 hours. Serum contained groups were treated with 1,5,10 or20% CSE. Hydrogen peroxide 200μM was used to induce oxidative stress and served as negative control for recording proliferative activity. (*) Indicates significant difference at 5, 10 or 20% CSE ($p<0.05$) compared to the control group. Data collected from 3 independent experiments (with 8 measurements per treatment for each condition, n=24) were combined and are represented as +/-S.D.

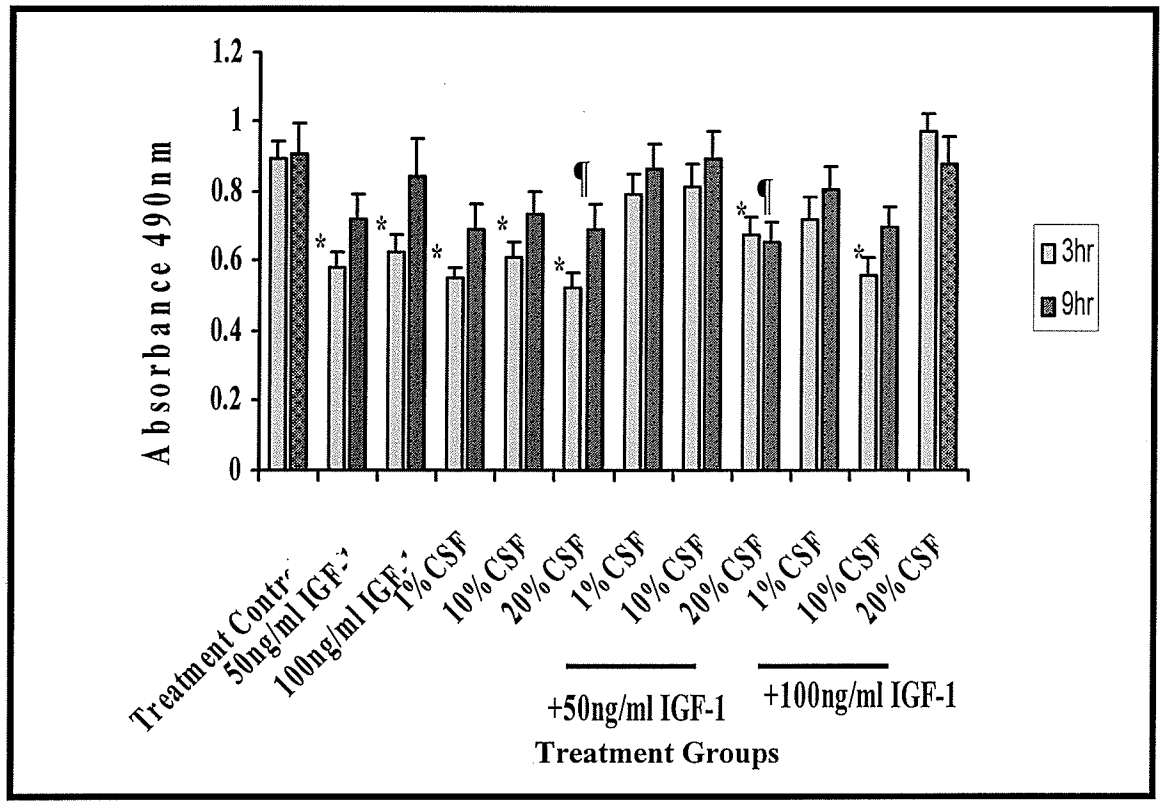

Figure 36: Effects of combined IGF-1 with CSE on cellular metabolic activity from gestational day 21 fetal rat mandibular condylar fibroblasts. MTS Activity recorded in gestational day 21 fetal rat mandilbular condylar fibroblasts exposed to 24 hour CSE treatments. At 3 hours, maximum activity recorded for serum starved at 24 hour incubation with significant difference (* $p<0.05$) at 50ng/ml, 100ng/ml, 1%,10%, 20% , 20% with 50ng/ml, or 10% with 100ng/ml CSE compared to controls. At 24 hours (¶ $p<0.05$) at 20%, 50ng/ml with 20% CSE compared to controls. Data collected from 3 independent experiments (with 8 measurements per treatment for each condition, n=24) were combined and are represented as +/-S.D.

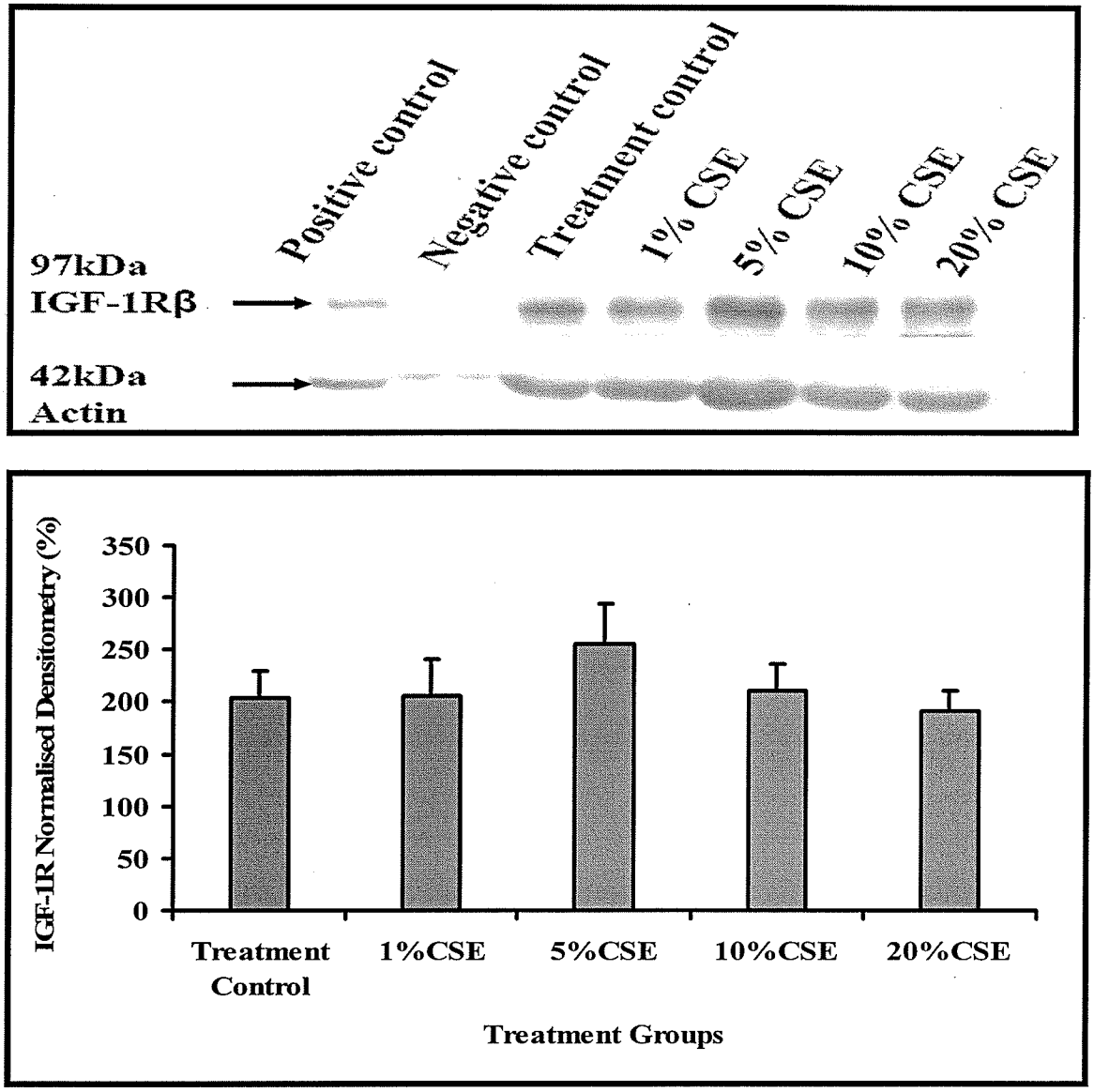

Figure 37: Effect of CSE on IGF-1R β protein expression from gestational day 21 fetal rat mandibular condylar fibroblasts Representative Western blot showing IGF-1R expression in mandibular condylar fibroblasts treated with 1,5, 10 or 20% CSE concentrations for 24 hour time period. Hela cells lysate served as positive control and mouse liver extract as negative control. Beta actin was probed for uniform loading. Densitometric quantitation represents IGF-1Rβ native expression for 24 hour time point in fetal rat mandibular condylar fibroblasts exposed 1, 5, 10 or 20% CSE concentrations. Statistical representation of +/-SE from 3 independent blots.

Physical Data	TPM rag/cig 30mm	FTC Tar mg/cig 30mm	Nictoine mg/cig 30mm	Butt size mm			
2R1	38.8	32.9	2.19	30			
	CRW gm/cig	RTD cm of H2O	Static Burning sec/40mm	Length mm/cig	Circ. mm/cig	Paper porosity sec/50cc	Paper additive type Phosphate
2R1	1.184	8.9	660	85.5	25.0	47.6	0.16
2R1	Water mg/cig	Puff count/cig	CO mg/cig				
	3.70	11.2	22.2				

Table 1: Describes the chemical constituents of reference cigarette 2RI. Abbreviations: CRW Cigarette (cig) rod weight, RTD resistance to draw, Circ; Circumference, TPM: Tar per minute. **Standard 2RI Smoke Analysis-FTC Method.** (Meetings 1984 Tobacco and Health Research Institute Lexington Kentucky USA.)

Protein of Interest	Primary Antibody	Dilution of primary antibody	Secondary Antibody	Dilution of secondary Antibody
IGF-1R α-subunit	Polyclonal Rabbit anti-human [1]	1:1000*	Polyclonal goat anti-rabbit [5]	1:5000 *
IGF-1R β-subunit	Polyclonal Rabbit anti-human [2]	1:1000*	Polyclonal goat anti-rabbit [5]	1:5000 *
Phospho IGF-1R β Tyr 1136/1136	Monoclonal rabbit anti-human [3]	1:1000**	Polyclonal goat anti-rabbit [5]	1:10000 *
Beta Actin antibody [AC-15] (ab6276)	Monoclonal mouse anti-human [4]	1:5000*	Polyclonal Goat-anti mouse [6]	1:10000 *

Table 2: Antibodies used for Western Blot Analysis. The table describes the antibodies and their sources. [1] IGF-1R α (N-20) (Santa Cruz Biotechnology, Inc., Santa Cruz, CA, USA), [2] IGF-1R β (C-20) (Santa Cruz Biotechnology, Inc.), [3] Phospho IGF-1R β Tyr 1135/1136 Cell Signaling Technology, Inc. USA), [4] Actin antibody [AC-15] to beta Actin Abcam Inc., USA. 5. Biorad purified IgG horse radish peroxidase conjugate secondary antibody (Bio-Rad Laboratories, Hercules, CA, USA). * Diluted in 1X TBST (0.05% Tween 20) with 5% skim milk powder. **Diluted in 1X TBST (0.1% Tween 20) with 1% BSA.

Discussion

There exists sufficient evidence in the literature about the role of the IGF axis in pulmonary development (Le Roith et al., 1995; Moats-Staats et al., 1994; Mouhieddine et al., 1994,; Liu et al., 1993). The specific role of IGF-1R in different stages of lung development is not known. However, the first link of IGFs to lung growth was identification of IGF receptors in lung membranes of fetal porcine lungs thus confirming *in vivo* presence of IGFs likely from the time of lung organogenesis (Stiles et al., 1990). Our initial approach to study pre and post natal pattern of IGF-1R expression was an important step toward the beginning of a foundation to compare the expression pattern of IGF-1R in primary cells when treated with cigarette smoke extracts for later experiments.

Our animal model of study was randomly bred Sprague Dawley rat species. The IGF-1R in this species has been sequenced and analyzed biochemically to be as close as 94% to human IGF-1R (Le Roth et al., 1995). Therefore receptor studies in this model could be possibly comparable to humans.

Inspite of the known fact that teratogens like cigarette smoke cause maximum fetal damage during the first trimester of pregnancy, we considered to study the third trimester for our experimental animal models. Specific studies on maternal smoking during third trimester are considered to induce considerable fetal growth retardation (Bernstein et al., 2005).Thus maternal smoking during third trimester could be as fatal as the first (Bernstein et al., 2005). Preliminary studies in normal species can help us understand and further assess the changes in IGF axis. This will determine future areas of investigation in a transgenic animal model.

IGF-1R protein expression during normal lung development

Protein expression studies for IGF-1R showed the presence of receptor in nearly all stages of lung development. Primary lung fibroblast cells in culture from gestational day 21 and post-natal day one, three, seven, eight or nine day age groups came to confluence at different time points (data not shown). The lung fibroblasts from the gestational day 21 reached confluency within 48-72 hours in culture. The other postnatal age groups reached confluence around 7-10 days. This observation was suggestive of the beginning of alveolarisation with differences in fibroblast density as they transit from pre to post natal ages, not only *in vivo* conditions but also *in vitro* conditions as recorded in our studies. Histological development is also suggestive of differences in lung development during the process of alveolarisation from pre to post natal stages.

Our thorough gestational profile of examining the receptor expression was our preliminary experiments to identify the presence or absence of the receptor in primary lung fibroblasts. This was performed due to lack of sufficient evidence in the literature regarding IGF-1R in lung tissues during development in the animal model in our study. Some *in vivo* studies (Silva et al., 2006; Maitre et al., 1995; Moats-Staats et al., 1995) were also suggestive of absence of IGF receptors, ligands and binding proteins in certain age groups as a phasic response of the system to undergoing tissue remodeling. Studies by Burri et al., 1974; 1975; 1984 on the lung development in rat do show lung fibroblasts to undergo increase and decrease in density relative to different stages of lung development. Fetal rat lungs are not functional until day two postnatal and neonatal pups breathe through smooth walled saccules (Burri et al., 1974; 1975; 1984). In our studies increased IGF-1R expression in day one is due to increased mesenchymal fibroblasts,

however the receptor expression reduced at day three. Increased expression at day seven or eight post natal is possibly due to increased proliferation of fibroblasts in the mid first postnatal week. On day nine and onwards the receptor expression is reduced possibly due to increase in alveoli formation and beginning of late postnatal phase, thereby promoting possibly an apoptotic mechanism in lung mesenchymal components (Burri et al., 1974; 1975; 1984). However those studies have not studied the IGF-1R during lung development. Studies by Modha et al., 2004 demonstrated developmental IGF-1R protein profile in rat mammary gland. This study is in accordance with our observation of differential expression of IGF-1R at different ages. Our study suggested that during the alveolarisation period reduced IGF-1R expression possibly due to apoptotic mechanisms predominated the proliferative ability of mesenchymal cells. More than 20% of lung fibroblasts undergo apoptosis during early post natal period (Sreenivasan et al., 2002; Bruce, 1999). This process probably keeps the development of the lung in homeostasis with other components of the lung tissue. Our qualitative expression of immunohistology to IGF-1R antibody reconfirmed the receptor expression from gestational day 21, seven, eight or nine day old lung paraffin sections. Abundant expression in day 27 old adult rat in bronchiolar epithelium (data not shown) suggested the presence of the receptor in adult stages as well.

In summary, reduced expression of IGF-1R in the mesenchymally derived lung cells coincided with increased process of alveolarisation. This experiment formed the basis for our further experiments to assess tobacco smoke exposure in pre and post natal lung cells (gestational day 21 and day one lung fibroblasts).

Cigarette Smoke Extract (CSE) Application in cell cultures

The rationale of applying cigarette smoke extract in different dilutions instead of specific tobacco components was to assess the overall damage *in vitro* to cells from different systems and age groups. Before the application of CSE in our *in vitro* model of study we had a few considerations in mind such as the organs and the type of cells for the pathogenesis of interest. Lungs are potentially the prime organs exposed to active smoking and their biological barriers to smoke constituents will differ from other systems such as bone or skin (Bernhard and Wick G 2005). CSE is a complex mixture of unknown chemicals and thus the basic analysis of the CSE constituents is to allow for comparisons within *in vivo* and *in vitro* studies since this is the prime objective of our *in vitro* model under investigation with CSE treatments. However within the limited time span of this project we formed a baseline of effects of whole cigarette smoke extract on cells from different systems. Previous researchers in our laboratory focused on assessing the changes induced by commercially prepared nicotine on the lung cells. In the present context, known nicotine content in 2RI research cigarette formulation is about 2.19 mg/cigarette. Concentrations at dilutions of 1% and 10% were considered equivalent to smoking four cigarettes/day and two packs (20 cigarettes /pack) of cigarettes/day, respectively by Hasgall et al., 2007. However, we do not agree with the explanation given by Hasgall and colleagues on the corresponding number of cigarettes to different percentages because a 100% CSE is derived from one cigarette combusted and smoked through 50ml of culture media. Therefore, the percentages of treatment actually represent the number of puffs/ml from one cigarette. For a 100% CSE we had consistent 12 drags or puffs in our machine. Therefore 1% CSE represents 0.028 puff/ml and so on.

It is also interesting to note that the number of cigarettes around 22-24 packed by the manufacturers per pack of cigarettes possibly has a close link to the hourly drop in nicotine content in the biological system resulting in craving for hourly consumption of cigarettes. Thereby catering to the 24 hour period of consumption of per cigarette each hour. Further in depth standardized chemical analysis of nicotine concentration will help us to determine the role of these specific constituents on cellular organs and tissues.

IGF-1R Expression in CSE treated primary lung and condylar cells.

IGF-1 receptor total protein expression in CSE treated cells

IGF-1R is the predominant receptor in the IGF axis. Ligand-receptor interaction initiates the signal transduction mechanism. We analyzed the receptor expression in all cell types through Western blotting. The pattern of expression was different at the various concentrations of CSE treatment.

There were differences in receptor expression in gestational day 21 of the two cell types in lung tissues. Their response to the CSE is very interesting. In type II cells receptor expression increase at 5% CSE treatment was higher compared to the lung fibroblast in the same age and concentration. The receptor expression increased at 1 or 5% in type II AECs and reduced thereafter whereas in lung fibroblasts reduced receptor expression noted at 1 or 10% CSE treatments. Visual and densitometric assessment of the pattern of the receptor expression in both types is also suggestive of the hetergeneous expression of these receptors (Le Roith et al., 1995). Two forms of this receptor have been cited in the literature, the heterogeneity in receptor forms (Le Roith et al., 1995) in pre and post natal lung development and also in normal lung development and

malignancies (Kaiser et al., 1993). This suggests that comparative differences in the epithelial-mesenchymal interactions and expression of this receptor in response to injurious stimuli like cigarette smoke is differentially regulated. The increase in expression is probably a response to injurious stimuli in an attempt to initiate repair mechanisms. IGF axis is considered a survival axis. IGF-1R is known to initiate anti-apoptotic mechanisms. Signaling through this receptor suggests that possibly repair mechanisms were initiated which can either initiate cell survival growth mechanism or cell death mechanisms through cross talk with other down stream signaling pathways (Narasaraju et al., 2004).

In the postnatal day one lung fibroblasts the receptor expression increased at 5, 10 or 20% CSE . This pattern differed from the lung fibroblasts and epithelial cells of gestational day 21 at higher concentrations onwards. This suggests that possibly the new born lung fibroblasts are more resistant to whole CSE. This also suggests how sensitive the fibroblasts from gestational day 21 are, when compared to post natal lung cells from new born lung fibroblasts to CSE. Up regulation of the IGF-1R at higher doses of CSE influencing the mesenchymal proliferation perhaps may lead to the fibrosis in these lung cells (Chetty et al., 2004).

Our study is consistent with studies on hypoxia-induced injury (Narasaraju et al., 2006) in lung type II which also probably triggered IGF signaling pathways by increasing expression of IGF-1R in type II cells, thereby initiating a process to regenerate normal alveolar epithelium. Literature evidence to support IGF-1R expression in type II cells is very limited. Evidence provided in the literature for receptor expression in type II cells was more emphasized in type II cells from adult rodents (Narasaraju et

al., 2006). Thus it was a challenge to localize the receptor expression in these prenatal cells. Subsequent repetitive experiments with consistent results proved that possibly we had targeted the receptor in type II cells based on their immunogenicity to the probed antibody. However, receptor purification studies and analytical biochemistry of IGF-1R in these cell types may assure us the configuration and sequence of the receptors. These studies were beyond the scope of the present project.

On the contrary, the results suggest that within the same age group two types of fibroblasts from two different systems responded differently. Lack of IGF-1R alteration in the mandibular condyles suggest the ability of these mesodermally derived fibroblasts from osteogenic origin to resist the potential negative effects of CSE on this receptor in this specific region at a 24 hour time point. We did anticipate increased receptor expression to CSE; however, lack of alteration of IGF-1R protein expression in MCCs suggest that possibly not all systems during development respond to CSE stimulation over a 24 hour time point. However bone density studies in these regions can suggest possible alteration to bony regions and its susceptibility to fracture. Studies on bone mineral density in fetal animals and humans subjected to maternal smoking conditions have shown negative results with decreased bone density (Seller and Bnait 1995; Jones et al., 1999; Zaren et al., 1996).

In the background we wanted to assess if the protein expression of IGF-1R correlated with its gene expression. We performed real time PCR analysis however due to technical errors and the wrong choice of primer design appropriate for the apparatus we could not assess the comparative profile of proteins and genes affected by CSE.

In summary, a contrasting behaviour of IGF-1 receptor expression was seen in these primary cells from pre and post natal stages. There is a definite temporal pattern of expression involved. How far these systems have an effect on each other will remain questions to be answered in future research. In retrospect, expression of surfactant proteins from type II cells to CSE exposure were not assessed and probably these studies could suggest if the IGF-1R expression profile was comparable to the surfactant expression in cultures. Previous studies done in our laboratory (Merluza et al., 2006) have shown the secretion of surfactant proteins in culture however their expression being relatively unaffected by the nicotine exposure treated. Thus a further experiment to assess surfactant protein expression in type II cells treated with CSE remains to be observed. We hypothesize that surfactant secretion will increase in lower doses of stimulation with CSE and decrease with higher concentrations.

IGF-1 receptor activated protein expression in CSE treated cells

Autophosphorylation studies

To further investigate the activation of receptor for downstream signaling mechanism we performed autophosphorylation studies in both lung fibroblasts and type II alveoloepithelial cells from gestational day 21. We induced the cells with IGF-1 at different concentrations. We probed with antibody specific to the tyrosine kinase domain at 1135/36 subunit of the IGF-1R. This region is very specific to initiate signaling mechanisms in most cells. In the lung fibroblasts we noticed increased autophosphorylated expression in 1, 5 or 10 % CSE concentrations. With IGF-1 stimulation however the pattern of expression was highly variable in type II cells which

showed increased receptor activation at only 1% CSE and not at higher concentrations. This suggested the reduced sensitivity of type II cells relative to lung fibroblasts in initiating signaling. From our previous discussion we know that in type II cells the total receptor expression increased from 1 to 5 % CSE and the decrease in 10% CSE was evident and not absent. However, lack of receptor activation in 5 or 10% CSE in type II cells suggests that possibly the receptor to CSE exposure became a dormant or to say so a dead entity. These cells failed to thrive upon the removal of injurious stimuli like CSE (data not shown). We speculate that possibly the IGF receptor is an important component in cells of fetal origin to maintain repair, growth and proliferative mechanisms. However, further receptor inhibitor and antagonistic studies in these cells will prove if the increase or decrease in expression of these receptors is primarily due to IGF axis and not a cross reaction from other receptors like estrogen and insulin receptors which share similar tyrosine kinase beta subunits.

IGF-1R and Insulin receptors are similar in structure and also share a common signaling pathway with phosphorylation of IRS-1 subunits (Lorenzino et al., 1998, White and Yenush 1998, Roth et al., 1991). The process of autophosphorylation is common to both receptors to activate downstream pathways such as the P13/Akt pathways (Myers et al 1993). It is possible that the observed receptor activation through autophosphorylation may have resulted from the activation of insulin receptor by IGF-1. Some studies have suggested that Crk proteins are preferentially activated by IGF-1R (Butler et al., 1998, Beitner-Johnson et al., 1996). Thus phosphorylation of Crk substrate is probably an end point to measure for IGF-1R signalling. So far the role of Crk

proteins in IGF-1R signal transduction in type II and lung fibroblasts have not been studied. However, these studies were not done in the present context as well.

Morphological Assessment

Phenotypic characteristics of CSE treated lung cells showed a very consistent pattern. At lower concentrations from 1 to 10% CSE not much different phenotypic differences were observed upon CSE treatments. The cells remained attached to the culture dishes and retained their fibroblast or type II epithelial type morphological features. However under higher magnification we did observe phenotypic changes in membranes, cell nuclei with membrane blebbings, nuclear condesations suggestive of probably apoptotic mechanisms occurring. At higher concentrations of 20% or above CSE we observed increased number of floating cells. Thus the safe dosage of CSE in culture for lung cells was determined between 1-10% for type II alveoloepithelial cells and lung fibroblasts from gestational day 21. However for cells from newborn lung fibroblasts we recorded a safe dosage of 1-20% and for mandibular condylar fibroblasts 1-30% CSE. Even though these phenotypic characteristics are typically observed in dying cells (Peruzzi et al., 1999), further test are required to distinguish cell senescence as a result of aopoptosis or necrosis. In the background we performed comet assay to assess the DNA damage in type II cells (data not shown); however, we ran into some technical optimization of the technical procedure. We observed disintegrated fragments of the nucleus and we may speculate either technical issues or the CSE at 1% is damaging to the DNA. Our controls showed comet heads, however, due to a weak signal with sybr green fluorescence dye the image quality recorded was weak. Perhaps DNA

fragmentation in DNA gels could be an alternative method to assess DNA damage in these cells. CSE studies on type II cell lines A 549 (Jiao Z et al 2008, Hoshino Y et al., 2001) showed morphological features as described in our studies. CSE contains abundant carcinogenic substances and abundant oxidants (Jiao Z et al 2008). Perhaps most cells undergo the three observed effects as seen in vascular endothelial cells exposed to CSE (Bernhard D and Wick G 2005) characterized by (1). damage phase which may cause oxidation of cellular proteins, (2). alert and repair phase where cytokines and chemokines are released and (3). decision phase characterized by cellular death or survival. We speculate similar processes occurring in cells exposed to CSE from different tissue sources.

CSE effects on cell viability, cell proliferation and metabolic mitochondrial dehydrogenase enzyme (MTS) Studies

In type II AECs, CSE inhibited the cell viability, as determined by trypan blue exclusion assay at 24 hours. However, we did not see the effect until the 12^{th} hour of treatment with CSE. The reduced viability was more significant at 20% CSE concentrations. Thus the present study demonstrated that CSE inhibited the growth of type II cells in a dose and time dependent manner. Probably the growth inhibition of cells was due to changes in cell cycle in G0-G1 phase (Jiao Z et al., 2008). Further studies on assessing the time required to restore the DNA damage before replication in cell cycles in G1-S phase may explain the possible slow process of growth in CSE treated cells. Extended CSE treatments to 48, 72 or 96 hours (data not shown) showed more detrimental effects which increasing time and doses of CSE. This observation

suggests that possibly the extended periods of incubation did not promote increased viability or proliferation and thus the period of cytotoxic effects on these cells start within a 24 hours time point. Our parallel studies on CSE induced proliferation through crystal violet assay and MTS mitochondrial dehydrogenase assay showed similar trends with slow rate of proliferation in 10 or 20% CSE. A striking contrast in MTS activity was observed in newborn rat lung fibroblasts. We found increased metabolic response in the 24 hours serum starved CSE treated state at higher concentrations of CSE. This reverse trend in these cell types probably could be a result of higher metabolic activity in these cells.

Similar trends of inhibited growth was seen in all types of fibroblasts, except the severity of damage at 20% CSE was comparatively lower than type II AECs. Our CSE treatment to assess cellular viability of mandibular cells suggest that these cells are resistant to 20% CSE with a appreciable cell viability of about 70% after treatment.

IGF-1 Ligand in combination with CSE effects on cell proliferation and metabolic mitochondrial dehydrogenase enzyme (MTS) studies in pre and post natal fibroblasts.

The concomitant ligand studies were done on these cell types to assess if IGF-1 has profound mitogenic action on these cells. We wanted to assess if the IGF-1 in combination with CSE may enhance the proliferative effects. In our studies there was a contrasting difference in the way IGF-1 stimulated pre and post natal lung fibroblasts. It was found to be more proliferative to post-natal lung fibroblasts than from gestational day 21 fibroblasts (Silva et al., 2006). This observation was in accordance with the

mitogenicity of IGF-1 which is higher in postnatal development. During development in *in vivo* studies, IGF-1 concentrations reduce during near term state and the increase in concentration has been observed in the early post natal phase (Silva et al., 2006). In our study we have observed that even the stimulation with exogenously supplied IGF-1 in late gestation lung fibroblasts did not stimulate the cellular growth and proliferation. Even though we did a concentration curve to assess the maximum response of IGF-1 in these cells at 50 or 100ng/ml we probably may go up to higher concentrations to re-assess this observation. IGF-1 in combination with CSE did not enhance proliferative or metabolic effect in these cell types, thus suggesting the lack of additive effect of IGFs in combination with CSE.

On the contrary the combined effect of CSE with IGF-1 on cells from condylar region showed increased MTS activity to IGF-1 at 50ng/ml dosage and in combination with CSE at 10% concentration. However mandibular condylar cells have shown increased proliferative response to CSE alone and in combination with IGF-1. Lack of sufficient literature evidence of genotoxic agents on these cells is a limiting factor to provide sufficient evidential support.

Significance of our *in vitro* study to *in vivo* clinical application

Maternal IGFs does not cross the placental barrier (Liu et al., 1994). Maternal administration of IGFs does not directly affect fetal circulatory levels of IGFs (Liu et al., 1994). Circulatory levels of IGF-1 in fetal and cord blood correlate with fetal size (IDECG, 1996). Thus, it has been a clinical proposal by United States Patent 5858966 for administration of IGFs in fetal circulation through placental route may be of

advantage to the fetal organs exposed to maternal smoking, which is an important indicator for fetal growth retardation. The entire project is the projection of the effect of one cigarette in a 24 hour time span on cells. This application of the one cigarette *in vitro* is actually the effect of number of puffs from one cigarette. However, we are surprised with the dynamic range of effects *in vitro* of one cigarette over the said period of time is probably a factor of the number of puffs of smoke per cigarette. In speculation the effect of each puff on developing fetus is immeasurable. As documented by Time magazine in 1935 by Antioch physicians that maternal smoking may send fetal heart beats up from 144 to 149 per minute upon stethoscopic evaluation of heartbeats, made them to conclude that maternal smoking during pregnancy may have permanently harmful effects upon the child. It is challenging to assess if the effects observed in our study is comparable to smoking individuals. To certain extent we do expect the results as reported by our study. However, other nutritional status and genetic make up of the individual cannot be ignored. This is probably also a genetically determined factor where the rate of clearance of tobacco metabolites is handled by genes such as Glutathione synthase transferase, or NAT genes responsible for detoxification of tobacco metabolites. These studies show that only if genetic defects in these genes or absence of these genes can define definite links of tobacco smoking and cellular effects. In our model of study we could not assess the genetic constituent of randomly bred Sprague Dawley rats for tobacco detoxification genes. On the other hand the significance of our study with respect to type-II AECs *in vitro* conditions compared to *in vivo*, possibly may not match to the *in vivo* effects. In the given present conditions of CSE serum starved treatments *in vitro* we hypothesize that surfactant quality will be affected. However,

clinical profile of lack of substantial links of maternal smoking and neonatal respiratory distress suggests that probably maternal smoking enhances the pulmonary maturation perhaps due to the combined effects of hormones. Therefore, *in vitro* conditions comparable study of effects of CSE with or without serum may suggest a profile of surfactant proteins in both conditions. The significance of our other tissue under investigation mandibular condylar cells one of the pressure bearing surfaces of the mandible suggested that even though by 24 hour exposure the cells from this region were did not showed altered IGF-1R expression, however by 96 hours time point we did anticipate receptor expression change as suggested by our phase contrast microscopy. It will be interesting to study the effects of this agent in the first trimester of pregnancy when this region of maxillofacial structure is more prone to developmental defects. In parallel follow up epidemiological studies with assessment of TMJ functionality of victims of maternal smoking can add valuable information if the maternal smoking in first trimester affected long term TMJ functioning and dental occlusion. The profile of IGF-1R response to CSE and IGF-1 suggested that possibly the route of exposures to developing fetus is both circulatory and amniotic, different tissues responded to the same teratogenic agent differentially. However, we do anticipate the detrimental effects of cigarette smoke in most tissues during development, which probably occur at different timepoints. Thus, over all growth restricting predominant effects of cigarette smoke inspite of the natural growth promoters within the physiological system.

Conclusions

In conclusion we found the predominance of CSE on numerous cellular systems was causing extensive detrimental changes. Among them all, the most affected were the type II alveolar lung cells to CSE. Possibly among the various cell types that compose the lung the epithelial cells of alveolar structure appear to be a major target of injury. However, a generalized process of inhibition to growth was seen in all cell types and the differential expression of receptor in these cell types suggest an intricate mechanism involved. Since the chemical composition of cigarette smoke is complex it is not easy to predict which compound was perhaps involved in increased toxicity and receptor expression. Our present *in vitro* study strongly suggests that cigarette smoke exposure may involve IGF axis-mediated differential cellular mechanism, predominantly more so in the primary developing fetal lung type II cells. The differential effects of CSE on mesodermally derived cells from the mandibular condyles are well noted in our study. However we could not find a definite cause and effect link among the hard and soft tissue profiles of CSE and IGF treatments. We speculate that *in vivo* future studies will determine if these observed patterns of cell differentiation and IGF axis alteration to smoke constituents follow the same pattern as our *in vitro* studies.

Future Studies

Directions from the existing project to future approach form a baseline of proposal for a new project. In the present context there are many unanswered questions left in which further research can help us to understand the molecular and cellular processes in more depth. In our present study model we found considerable changes *in vitro* in the receptor expression. Parallel *in vivo* studies of organ culture may reflect the possible *in vivo* morphological changes to CSE. This study addressed how the receptors are undergoing changes in expression to CSE. However, the biochemical analysis of these structures in the specific sites remain to be localized. Through literature evidence it is known that estrogen induces IGF-1R expression in various tumor cell lines (Stewart et al., 1990). A parallel study whereby inhibiting and antagonistic agents for the corresponding tyrosine kinase domains of estrogen receptors, insulin receptors and growth hormone receptors may allow us to compare and understand the role of IGF receptors more specifically without any bias from receptors with similar characteristics. The role of growth hormone (GH) and insulin known to regulate IGF-1 expression in future studies during development may provide an insight to the extent of IGF axis predominance. IGFs are known as weak mitogens for type II cells. Further parallel studies to assess the paracrine nature of IGFs on type II cells and the role of binding proteins may suggest intricate mechanisms of IGF receptor changes as observed in our study. Lack of surfactant protein studies in our project suggest a possible starting point for the next step in this research project. The concurrent pattern of surfactant secretion to smoke exposure can decipher the effect of cigarette smoke on type II cells specific functions.

In summary, these studies may contribute in addition information about IGF axis during fetal lung development exposed to genotoxins. This will help us to determine if changes observed in IGF axis in lungs and craniofacial structures have similar observed effects in humans from second hand smoke. Our observations of bench research need consistent team effort with communication with epidemiologists and clinical specialists of concerned specialties which may help us move towards a more translational approach of cellular knowledge to clinical applications. Thus instead of moving in directions in our own isolations based on our laboratory focus, a holistic team approach may help us find quicker cures and re-emphasize the practice of consistent good research.

REFERENCES

Avery JK, Bernick S. 1994 Structure and Function of the temporomandibular joint In Avery JK (Eds.) Oral Development and Histology pp. 214-225 New York Thieme Medical Publishers, Inc.

Barnard R Haynes KM Werther GA Waters MJ 1988 The odontogeny of growth hormone receptors in the rabbit tibia. Endocrinology 122:2562-2569

Beitner-Johnson D, Blakesley VA, Shen-Orr Z, Jimenez M, Stannard B, Wang LM, Pierce J, Le Roith D 1996 The proto-oncogene product c-Crk associates with insulin receptor substrate-1 and 4PS. Modulation by insulin growth factor-1 (IGF) and enhanced IGF-1 signaling. Journal of Biological Biochemistry 271:9287-90.

Bernhard D, Wick G 2005 *In vitro* models for the analysis of cigarette smoke effects In Wang XL and Scott DA (Eds). Molecular Mechansims of Tobacco-Induced Diseases pp. 29-54 New York Nova Science Publishers Inc.

Bernstein IM, Mongeon JA, Badger GJ, Solomon L, Heil SH, Higgins ST 2005 Maternal smoking and its association with birth weight. Obstet Gynecol 106:986-91.

Blakesley VA, Scrimgeour A, Esposito D, LeRoith D. 1996 Signaling via the insulin-like growth factor-1 receptor: does it differ from insulin receptor signaling? Cytok & Grow. Fact. Rev. 7, 153-159.

Boyden EA 1974 The mode of origin of pulmonary acini and respiratory bronchioles in the fetal lung. American Journal of Anatomy, 141, 317-328

Bradley KH, Kawanami O, Ferrans VJ, Crystal RG 1980 The fibroblast of human lung alveolar structures: a differentiated cell with a major role in lung structure and function. Methods Cell Biol. 21A:37-64

Burdi AR 1992 Morphogenesis In Sarnat BG, Laskin DM (Eds.) The Temporomandibular Joint A Biological Basis for Clinical Practice pp.36-47 Philadelphia W.B.Saunders company.

Burgi H, Muller WA, Humbel RE, Labhart A, Froesch ER 1966 Non suppressible insulin-like activity in human serum: physicochemical properties, extraction and partial purification. Biochim. Biophys.Acta 121, 349-359.

Burri PH, Dbaly J, and Weibel ER. 1974 The postnatal growth of the rat lung. I. Morphometry. Anat Rec 178: 711-730

Burri PH. 1974 The postnatal growth of the rat lung. III. Morphology. Anat Rec 180: 77-98

Burri PH. 1984 Fetal and postnatal development of the lung. Annu Rev Physiol 46: 617-628.

Burri PH.1975 Postnatal growth and maturation of the lung. Chest 67: 2S-7S,

Butler AA, Yakar S, Gewolb IH, Karas M, Okubo Y, Le Roith D 1998 Insulin-like growth factor-I receptor signal transduction: at the interface between physiology and cell biology. Comparative Biochemistry and Physiology 121: 19-26

Carp H, Janoff A. 1978 Possible mechanisms of emphysema in smokers. In vitro suppression of serum elastase-inhibitory capacity by fresh cigarette smoke and its prevention by antioxidants. Am Rev Respir Dis, 118:617-621

Carpentier JL, Foti M, Moukil MA, Dudognon P 2004 Insulin and IGF-1 receptor trafficking and signaling In Bock G, Goode J (Eds). Biology of IGF-1: its interaction with insulin in health and malignant states pp. 125-147 Chichester, John Wiley & Sons Ltd.

Centers for Disease Control and Prevention (CDC 2004), Office on Smoking and Health, Department of Health and Human Services. The Health Consequences of Smoking: A Report of the Surgeon General Atlanta Georgia, U.S.

Centers for Disease Control and Prevention (CDC) 2007. Smoking and Tobacco Fact Sheet:Women and Smoking .

Chen J, Chen Z, Narasaraju T, Jin N and Liu L 2004 Isolation of highly pure alveolar epithelial type I and type II cells from rat lungs. Laboratory Investigation; 84, 727–735.

Chen Z, Jin N, Narasaraju T, Chen J, McFarland LR, Scott M, Liu L. 2004 Identification of two novel markers for alveolar epithelial type I and II cells Biochemical and Biophysical Research Communications;319 (3), pp. 774-780.

Chetty A, Andersson S, Lassus P, Nielsen H 2004 Insulin-like growth factor-1 (IGF-1) and IGF-1 Receptor (IGF-1R) expression in human lung in RDS and BPD. Pediatr Pulmonol 37: 128-136

Chung KC, Kowalski CP, Kim HM, 2000. Maternal cigarette smoking during pregnancy and the risk of having a child with cleft lip/palate. Plast Reconstr Surg;105:485–491.

Clemmons DR (1997) Insulin-like growth factor binding proteins and their role in controlling IGF actions. Cytokine & growth factor reviews; 8, 45-62.

Crapo JD, Barry BE, Gehr P, Bachofen M, Weibel ER 1982 Cell number and cell characteristics of the normal human lung. Am. Rev. Respir. Dis;125:332-337.

Cunningham J, Dockery DW and Speizer FE 1994 Maternal Smoking during pregnancy as a Predictor of Lung Function in Children American Journal of Epidemiology;139, No. 12: 1139-1152

D'ercole AJ, Applewhite GT, Underwood, LE 1980. Evidence that somatomedin is synthesized by multiple tissues in the fetus. Develop Biol 75, 315-328.

Daughaday WH, Hall K, Raben MS, Salmon Jr, WD, Brande JL, Wyk JJ 1972. Somatomedin: proposed designation for sulfation factor. Nature 235, 107.

Daughaday WH, Hall K, Salmon Jr, WD, Brande van den JL, Wyk van, J.J. 1987. On the nomenclature of the somatomedins and insulin-like growth factors. J. Clin.Endocrinol.Metab. 65, 1075-1076.

Delatte M, Von den Hoff JW, Maltha JC, Kuijpers-Jagtman AM. 2004 Growth stimulation of mandibular condyles and femoral heads of newborn rats by IGF-I.
Durkin JF, Heeley JD, Irving JT. The cartilage of the mandibular condyle. Oral Sci Rev. 1973;2:29–99.

Duterloo HS. 1967 Invivo implantation of the mandibular condyle of the rat. Unpublished dissertation. Nijmegen, the Netherlands, University of Nijmegen

Enlow DH. 1992 The condyle and facial growth In Sarnat BG, Laskin DM (Eds.) The Temporomandibular Joint A Biological Basis for Clinical Practice pp.48-59 Philadelphia W.B.Saunders company.

Ermis B, Altinkaynak K, Yildirim A, Ozkan B 2004 Influence of Smoking on Serum and Milk of Mothers, and Their Infants' Serum Insulin-Like Growth Factor-I and Insulin-Like Growth Factor Binding Protein-3 Levels Horm Res ;62:288-292.

Etherton TD. 2004 Somatotroph function: the somatomedin hypothesis revisited. J.Anim.Sci. 82E, E239-E244.

Evans HM, Long LA. 1921. Effect of the anterior lobe of the hypophysis administered intraperitoneally upon growth and maturity and estrous cycles of the rat .Anat record 21, 62.

Floros J, Post M, Smith BT 1985. Glucocorticoids affect the synthesis of pulmonary fibroblast pneumocytes factor at a pre translational level. J. Biol. Chem 260: 2265-2267

Fowler PA, Cassie S, Rhind SM, Brewer MJ, Collinson JM, Lea RG, Baker PJ, Bhattacharya S and O'Shaughnessy P J 2008 Maternal Smoking during Pregnancy Specifically Reduces Human Fetal Desert Hedgehog Gene Expression during Testis Development The Journal of Clinical Endocrinology & Metabolism Vol. 93, No. 2 619-626

Franks LM., Cooper TW., 1972 The origin of human embryonic lung cells in culture: a comment on cell differentiation, in vitro growth and neoplasia. Int. J. Cancer 9: 19-29.

Godfrey K, Walker-Bone K, Robinson S, Taylor P, Shore S, Wheeler T, Cooper C. 2001 Neonatal bone mass: influence of parental birthweight, maternal smoking, body composition, and activity during pregnancy. J Bone Miner Res. Sep;16(9):1694-703.

Guerreiro AS, Boller D., Doepfner KT, Arcaro, A. 2006 IGF-IR: potential role in antitumor agent. Drugs News Perspect. 19, 261-269.

Hall BK, 1970 Differentiation of cartilage and bone from common germinal cells. J. Exp. Zool. 173:383-393

Han VK, Lund PK, Lee DC, D'ercole, AJ 1988. Expression of somatomedin/insulin-like growth factor messenger ribonucleic acids in the human fetus: identification, characterization, and tissue distribution. J. Clin. Endocrinol. Metab. 66,422-429.

Hance AJ, Crystal RG 1975. The connective tissue of lung. Am Rev Respir Dis 112: 657-711.

Harding R, Bocking AD, Sigger JN 1986 Influence of upper respiratory tract on liquid flow to and from fetal lungs. J Appl Physiol 61:68-74.

Hartsfield JK Jr, Hickman TA, Everett ET, Shaw GM, Lammer EJ, Finnell RA. 2001 Analysis of the EPHX 1113 polymorphism and GSTM1 homozygous null polymorphism and oral clefting associated with maternal smoking. Am J Med Genet. Jul 22; 102(1):21-4.

Hasgall P, Bellehsen L, Hammel I, Amichai D, Levi-Schaffer F 2007 In Vitro Exposure To Cigarette Smoke Activates Eosinophils: Implications For Lung Inflammation. The Internet Journal of Asthma, Allergy and Immunology. Vol 10 Number 10

Hassib N 2006 Reducing Birth Defects - The Cost-effective and Global Way Forward; pp. 201-238 In Janet V. Engels (Ed.) Birth defects: New research. pp 201-238 Nova science publishers.

Hislop A, Reid L. 1974 Development of the acinus in the human lung. Thorax, 29, 90-94.

Hislop AA 2002 Airway and blood vessel interaction during lung development. Journal of Anatomy 201, 325-334.

Holly Jeff 2004 Physiology of the IGF system In Bock G, Goode J (Eds). Biology of IGF-1: its interaction with insulin in health and malignant states pp. 19-35 Chichester, John Wiley & Sons Ltd.

Hong, Yun-Chul MD; Lee, Kwan-Hee MS; Son, Byong-Kwan MD; Ha, Eun-Hee MD; Moon, Hye-Sung MD; Ha, Mina MD 2003 Effects of the GSTM1 and GSTT1 Polymorphisms on the Relationship Between Maternal Exposure to Environmental Tobacco Smoke and Neonatal Birth Weight. Journal of Occupational & Environmental Medicine. 45(5):492-498

Hooper SB, Harding R, 1995 Fetal lung liquid: a major determinant of the growth and functional development of the fetal lung. Clinical and experimental pharmacology and physiology, 22, 235-247.

Hooper SB, Wallace MJ. 2004 Physical, endocrine and growth factors in lung development In Harding, R., Pinkerton, K.E., Plopper, C.G. (Eds.). The lung development, aging and the environment pp.132-148. London: Elsevier Academic Press.

Huizink AC, Mulder EJH. 2006 Maternal smoking, drinking or cannabis use during pregnancy and neurobehavioral and cognitive functioning in human offspring. Neurosci and Biobehav Reviews 30:24-41

IDECG 1996 Causes and Consequences of Intrauterine Growth Retardation, Proceedings of an IDECG workshop, November 1996, Baton Rouge, USA, Supplement of the European Journal of Clinical Nutrition (International Dietary Energy Consultative Group – IDECG,100 pages).

Inselman LS, Mellins RB 1981 Growth and development of the lung. Journal of Paediatrics, 98, 1-15.

Isaksson OGP, Eden S, Jansson J-O 1985. Mode of action of pituitary growth hormone on target cells. Ann Rev Physiol 47:483-499

Jacobs R. Economic policies, taxation and fiscal measures 2001 In J Samet, Soon-Young Yoon (Eds.) Women and the tobacco Epidemic: Challenges for the 21st Century. World Health Organization, Geneva: 177-200.

Jakob A, Hauri C, Froesch ER. 1968 Non suppressible insulin-like activity in human serum: differentiation of two distinct molecules with non suppressible ILA. J.Clin. Invest. 47, 2678-2688.

Janoff A, Pryor WA, Bengali Z, 1987 NHLBI workshop summary. Effects of tobacco smoke components on cellular and biochemical processes in the lung. Am Rev Respir Dis,. 136(4): 1058-64

Javaid M. 2003 Prenatal and childhood influences on osteoporosis. Best Practice & Research Clinical Endocrinology & Metabolism , Volume 16 , Issue 2 , Pages 349 - 367

Jiao Z, Qilin AO, Xiaona GE, Xiong M 2008 Cigarette smoke extract inhibits the proliferation of alveolar epithelial cells and augments the expression of P21 WAF1. J Huazhong Univ Sci Technol [Med Sci]. 28(1): 6-10

Joad J, Effects of environmental tobacco smoke on lung development, in The Lung: Development, Aging and the Environment. 2004 Elsevier 291-298

Johansson J, Curstedt T. 1997 Molecular structures and interactions of pulmonary surfactant components. Eur J Biochem 244 (3); 675-93.

Jones GRM, Dwyer T 1999 Maternal smoking during pregancy, growth and bone mass in pre pubertal children. Journal of Bone Mineral Research 14, 146-151

Jurisicova A, Taniuchi A, Li H, Shang Y, Antenos M, Detmar J, Xu J, Matikainen T, Hernández A B, Nunez G and Casper RF 2007. Maternal exposure to polycyclic aromatic hydrocarbons diminishes murine ovarian reserve via induction of Harakiri J. Clin. Invest. 117(12): 3595-3595

Kabesch M, Hoefler C, Carr D, Leupold W, Weiland SK, Mutius E 2004 Glutathione S transferase deficiency and passive smoking increase childhood asthma Thorax 59:569-573

Kaiser U, Schardt C, Brandscheidt D, Wollmer E, Havemann K 1993 Expression of insulin-like growth factor receptor I and II in normal human lung and in lung cancer J Cancer Res Clin Oncol 119:665-668

Kapoor D, Jones TH 2005 Smoking and hormones in health and endocrine disorders. European Journal of Endocrinology 152-491-499

Kim JJ, Accil D 2002 Signalling through IGF-1 and insulin receptors: where is the specificity? Growth Horm IGF Res 12:84-90

Klapper DG, Svoboda ME, Van Wyk JJ. 1983. Sequence analysis of somatomedin-C:confirmation of identity with insulin-like growth factor I. Endocriniology 112, 2215-2217.

Kuhn C. 1978 Ultrastructure and cellular functionin the distal lung. In The Lung: Structure, Function and Disease. Edited by W.M. Thurlbeck and MR Abell. Wiliams & Wilkins, Baltimore, pp. 1-20.

Lammer EJ, Shaw GM, Iovannisci DM, Van WJ, Finnell RH.2004 Maternal Smoking and the Risk of Orofacial Clefts: Susceptibility With NAT1 and NAT2 Polymorphisms. Epidemiology. 15(2):150-156, March 2004.

Lannan S, Donaldson K, Brown D and MacNee W 1994 Effect of cigarette smoke and its condensates on alveolar epithelial cell injury in vitro. Am J Physiol Lung Cell Mol Physiol 266: L92-L100,

Laron Z. 2004 IGF-1 and insulin as growth hormones In Bock G, Goode J (Eds). Biology of IGF-1: its interaction with insulin in health and malignant states pp. 56-83 Chichester, John Wiley & Sons Ltd.

Le Roith D, Werner H, Beitner-Johnson D, Roberts Jr CT. 1995 Molecular and cellular aspects of the insulin-like growth factor-I receptor. Endocr. Rev. 16, 143-163

Le Roith D, Bondy C, Yakar S, Liu JL, Butler A. 2001 The somatomedin hypothesis. Endocr. Rev. 22, 53-74.

Leanderson P, Tagesson C. 1992 Cigarette smoke-induced DNA damage in cultured human lung cells: role of hydroxyl radicals and endonuclease activation. Chem Biol Interact 81(1-2) : 197-208

Lindahl A, Isgaard J, Isaksson OGP 1987 Differential effects of growth hormone and insulin-like growth factor -1 in vitro on colony formation of epiphyseal chondrocytes isolated from hypophysectomized rats. Endocrinology 121:1061-1069

Little J, Cardy A, Munger RG. WHO 2004 Tobacco smoking and oral clefts: a meta-analysis. Bull World Health Organization 82: 213-8.

Liu JP, Baker J, Perkins AS et al. 1993 Mice carrying null mutations of the genes encoding insulin-like growth factor 1 and type 1 IGF receptor Cell 75:59-72.

Liu L, Harding J E, Evans P C, Gluckman P D. 1994 Maternal IGF-1 alters feto-placental carbohydrate and protein metabolism in pregnant sheep Endocrinology 135 895-90.

Lorenzino L 1998 Structure and function of the insulin-like growth factor I receptor. Breast cancer research and treatment 47: 235-253

Luder HU 1993 Macroscopic and microscopic joint morphology, relationship to metabolic activity. In McNamara JA Jr, (Eds.) Postnatal development, aging, and degeneration of the temporomandibular joint in humans, monkeys, and rats. Ann Arbor: Center for Human Growth and Development, University of Michigan, vol. 32, pp.41-109

Maitre B, Clement A, Williams MC, Brody JS 1995 Expression of insulin-like growth factor receptors 1 and 2 in the developing lung and their relation to epithelial cell differentiation. Am J Respir Cell Mol Biol 13:262-270

Maor G, Laron Z, Eshet R, Silbermann M 1993. The early postnatal development of the murine mandibular condyle is regulated by endogenous insulin-like growth factor-1. J Endocrinol 137:121-126

Martin JA 2006. Births: Final Data for 2004. National Vital Statistics Reports, vol 55, no.1

Mason RJ, and Shannon JM. 1997 Alveolar type II cells. In Crystal, R.G., West, J.B. (Eds.) The Lung: Scientific Foundations pp. 543-555 New York, Raven Press, Ltd.

McClure BG, Dornan JC 1989 Fetal lung maturation. Fetal Medicine, 1, 223-234

Meikle MC 1973 In vivo transplantation of the mandibular joint of the rat: An autoradiographic investigation into cellular changes at the condyle. Arch. Oral. Biol. 18:1011-1020

Merluza J 2006 Nicotine and cotinine effects on fetal rat lung Type II Alveolar cells. MSc Thesis Department of Oral Biology Univerity of Manitoba.

Min Shi, Christensen K, Weinberg CR, Romitti P, Bathum L, Lozada A, Morris RW, Lovett M, and Murray JC 2007 Orofacial Cleft Risk Is Increased with Maternal Smoking and Specific Detoxification-Gene Variants Am J Hum Genet. 80(1): 76–90.

Moats-Staats BM, Price WA, Xu L, Jarvis HW, Stiles AD 1995 Regulation of the insulin-like growth factor system during normal rat lung development. Am J Respir Cell Mol Biol 13:262-270.

Modha G, Blanchard A, Iwasiow B, Mao XJ, Troup S, Adeyinka A, Watson P, Shiu R, Myal Y 2004 Developmental changes in Insulin-like growth factor-I receptor gene expression in the mouse mammary gland. Endocrine Research Vol 30, No 1, pp. 127-140, 2004.

Mouhieddine OB, Cazals V, Maitre B, Bouc YL, Chadelat K, Clement A 1994 Insulin-like growth factor-2, type 2 IGF receptor and IGF-Binding protein-2 gene expression in rat lung alveolar epithelial cells: relation to proliferation. Endocrinology vol 135; 83-91.

Murray JF 1986 The normal lung: The basis for diagnosis and treatment of pulmonary disease, pp. 2-4 Philadelphia, W.B Saunders.

Narasaraju TA, Chen H, Weng T, Bhaskaran M, Jin N, Chen J, Chen Z, Chinoy MR, Liu L 2006 Expression profile of IGF system during lung injury and recovery in rats

exposed to hyperoxia: A possible role of IGF-1 in alveolar epithelial cell proliferation and differentiation. J Cell Biochem. 97:984-998.

National Institute on Drug Abuse NIDA InfoFacts: Cigarettes and Other Tobacco Products Available from: http://www.nida.nih.gov/infofacts/tobacco.html

Peltomaki T, Kylamarkula S, Vinkka-Puhakka H, Rintala M, Kantomaa T, Ronning O 1997 Tissue-separating capacity of growth cartilages. Eur J Orthod 19:473-481

Perez-Gil J, Keough KMW. 1998 Interfacial properties of surfactant proteins Biochimica et Biophysica Acta - Molecular Basis of Disease, 1408 (2-3), pp. 203-217.

Poswillo DE, Robinson P. 1992 Congenital and Developmental anomalies. In Sarnat BG, Laskin DM (Eds.) The Temporomandibular Joint A Biological Basis for Clinical Practice pp.183-206 Philadelphia W.B.Saunders company

Reid LM 1979 The pulmonary circulation: remodeling in growth and disease. American review of respiratory disease, 119, 531-546.

Retrieved from: http://www.libraryindex.com/pages/2112/Tobacco-What-What-Does-HEALTH-CONSEQUENCES.html

Roberts Jr CT. 1996 Control of insulin-like growth factor (IGF) action by regulation of IGF-I receptor expression. Endocrine Journal 43, S49-S55.

Ross R 1968 The connective tissue fiber forming cells. In Treatise on collagen, Vol. 2, part A. Edited by B.S. Gould. Academmic Press, New York, pp.2-82.

Roth RA, Yonezawa K, Pierce S, Steele-Perkins G 1991 Substrates of the insulin and IGF-1. In Modern concepts of Insulin-like growth factors, edited by EM Spencer. Elsevier, Amsterdame, pp. 505-515

Salmon Jr, WD, Daughaday WH. 1956. Sulfation factor, a serum component mediating the action of growth hormone in stimulating incorporation of sulfate into cartilage. J. Clin. Invest. 35, 733.

Salmon Jr, WD, Daughaday WH. 1957. A hormonally controlled serum factor which stimulates sulfate incorporation by cartilage in vitro. J Lab Clin Med, 49, 825-836.

Sapp JP, Cherrick HM 1992 Pathological aspects of developmental, inflammatory, and neoplastic disease. In Sarnat BG, Laskin DM (Eds.) The Temporomandibular Joint A Biological Basis for Clinical Practice pp.150-164 Philadelphia W.B.Saunders company.

Sarfstein R, Maor S, Reizner N, Abramovitch S, Werner H 2006 Transcriptional regulation of the insulin-like growth factor-1 receptor gene in breast cancer. Molecular and cellular endocrinology 252; 241-246

Schaeffer WI. 1979 Proposed usage of animal tissue culture terms (revised 1978). Usage of vertebrate cell, tissue and organ culture terminology. In vitro 15:649-653.

Seller MJ, Bnait KS 1995 Effects of tobacco smoke inhalation on developing mouse embryo and fetus. Reproductive toxicology 9, 449-459

Silva D, Venihaki M, Guo WH, Lopez MF, 2006 IGF-2 Deficiency results in delayed lung development at the end of gestation. Endocrinology 147(12): 5584-5591

Sims JR, Karp S, Ingber DE. 1992 Altering the cellular mechanical force balance results in integrated changes in cell, cytoskeletal and nuclear shape. J Cell Sci Suppl 103: 1215-1222

Smale ST, Baltimore D. 1989. The "initiator" as a transcription control element. Cell 57, 103-113

Srinivasan S, Strange J, Awonusonu F, Bruce MC 2002 Pre and post lung development, maturation and plasticity. Insulin-like growth factor- I receptor is down regulated after alveolarisation in an apoptotic fibroblast subset. Am J Physiol Lung Cell Mol Physiol 282: L 457- L 467

Stewart A, Johnson M, May F, Westely B 1990. Role of insulin-like growth factors and type I insulin-like growth factor receptor in the estrogen-stimulated proliferation of human breast cancer cells. Journal of Biological Chemistry 265: 21172-21178.

US Patent5858966 FetalGrowth retrieved from website :
http://www.freepatentsonline.com/5858966.html

Uhal BD, 1997 Cell cycle kinetics in the alveolar epithelium, American Journal of Physiology, 272, L1031-45.

Visnapuu V, Peltomaki T, Ronning O, Vahlberg T and Helenius H 2001 Growth hormone and insulin-like growth factor I receptors in the temporomandibular joint of the rat Journal of Dental Research, Vol 80 Mar;49(3):165-75. Archives of Oral Biology

Visnapuu V, Peltomaki T, Kantomaa T, Isotupa K, Helenius H 2000. Distribution and characterization of proliferative cells in the rat condyle during growth. Eur J Orthod 22:631-638.

Ware WH, Fujimoto JT 1992 Experimental Studies In Sarnat BG, Laskin DM (Eds.) The Temporomandibular Joint A Biological Basis for Clinical Practice pp.207-236 Philadelphia W.B.Saunders company

Weibel ER, Geher P, Haies D, Gil J, Bachofen, M. 1976 The cell population of the normal lung. In A. Bouhuys. (Ed.) Lung cells in disease pp. 3-16. Elsevier/North Holland Biomedical Press, Amsterdam.

Werner H, Woloschak M, Adamo M, Shen-Orr Z, Roberts Jr CT, Le Roith D.1989. Developmental regulation of the rat insulin-like growth factor I receptor gene. Proc Natl Acad Sci USA 86, 7451-7455.

White MF, Yenush L 1998 The IRS-signaling system: a network of docking proteins that mediate insulin and cytokine action. Current topics in microbiology and immunology 228: 179-208

Williams MC 1977. Conversion of lamellar body membranes into tubular myelin in alveoli of fetal rat lungs. J. Cell Biol 72: 260-277

Williams MC 1978 Freeze-fracture studies of tubular myelin and lamellar bodies in fetal and adult rat lungs. J. Ultrastruct. Res 64:352-361

World Health Organization. WHO 2008 Report on the global tobacco epidemic 2008. Geneva: World Health Organization; 2008 [cited 2008 Mar21]. Retreived from: http://www.who.int/tobacco/mpower/en/.

Yakar S, Liu J, Stannard B, Butler A, Acilli D, Sauer B, LeRoith D. 1999 Normal growth and development in the absence of hepatic insulin-like growth factor.Proc.Natl.Acad.Sci.USA. 96, 7324-7329.

Zaren BLG, Gebre-Medhin M 1996 Maternal smoking and body composition of the newborn. Acta Paediatricia 85, 213-219.